On Spectrum Sensing, Resource Allocation, and Medium Access Control in Cognitive Radio Networks

by

Madushan Thilina Karaputugala Gamacharige

A Thesis submitted to The Faculty of Graduate Studies of

The University of Manitoba

in partial fulfillment of the requirements for the degree of

Doctor of Philosophy

Department of Electrical and Computer Engineering

University of Manitoba

Winnipeg

January 2015

Abstract

The cognitive radio-based wireless networks have been proposed as a promising technology to improve the utilization of the radio spectrum through opportunistic spectrum access. In this context, the cognitive radios opportunistically access the spectrum which is licensed to primary users when the primary user transmission is detected to be absent. For opportunistic spectrum access, the cognitive radios should sense the radio environment and allocate the spectrum and power based on the sensing results. To this end, in this thesis, I develop a novel cooperative spectrum sensing scheme for cognitive radio networks (CRNs) based on machine learning techniques which are used for pattern classification. In this regard, unsupervised and supervised learning-based classification techniques are implemented for cooperative spectrum sensing. Secondly, I propose a novel joint channel and power allocation scheme for downlink transmission in cellular CRNs. I formulate the downlink resource allocation problem as a generalized spectral-footprint minimization problem. The channel assignment problem for secondary users is solved by applying a modified Hungarian algorithm while the power allocation subproblem is solved by using Lagrangian technique. Specifically, I propose a low-complexity modified Hungarian algorithm for subchannel allocation which exploits the local information in the cost matrix. Finally, I propose a novel dynamic common control channel-based medium access control (MAC) protocol for CRNs. Specifically, unlike the traditional dedicated control channel-based MAC protocols, the proposed MAC protocol eliminates the requirement of a dedicated channel for control information exchange.

Acknowledgements

This dissertation would not have even been possible without the help and dedication of some special people in many ways. Undoubtedly, I would like to express my foremost heartiest gratitude to my dissertation advisor Professor Ekram Hossain for his excellent guidance, encouragement and dedication that pushed me far beyond my expectation. Specially, no matter how busy he was, he could always find time to discussions. Thank you for all of that!

I gratefully acknowledge the members of the dissertation examination committee Professor Pradeepa Yahampath, Professor Pourang Irani and Professor Abraham Fapojuwo for their constructive criticism, valuable comments and suggestions on this study. My special thank also should goes to other faculty staffs for their collaboration for improving my knowledge in numerous ways. I make this an opportunity to acknowledge the financial support from UMGF and NSERC to carry out my PHD. Specially, I would like to thank all my group members, lab colleagues and the Sri Lankan community in Winnipeg for all kind of supports given to me during my study.

No single piece of this dissertation would be a reality without the seamless support of my parents, Hemalatha and Dharmasena, who always encourage my dreams and aspirations no matter which direction I chose. I would have never been in this position without their love, care, dedications and support. The minimum I can give back is to dedicate this dissertation to my parents.

I would like to acknowledge my sisters, Samanthi and Keshala, and my brother-in-law, Lakmal, for providing constant support and keeping me in good mood by taking care of everything back home on my behalf.

Most importantly, I have no word to express my gratitude to my loving wife, Saranga. Her continuous understanding, support, encouragement, patience and proof reading made

my life easy. Her love and care makes anywhere we live together called home. Nothing is possible without her dedication. Thank you for all of that!

Table of Contents

List of Figures

List of Tables

List of Abbreviations

ACK	Acknowledgement
BF	Beacon falsification
CR-BS	Cognitive base station
CC	Control channel
CCC	Common control channel
CINR	Channel to interference noise ratio
C-MAC	Cognitive medium access control
CPE	Consumer/customer premise equipment
CR	Cognitive radio
CRN	Cognitive radio network
CSI	Channel state information
CSS	Cooperative spectrum sensing
CTS	Clear to send
D2D	Device-to-device
DCC	Dedicated control channel
DCCC	Dynamic common control channel
DCCC-MAC	Dynamic common control channel-based MAC
DSA	Dynamic spectrum access
ECMA	European computer manufacture association

EM	Expectation maximization
FCC	Federal Communications Commission
FD	Full duplex
FDMA	Frequency division multiple access
GMM	Gaussian mixture model
GPS	Global position system
IEEE	Institute of Electrical and Electronic Engineers
ISM	Industrial Scientific and Medical
KNN	K-nearest neighbour
MAC	Medium access control
MBAN	Medical body area network
MIMO	Multiple input multiple output
ML	Maximum likelihood
NDCC	Non-dedicated control channel
OFDMA	Orthogonal frequency division multiple access
OSA	Opportunistic spectrum access
PU-BS	Primary base station
PR	Primary receiver
PT	Primary transmitter
PU	Primary user
PUEA	Primary user emulation attack
QoS	Quality of service
REM	Radio environmental map
RF	Radio frequency
RS	Relay station

ROC	Receiver operating characteristic
RTS	Request to send
SF	Spectral footprint
SPTF	Spectrum Task Force
SSDF	Spectrum sensing data falsification
SVM	support vector machine
TDMA	Time division multiple access
WLAN	Wireless local area network
WRAN	Wireless regional area network
w.r.t.	With respect to

List of Symbols

$a^{(l)}$	Label of l-th training energy vector
$\overline{a}$	Channel availability (idle/busy) vector corresponding to a training an energy vector
A	Indices of the dummy rows
B	Bandwidth
BCh_{req}	Current best number of subchannel requirement of users
$c_{n,k}$	Cost for assigning k-th subchannel to n-th user
$\mathbf{C}_{srt}$	Cost of sorted best $\mathcal{K}^*$ subchannels of each user
$\mathbf{Ch}_{req}$	Number of subchannels allocated to each user
D	Index matrix
$\mathbf{D}_0$	Index matrix which stores the indices of subchannels used in the previous iteration
F_{opt}	Availability of optimal solution
FCh_{sat}	Each user is satisfied with its required rate or not
$FDif$	Start of the SF difference based update
$FInit$	Availability of initial feasible upper bound
$h(m,n)$	Channel gain power between location m and m
L	Number of training samples for SVM
M	Total number of PUs
N	Total number of SUs in the cognitive network

$\overline{N}$	Number of SUs expected to cooperate for spectrum sensing
N_i	Number of SUs transmitting their sensing results to CR-BS in the i-th mini-slot
$\overline{N}_i$	Average number of SUs successfully transmitting sensing results in the i mini-slot
N_b	Minimum number of mini-slots required to send the sensing results from $\bar{N}$ SUs to CR-BS
$\overline{N}_{N_b}$	Number of SUs transmit their sensing results within N_b mini-slots or number of SUs participate for cooperative spectrum sensing or number of SUs scheduled for data transmission
$PL(.)$	Path loss
P_b	Probability that a PU is active in a given channel
$\{P_{n,k}\}$	Transmit power allocated on k-th subchannel to n-th user
P_s	Transmission probability of an SU within a mini-slot in the CCC selection phase if the SU has not successfully transmitted in the previous mini-slot
$\mathbf{S}$	Vector of the states of all PUs
$\mathbf{S}_k$	Vector of the states of all PUs on k-th channel
$S_{n,k}$	State of n-th PU's activity on k-th channel
SF	Current value of spectral footprint
SFB_{found}	Availability of new bound due to the increment of unsatisfied users' subchannel requirements
SFn	Collection of SFs of individual users
SFn_{best}	Collection of the current best SFs of individual users
SFn_{prev_best}	Collection of the best SFs before finding current SFn_{best}
SF_{best}	Current best spectral footprint
$\{SF_n\}$	Spectral footprint of n-th user
t	Number of times the algorithm executes

t_{D-ms}	Mini-slot duration in the data transmission phase
t_{IB}	Time to select the best idle channel based on individual sensing
$t_{I_{ccc}}$	Time required to inform the CCC to the SUs
t_{SSR}	Time duration to send sensing results to the Co-BS
t_{SSR-ms}	Mini-slot duration in the CCC selection phase
$t_{S_{ccc}}$	Time required to execute the CCC selection process based on SVM
t_{D-TS}	Time to transmit $Transmission\_Setup$ message
T_B	Time duration for the beaconing phase
T_D	Time duration for the data transmission phase
T_k	Number of times the k-th channel is sensed
T_S	Total time for spectrum sensing
T_{SCCC}	Time duration for the CCC selection phase
$\mathbf{T}$	Assignment-cost-table
$\mathbf{T}_0$	Previous assignment-cost-table
$\mathbf{U}$	Dual variables corresponding to the rows in $\mathbf{T}$
$\mathbf{V}$	Dual variables corresponding to the columns in $\mathbf{T}$
W	Maximum size of contention window
$\mathbf{w}$	Weighting vector
$\{X_{n,k}\}$	if k-th subchannel is assigned to the n-th user $\{X_{m,k}\} = 0$
$\mathbf{y}^{(l)}$	l-th training energy vector
$\overline{\mathbf{y}}$	Set of training energy vectors
α	Bandwidth weighting factor
α_k	Centroid of the cluster
β	Power weighting factor
$\mathcal{C}_k$	Set of training vectors in cluster k

δ_t	Slack variable
$\delta^{(l)}$	Slack variable, $l = 1, \ldots, L$
η	Noise spectral density
Γ	Number of SUs contending for channel access
Γ_{th}	Energy threshold
$\overline{\kappa}$	Average number of idle channels available for cognitive transmission
$\mathcal{K}$	Total number of channels available for sensing
$\{\mathcal{K}_n\}$	Number of subchannels assigned to n-th user
$\overline{\mathcal{K}}$	Number of channels sensed at a given frame
$\overline{\boldsymbol{\mathcal{K}}}$	Set of channels sensed
$\boldsymbol{\mathcal{K}}$	Set of channels available for sensing
$\nu_{m,n}$	Multi-path fading component
$\mathbf{P}_{\boldsymbol{\Theta}}$	Relative channel idle probability w.r.t. the CCC
$\phi(.)$	Mapping function
$\{\phi_n\}$	Minimum rate requirement of n-th user
$\psi_{m,n}$	Shadow fading component between location m and n
$\Phi(.)$	Multivariate Gaussian distribution
ω_n	Weight factor for the nth component of the energy vector
ω_k	Primary users' activity on k-th subchannel
ω_k	Threshold activity factor
τ	Sensing duration
w_0	Bias value used in the SVM to determine the classification hyperplane
ξ	Soft margin constant

Publications

- Book Chapters:

  1. K. M. Thilina, and E. Hossain, "Cognitive Radio Networks and Spectrum Sharing" book chapter in *Transmission Techniques for Digital Communications (Eds. Sarah Kate Wilson and Stephen Wilson)*, Elsevier - to appear

- Journal Publications:

  1. **K. M. Thilina**, E. Hossain, and D.I. Kim, "DCCC-MAC: A Dynamic Common Control Channel-Based MAC Protocol for Cognitive Radio Networks," *IEEE Transactions on Vehicular Technology*, to appear.
  2. **K.M. Thilina**, H. Tabassum, E. Hossain, and D.I. Kim, "Medium access control design for full duplex wireless systems: challenges and approaches," *IEEE Communications Magazine* , vol.53, no.5, pp.112,120, May 2015
  3. **K. Thilina**, E. Hossain, and M. Moghadari, "Cellular OFDMA Cognitive Radio Networks: Generalized Spectral Footprint Minimization," *IEEE Transactions on Vehicular Technology*, August 2014.
  4. **K. M. Thilina**, K. W. Choi, N. Saquib, and E. Hossain, "Machine Learning Techniques for Cooperative Spectrum Sensing in Cognitive Radio Networks," *IEEE Journal on Selected Areas in Communications*, vol. 31, no.11 pp. 2209–2221, November 2013.

5. **K. G. M. Thilina** and E. Hossain, "Optimal-Switching Adaptive Modulation for Multiuser Relay Networks with Feedback Delays," *IEEE Transactions on Wireless Communications*, vol 12, no. 8, pp. 3682–3695, August 2013.

- Conference Publications:

1. **K. M. Thilina**, M. Moghadari and E. Hossain, "Generalized Spectral Footprint Minimization for Multiuser Cognitive Radio Networks," in Proc. *IEEE Int. Conf. on Communication (ICC'13)* , Sydney, Australia, 10-14 June 2013.
2. **K. M. Thilina**, K. W. Choi, N. Saquib, and E. Hossain, "Pattern Classification Techniques for Cooperative Spectrum Sensing in Cognitive Radio Networks: SVM and W-KNN Approaches," in Proc. *IEEE Global Communications Conference (Globecom'12)*, Anaheim, California, USA, 2012.
3. **K. M. Thilina**, and E. Hossain, "Selective Relaying in Multi Relay Networks with Feedback Delays," in Proc. *IEEE ICC'12)*, Ottawa, Canada, 10-15 June 2012.
4. **K. M. Thilina** and E. Hossain, "Adaptive Modulation for Multiuser Amplify-and-Forward Relay Networks with Feedback Delays," in Proc. *IEEE Globecom'11*, Houston, TX, USA, 5-9 December 2011.

Chapter 1

Introduction

1.1 Introduction

With the advances of information and communication technologies and the development of world economy, there has been an explosive demand for wireless communication services. Specially, wireless internet access through the smart-phones, tablets, and laptops has become the primary means of personal communication. The wireless communication applications go beyond the personal communication services to perform sensing, monitoring (e.g., surveillance systems and embedded health monitoring systems), traffic controlling, and so on. This proliferation of wide range of wireless communication services is challenged by the scarcity of the radio spectrum since most of the available (and useful) radio spectrum have already been allocated by the regulatory communities for different services. The scarcity of the radio spectrum and exponential growth in the demand for wireless services have motivated researchers to develop new technologies for wireless and mobile communication to provide a ubiquitous, efficient, and seamless connectivity.

1.1.1 Basics of Cognitive Radio: Motivation and Definition

As has been just mentioned, most of the useful frequency bands have already been assigned to network operators as a large chunk of frequency spectrum by granting exclusive right to use for a long-term over vast geographical areas [7, 8]. Specially, under current allocation policies, a chunk of frequency spectrum is licensed to one operator for a given geographical location and a particular application while not allowing the transfer of the right to use that spectrum to other operators. These policies limit the flexibility of spectrum exploitation as they result in spectrum underutilization. Therefore, the traditional wireless communication systems have to utilize only the dedicated spectrum band irrespective of the traffic condition. Further, this long-term large chunk assignment limits the feasibility of short term small spectrum band licensing to meet temporary traffic demand. At the same time, the allocated spectrum may not be fully utilized when the number of users is small while prohibiting other users from accessing the spectrum. In addition, the unlicensed spectrum bands such as the Industrial Scientific and Medical (ISM) bands have become crowded. Thus, the ISM bands also have a limited bandwidth availability for new services. However, a study by the Spectrum Task Force (SPTF) of the FCC [8] has shown that a large portion of the licensed spectrum bands are partly or highly unoccupied in a given area at a given time. As a matter of fact, FCCs reference [9] states that the licensed spectrum utilization over the time and geographical location varies from 15% to 85%.

The problem of spectrum scarcity in presence of spectrum underutilization has motivated researchers to investigate new spectrum management paradigm for wireless communication systems. Mitola [10] proposed a novel idea for the opportunistic use of underutilized portion of the spectrum, while providing a solution to mitigate the spectrum scarcity problem. This proposed spectrum management paradigm creates a landscape for new wireless services using the novel device called “Cognitive Radio. A *cognitive radio (CR)* is an

intelligent wireless communication device, which senses its operational electromagnetic environment and can dynamically and autonomously adjust its radio operating parameters [10–12]. In this context, opportunistic spectrum access (OSA) is a key concept which allows a CR device to opportunistically access the frequency band allocated to a licensed user when the license user transmission is detected to be inactive. The licensed users' inactive spectrum bands are referred as "spectrum holes" or "white spaces". These spectrum holes or white spaces are formally defined as [13]: "a band of frequencies assigned to a primary user (license user), but, at a particular time and specific geographic location, the band is not being utilized by that user".

To achieve OSA by dynamically and autonomously adjusting its radio operation parameters, cognitive radios should have two main characteristics [1]: cognitive capability and reconfigurability. The cognitive capabilities of a CR device is defined as the ability to sense the surrounding radio environment, analyze the sensed information, and make the spectrum access decision based on the analyzed information. Reconfigurability is defined as the ability of a CR to change its operating parameters based on the information obtained from spectrum analysis on-the-fly. Such CRs, when interconnected together (either through a cognitive base staton (CBS) or directly in a peer-to-peer manner), form a cognitive radio network (CRN). In such a CRN, the available spectrum is allocated among the CRs efficiently by using a smart spectrum management system.

1.1.2 Challenges in Cognitive Radio Networks

Cognitive radios should be capable of meeting their operational requirements while avoiding harmful interference caused to the primary network (or primary users (PUs)). To access the unlicensed spectrum without causing harmful interference to the PUs, the CRs should be equipped with some additional (compared to traditional wireless devices) functionali-

ties such as spectrum sensing, learning, spectrum management and opportunistic spectrum access.

Spectrum Management

The unique challenge imposed on CRNs due to their coexistence with primary networks is mainly related to spectrum management functionalities such as spectrum sensing, analysing, sharing, and spectrum mobility. The spectrum-sensing mechanism in cognitive radios should find answers to the following issues: where to sense, what to sense, how to sense, how long to sense, allowable interference limits and so on. Once spectrum sensing is completed, a CR should take a decision by analyzing the sensed information. Then, the spectrum management system should find answers to the spectrum-sharing specific questions such as how to access and how to allocate PUs' idle bands. Nevertheless, the spectrum management system should release the spectrum band being used by the CRs upon reappearnace of a PU in that spectrum band. Also, the cognitive communication should be shifted to another band if there are idle spectrum bands available. At this point, solutions to the spectrum-mobility-specific issues such as how to stop CR transmission, where to shift and how to change configuration parameters are of significant importance for smooth operation. Optimizing spectrum management issues in such a way that mitigates PU interference while improving cognitive throughput is not an easy task.

Resource Allocation

The resource allocation scheme in a CRN is the entity which is responsible for avoiding harmful interference caused to the PUs while optimally utilizing the available resources (i.e., power and spectrum). For this, the resource allocation schemes need to consider the effect of PU activities in different bands. Therefore, the resource allocation schemes used

in legacy wireless networks are not suitable for CRNs. Also, different types of resource allocation methods will be required based on the CRN architecture (i.e., centralized or distributed CRN) or the type of operation mode of the CRN (e.g., overlay mode or underlay mode). While power control is a crucial component of resource allocation for CRNs operating in the underlay mode (i.e., mode in which PUs and CRs can access a spectrum band simultaneously), it is not that crucial in case of overlay mode (i.e., mode in which PUs and CRs do not access a spectrum band simultaneously).

Medium Access Control

The medium access control (MAC) is related to resource allocation. In the presence of multiple CRs, the MAC method is responsible for resource allocation among the CRs and coordinting the access of the CRs to the shared radio resources. In a centralized CRN (e.g., a cellular CRN), the MAC method is executed by the CBS in a centralized manner, while in a distributed CRN (e.g., an ad-hoc CRN), the CRs independently perform the MAC method. The MAC method should efficiently use the radio resources while limiting interference caused to the PUs. However, for efficient network operation, the siganling overhead of the MAC method should be low.

Security Issues

CRNs are susceptible to all traditional wireless network specific attacks [14, 15] such as radio frequency (RF) jamming (data and control channel) [16, 17], MAC address snooping [17], spurious MAC frame (e.g., RTS, CTS, ACK frames) transmission [17], eavesdropping [18] and cheating on contention (violating back off rules) [19]. In addition to these traditional attacks, CRNs undergo new security attacks due to the unique behaviour of cognitive radios. The main CRN-specific attacks are as follows: primary user emula-

tion attacks (PUEA) [20–22], spectrum sensing data falsification (SSDF) [23–25], beacon falsification (BF) [26, 27], and cross-layer attacks [28–30].

1.2 Research Goal

The research work presented in this dissertation is motivated by three important but unexplored problems in the literature as follows:

- Develop a novel cooperative spectrum sensing scheme that has following advantages over the traditional cooperative spectrum sensing (CSS) schemes:
  - Capable of implicitly learning the surrounding environment (e.g., the topology of the PU and the CR networks and the channel fading) in an online fashion. Hence, the developed techniques should be much more adaptive than the traditional CSS techniques, which need prior knowledge about the environment for optimization.
  - Develop techniques which can describe more optimized decision region on the feature space than the traditional cooperative spectrum techniques (e.g., OR/AND-rule-based and linear fusion techniques) yield.
- Design and analyze a novel cognitive MAC protocol to eliminate the requirement of a dedicated control channel. The proposed cognitive MAC protocol offers the following main advantages over the existing dedicated control channel based cognitive MAC protocols:
  - Remove the requirement of a dedicated control channel (either in-band or out-of-band) by selecting a dynamically changing control channel from the set of PUs' idle channels in a given time frame. This dynamic control channel selection from the unlicensed band paves the way to designing cost-effective CRNs.

  - Dedicated control channel-based cognitive MAC protocols are vulnerable to jamming. However, in the proposed MAC protocol, due to its dynamic behaviour, the jammers would not be able to detect the control channel easily for jamming.

- Propose and solve a novel resource allocation metric that capture the behaviour of CRNs while offering the following advantages:

  - Generalized resource allocation scheme that paves the way to utilize the available spectrum and power optimally and opportunistically depending on the network operators' objectives.
  - Save some spectrum while maintaining the cognitive network coverage and interference thresholds at PUs.

1.3 Research Contributions

In a nutshell, the research presented in this dissertation investigates the following three problems in CRNs: spectrum sensing, resource allocation, and medium access control. I propose and design cooperative spectrum sensing techniques that adapt to the environment condition in an online fashion, propose and solve a generalized spectral footprint minimization based resource allocation problem, and design dynamic common control channel-based medium access control protocol for cognitive radio networks by eliminating the requirement of a dedicated control channel. The contributions can be summarized as follows:

- **Learning-based cooperative spectrum sensing schemes:** I propose, develop and explore machine learning-based cooperative spectrum sensing (CSS) schemes for CRNs. The machine learning techniques are often used for pattern classification,

where a feature vector is extracted from a pattern and is fed into the classifier which categorizes the pattern into a certain class. In the context of CSS, I treat an "energy vector", each component of which is an energy level estimated at each CR device, as a feature vector. Then, the classifier categorizes the energy vector into one of two classes: the "channel available class" (corresponding to the case that no PU is active) and the "channel unavailable class" (corresponding to the case that at least one PU is active). Prior to online classification, the classifier has to go through a training phase where it learns from training feature vectors.

In this regard, in Chapter 3, I propose to use unsupervised learning approaches such as the K-means clustering and the Gaussian mixture model (GMM) for CSS based on the energy vector . The K-means clustering algorithm partitions the features into K clusters. Each cluster is mapped to either the channel available class or the channel unavailable class. On the other hand, in the GMM, I obtain a Gaussian mixture distribution from training feature vectors, where each Gaussian distribution in the mixture distribution corresponds to a cluster. Due to their higher prediction capability, I also propose to use supervised learning approaches such as the support vector machine (SVM) and the K-nearest neighbor (KNN) for CSS. In the SVM, the support vectors (i.e., a subset of training vectors which fully specify the decision function) are obtained by maximizing the margin between separating hyperplanes and feature vectors. Specially, the performance of each of the classification techniques is evaluated in terms of the training time, the classification delay, and the ROC curve. The effect of the number of the CR devices in cooperation is also quantified.

- **Dynamic common control channel-based MAC protocol:** In Chapter 4, I propose a dynamic common control channel-based MAC (DCCC-MAC) protocol for CRNs. To the best of my knowledge, this protocol would be the first cognitive MAC protocol

in the literature that utilizes a dynamically changing in-band common control channel for exchanging control information instead of dedicated control channel. Specifically, for a set of cooperating secondary users (SUs), the common control channel during a given frame is selected by employing a SVM-based learning technique. The one-dimensional decision values of the SVM are processed for selecting the control channel. As an incentive, the SUs who participate in the CCC selection process are prioritized during the data transmission phase.

The proposed DCCC-MAC protocol is capable of learning the surrounding environment cooperatively in an online fashion. Since the CCC is selected based on the learning decision, the proposed MAC protocol eliminates the requirement of dedicated control channel for control information exchange. Also, due to the dynamic nature of the CCC, the proposed DCCC-MAC protocol is able to withstand against control channel jamming problem. Specially, this MAC protocol mitigates not only the multichannel hidden terminal problem but also the PU hidden terminal problem due to the cooperative nature in PUs idle channel detection. Finally, for this proposed MAC protocol, I derive a closed-form expression for saturation throughput.

- **Generalized spectral footprint based resource allocation:** In Chapter 5, I propose a novel resource allocation method for downlink transissions in a CRN which is based on the generalized spectral footprint minimization problem. The main benefit of this method is two folded: a) paves the way to optimally and opportunistically utilize the available radio resources depending on the network operators objectives. b) instead of utilizing all the available bands for transmitting, the CRN can save some spectrum bands for other applications while satisfying its own requirements.

  The proposed resource allocation method assumes a multiuser orthogonal frequency-division multiple access (OFDMA)-based CRN. The generalized spectral footprint

minimization problem is formulated under the required rate, interference, total power and sensitivity constraints. The formulated optimization problem is a non-convex mixed-integer programming problem. Therefore, I solve this optimization problem by dividing the original problem into a subchannel allocation master problem and a power allocation subproblem. Specially, I propose a lower-complexity modified Hungarian-based subchannel assignment algorithm by exploiting the local information in the available subchannel assignment cost-table, which is used for subchannel assignment. Moreover, the optimality of the proposed modified Hungarian-based subchannel allocation algorithm is proved. The power allocation subproblem is solved by adopting Lagrangian based approach. In particular, to provide insights into the system behaviour, I derive a closed-form expression for the number of subchannels required to satisfy a given QoS requirement when there is a single user in the network.

1.4 Organization of the Thesis

In Chapter 2, I present a high level overview on cognitive radio networks, different aspects of spectrum management and medium access control protocols. In Chapter 3, I present machine learning-based cooperative spectrum sensing techniques for CRNs. Chapter 4 presents novel dynamic common control channel-based medium access protocol for cellular CRNs. In Chapter 5, I present generalized spectral footprint-based downlink resource allocation scheme for multiuser multichannel cognitive radio networks. Finally, Chapter 6 summarizes the milestones achieved in this study and future research directions.

Chapter 2

Overview on Cognitive Radio Networks

In CRNs, dynamic spectrum access (DSA) is a key concept, which allows a cognitive radio (secondary user) to opportunistically access the frequency band allocated to a licensed (primary) user when the primary user transmission is detected to be absent in a given geographical area (spectrum overlay paradigm). Further, in CRNs, secondary users (SUs) can use the licensed spectrum if and only if they guarantee no harmful interference to primary user networks (spectrum underlay paradigm). Inefficient utilization of the available spectrum and power can degrade the performance of both the secondary (or cognitive) and the primary networks.

In DSA, to avoid the harmful interference at primary receivers and optimally utilize the available PUs' idle spectrum bands, the CRN should have an effective and efficient spectrum management framework and a MAC protocol. The cognitive spectrum management framework is responsible for addressing main challenges in spectrum management such as spectrum sensing, spectrum decision, spectrum sharing and spectrum mobility [1], whereas the cognitive MAC protocol is responsible for optimizing spectrum sensing and the spectrum access decision, controlling SU access in multichannel networks, allocating spectrum to CRs and scheduling data transmission and supporting spectrum trading func-

Table 2.1: Application specific standards

Application Scenario	Standards	Use case
Wireless Regional Area Networks (WRANs) using TV white space	IEEE 802.22	The fallow TV spectrum is used by networks (WRAN) centralized CRNs [26, 27, 33]
Local area applications within buildings	European Computer Manufacture Association (ECMA)-392	Personal and portable devices for exploiting TV white space [34]
Wi-Fi using spectrum holes in TV bands	IEEE 802.11af	IEEE 802.11 protocol stack is modified (i.e. PHY and MAC layers) to meet the channel access and coexistence with other CRNs in the spectrum holes in TV bands [35].
Medical Body Area Networks (MBAN)	IEEE 802.15.4j	Allowed to access 2.36GHz-2.4GHz band on cognitive basis for MBAN [36, 37]
Public Safety (FirstNEt)	3GPP (LTE)	Provide spectrum with priority to public safety network in addition to the licensed bands [38, 39]

tionalities [31].

2.1 Regulatory Aspects and Standardization

As any other wireless network, CRNs also require a standardization process to successfully develop and implement them in practice. Therefore, researchers and industry practitioners got together and formed groups (i.e. IEEE 802.18, 19, 21, 22 and so on) to standardize and regulate cognitive radio-specific activities. IEEE 802.18 is a regulatory and advisory board which is responsible for participating and monitoring radio regulatory activities in different projects such as IEEE 802.11, IEEE 802.15, IEEE 802.16 and etc. These communities have made significant efforts toward the standardization of cognitive radio networks by incorporating dynamic spectrum access technologies for different application. Some of the application specific standards are listed in Table 2.1 [32].

2.2 Cognitive Radio Network Architectures

A cognitive radio network (referred to as secondary network, unlicensed network, or dynamic spectrum access network) coexists with primary networks (also referred to as li-

censed networks) within the same geographical area, at the same time and utilize the same frequency bands. The CRs in CRNs are not licensed to operate in the spectrum band. Only the primary networks are licensed to operate, and they serve primary users who have the right to access the spectrum band licensed for use. The primary network can be classified as either a centralized (infrastructure-based) network or a distributed (or ad-hoc) network. Similarly, based on the network architecture, the cognitive radio network can also be classified as either a centralized or a distributed network. Generally, the PUs and the primary base stations (PBS) do not have the cognitive radio capabilities. Hence, it is the responsibility of cognitive users to sense the channel before cognitive transmission and vacate immediately after the appearance of primary users.

2.2.1 Centralized Cognitive Radio Networks

Centralized CRNs [1,11,42] are infrastructure-based CRNs which have a central controller or coordinator (see Fig. **??**), e.g., a CBS or a central access point. This central controller collects spectrum information from cognitive users over a licensed or unlicensed spectrum band (i.e., control channel), analyzes and makes information about spectrum availability (e.g., channels where PUs are absent) known to cognitive users via control channels. However, the information collection and exchange process between secondary users (SUs) incur additional significant signalling overhead with an increasing number of SUs. Apart from cognitive functionalities, a cognitive base station performs resource (e.g., channel and power) allocation for cognitive (or secondary) users. The IEEE 802.22 is the first worldwide standard to follow a centralized scheme and the IEEE 802.22 standard defines the specification for centralized cognitive communication networks [43].

2.2.2 Distributed Cognitive Radio Networks

Distributed CRNs [1, 11, 42] are ad-hoc or point-to-point communication systems where SUs communicate over licensed or unlicensed bands opportunistically as shown in Fig. **??**. These distributed CRNs do not have a central controller to coordinate opportunistic spectrum access and spectrum access decisions are jointly coordinated via a common control channel (CCC) [44]. Hence, the signalling overhead in distributed CRNs is considerably small compared to centralized CRNs even with a larger number of SUs. However, the spectrum access decision taken by distributed CRNs based on local information may not be optimal.

2.2.3 CR Operational Models

All the CRs in either centralized or distributed CRNs can use either of the following operational modes [11, 45]: underlay, overlay, and interweave (see Fig. 2.1). In the underlay model, the CRs allow concurrent transmission with primary users. Such CRNs protect the PUs by enforcing a spectral mask in such a way that guarantees the interference experienced at the PUs is below the acceptable noise floor. Overlay (e.g., relay-assisted) systems assist primary transmission and may utilize a small portion of the primary band for cognitive transmissions as an incentive. The interweave approach-based CRNs are derived from J. Mitolas doctoral thesis [10]. In such networks, CRs access the unlicensed band opportunistically when PU activity is not detected on the sensed spectrum bands.

2.2.4 Spectrum Access Model

Generally speaking, the so-called underlay, overlay, and interweave modes of CR operations use different forms of dynamic spectrum access (DSA) models. The DSA models in CRNs can be typically categorized into three access models as follows [31, 46, 47]: spec-

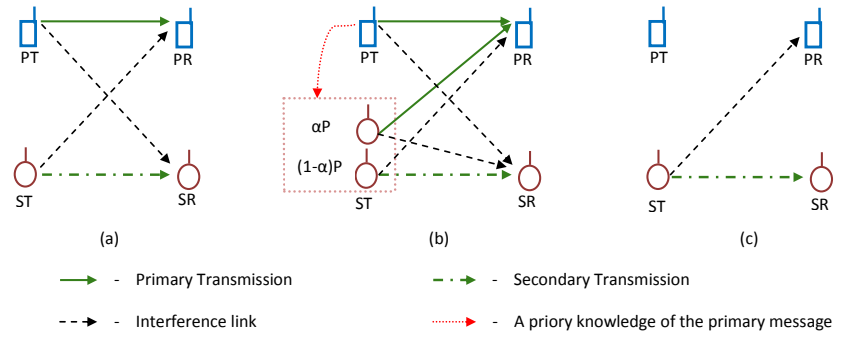

Figure 2.1: Cognitive radio operational models. a) Underlay operation b) Overlay operation c) Interweave operation.

trum exclusive-use model, spectrum shared-use model, and spectrum common-use model. In the spectrum exclusive-use model, when the licensed users do not use the bands, the spectrum licensee grants the spectrum access right to the CRs (i.e. overlay mode) under some constraints. In the spectrum shared-use model, the CRs (i.e., underlay, overlay, and interweave mode) are allowed to access the spectrum simultaneously with PUs as long as CRs do not create harmful interference at primary receivers. In the common-use model, all the CRs have same right to access the spectrum and this spectrum is not licensed to any party (i.e., unlicensed spectrum bands such as the industrial, scientific, and medical [ISM] bands).

2.3 Spectrum Management Framework

The number of accessible channels available in traditional wireless networks is fixed whereas the number of channels available for cognitive transmission rapidly varies with time and space. The number of channels available for cognitive transmission changes with the appearance of a primary user since the the spectrum band is licensed to PUs. This rapidly-fluctuating nature of available spectrum imposes unique challenges in cognitive ra-

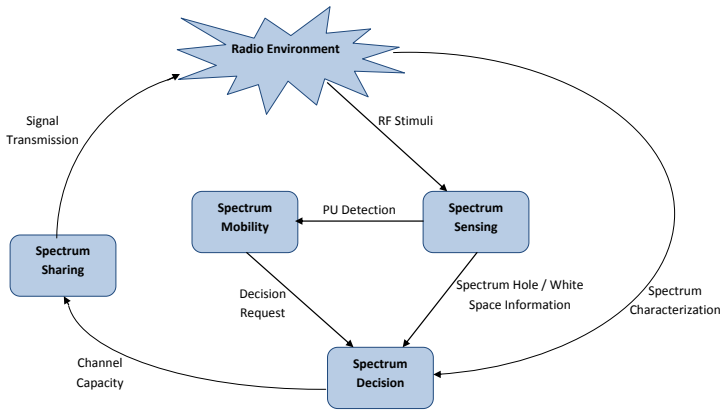

Figure 2.2: Spectrum management framework in CRNs [1].

dio spectrum management system such as interference avoidance, QoS provisioning, and seamless cognitive communication. In order to address these challenges, the CRNs should determine which portions of the spectrum bands are available for cognitive transmission, select the best channel to achieve required QoS, coordinate access to mitigate interference and collision, and vacate the channel upon the appearance of PUs. These capabilities are achieved by cognitive radio networks through four different spectrum management functionalities: spectrum sensing, spectrum decision, spectrum sharing, and spectrum mobility [1]. The relationship between the spectrum management functionalities are illustrated in Fig. 2.2.

2.3.1 Spectrum Sensing

Spectrum sensing is a process (which is implemented in CRs) for obtaining radio or spectrum information at a given time and a given location. The radio information obtained through spectrum sensing focuses on the following: obtaining PU-idle channels, calculate the interference experienced by the PUs, learning the PU traffic condition to enhance CRN operation, and estimating the channel gains between cognitive radios. The CRN makes

spectrum access and sharing decisions based on the data provided by sensing process. Therefore, the sensing data should be highly reliable and up-to-date for smooth operation of primary and cognitive networks. To achieve the above goals, the spectrum sensing mechanism should deal with the following issues [1, 32, 48]: when to sense [49], What and how to detect [50, 50–54], where to sense [55], how to sense [56–58] and how long to sense [50, 51, 59–61]

2.3.2 Spectrum Decision

Spectrum decision making in CRNs refers to the ability to select the best PU idle bands to satisfy the QoS requirements of CRs without causing harmful interference to primary users. In order to satisfy CRs' QoS requirements under CRN-specific constraints, at first the decision process characterizes each PU idle spectrum band, which is informed by the spectrum sensing, based on the local observation and statistical information of the primary networks such as primary user activity [62]. Then, the most suitable bands which satisfy these QoS requirements are selected based on spectrum characterization. Once the most appropriate bands for cognitive transmission are identified, the spectrum decision process reconfigures its transceiver parameters to support cognitive transmission on the selected bands. The spectrum decision flow is illustrated in Fig. 2.3 and the main questions to be answered in performing these functionalities are as follows [63]: How to characterize available spectrum bands? How to select the best PUs idle band to satisfy CRs QoS? and What is the best technique to reconfigure cognitive transceivers for the bands selected?

2.3.3 Spectrum Sharing

The spectrum sharing functionality in CRNs is responsible for satisfying the QoS requirements of CRs and avoiding/mitigating harmful interference caused to the PUs through the

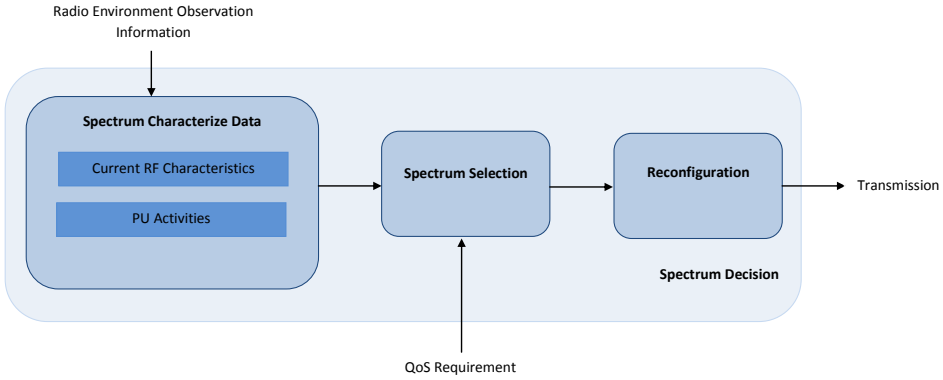

Figure 2.3: Spectrum decision flow.

CRN architecture, spectrum allocation and spectrum access mechanism. From spectrum-management perceptive, the quality and reliability of spectrum sharing depends on how the network information is exploited by the spectrum sensing and decision processes. The required information for spectrum sharing is exchanged through a control channel. The coordination in cognitive spectrum sharing is implemented by using cognitive MAC protocols. The folowing issues are important in the context of spectrum sharing in CRNs: network architecture, spectrum allocation and spectrum access mechanism.

- **Architecture-based spectrum sharing:** The network architecture-based spectrum sharing approaches in CRNs can be classified as centralized and distributed spectrum sharing. In centralized spectrum sharing, spectrum allocation and access are controlled by a central controller [64–66] whereas the spectrum allocation and spectrum access in distributed CNRs are performed by each CR [65, 67]. The control information in centralized spectrum sharing process is exchanged with the help of a dedicated common control channel or a dynamic common control channel [68]. Hence, the centralized spectrum sharing achieves comparatively higher performance over distributed sharing at a cost of higher information exchange and complexity.

- **How to allocate spectrum:** The spectrum allocation process is the fundamental

component in spectrum sharing and it is responsible for allocating the best frequency band and bandwidth in such a way that achieves CRs' QoS requirements while avoiding or mitigating harmful interference at the PUs. This spectrum allocation process can be classified as either cooperative [69] or non-cooperative [70] spectrum allocation. The cooperative spectrum sharing can achieve high performance compared to non-cooperation by introducing cooperation among all the active CRs and/or cooperation with primary networks. For cooperative spectrum sharing, game theory-based approaches, such as bargaining [71] and coalitional [72] games can be used. In non-cooperative spectrum sharing, CRs do not collaborate with each other and they try to maximize their performance as much as possible in a selfish manner.

- **How to perform multiple access:** This is the key spectrum sharing function. Once frequency bands (channels) are allocated to CRs, the CRs should know or should be informed about how to access the shared wireless spectrum in such a way that mitigates or avoids interference among CRs. The spectrum access technologies utilized in traditional wireless networks (i.e., CDMA, OFDMA, TDMA, FDMA and SDMA) can be used in CRNs. Orthogonal frequency-division multiple access (OFDMA) access technology is a very good candidate for CRNs due to its capability of altering waveform and flexibility in bandwidth allocation as well as immunity to frequency-selective fading.

2.3.4 Spectrum Mobility

The objective of spectrum mobility in a CRN is to maintain an ongoing cognitive transmission by seamlessly switching between PU idle channels upon appearance of PUs in the network, or due to low channel quality due to CRs' mobility [73]. This functionality can be divided into two subfunctions: spectrum handoff and connection management. The spec-

trum handoff process is responsible for switching an ongoing transmission from one channel to another PU idle channel, whereas the connection management process is responsible for adapting or reconfiguring switching parameters in the protocol stack. Compared to the traditional wireless systems, in CRNs, due the primary users' activity, spectrum mobility introduces a new set of challenges.

2.4 Spectrum Sensing Techniques

For OSA, there are two basic approaches for identifying spectrum opportunities in licensed bands: database-centric approach and spectrum sensing approach. In the database-centric approach, the information about spectrum opportunities are exchanged through a central database. It requires an essential modification for the existing wireless protocols for updating its spectrum utilization in a central database. Hence, database-centric approach suffers from high infrastructure cost as well from a limitation in the opportunistic spectrum access ability. On the other hand, the spectrum sensing-based approach requires sensing the unlicensed spectrum and accessing the spectrum opportunistically when an idle channel is found. As a result, this approach does not require any modification to the existing traditional wireless infrastructure. Spectrum sensing enables CRNs to opportunistically access the spectrum by adopting non-cooperative or cooperative spectrum sensing-based detection scheme.

2.4.1 Non-Cooperative Spectrum Sensing

The techniques for detecting spectrum holes by a CR can be classified as either blind detection [74] or feature detection [74, 75]. Blind detection in CRNs characterizes the available spectrum holes or PU idle channels without having any prior knowledge of primary transmission. The main drawback of blind detection techniques is that they cannot differentiate

a PU-transmitted signal from a CR-transmitted signal. Energy detection, autocorrelation detection, and higher-order-static detection are some of the well-known blind detection techniques studied for CRNs. The feature detection technique utilizes prior knowledge of the primary transmission to detect spectrum holes while differentiating PU signals from CR signals. Matched filter and cyclostationary detection are examples of feature detection techniques.

Energy Detection

The energy detection technique simply detects spectrum holes or PU idle channels based on the sensed energy at the receiver [76, 77]. To perform energy detection, CRs need to estimate the energy level for a time duration. Let τ_s be the spectrum sensing duration. If we denote the bandwidth by B, the energy detector takes $B\tau_s$ baseband complex signal samples during τ_s. Let $Z_n(i)$ denote the ith signal sample taken by SU n, $1 \leq n \leq N$, where N is the number of SUs in the CRN. The signal samples consist of the summation of the signals from all PUs in the active state and the thermal noise. That is,

$$Z_n(i) = \sum_{m=1}^{M} h_{m,n} X_m(i) + N_n(i), \tag{2.1}$$

where $h_{m,n}$ denotes the channel gain from m-th PU to n-th CR , $X_m(i)$ is the signal transmitted by m-th PU, $N_n(i)$ is the thermal noise at n-th CR and M is the number of PUs in the network. The energy detector of CR n estimates the energy level normalized by the noise spectral density, which is denoted by Y_n, from the signal samples as

$$Y_n = \frac{2}{\eta} \sum_{i=1}^{B\tau_s} |Z_n(i)|^2, \tag{2.2}$$

where $\eta = \mathrm{E}[|N_n(i)|^2]$ is the noise spectral density. The output of the n-th CR's energy detector, Y_n, is compared with the energy threshold Γ_{th} and the spectrum availability decision is made as follows:

$$A_n = \begin{cases} 1, & \text{if } Y_n \geq \Gamma_{th} \\ -1, & \text{otherwise.} \end{cases} \tag{2.3}$$

If $A_n = 1$ (i.e., at least one PU is active), the channel is considered unavailable for the CR network to access. The channel is available only when there is no PU in the active state (i.e., $A_n = -1$).

Cyclostationary Feature Detector

A cyclostationary feature detector exploits the inherent periodicity of PU-modulated signals for detecting spectrum holes. Specifically, a process is said to be wide-sense stationary if its mean and autocorrelation function are time independent and it becomes cyclic stationary if it shows wide-sense stationary behaviour periodically. This is the feature that a cyclostationary feature detector exploits in the process of PU idle channel detection. The periodicity property of PUs' modulated signals and the wide-sense stationarity property of uncorrelated noise makes it possible for the decoder to easily differentiate noise from the PUs signal. Therefore, the detector calculates the cyclic spectral density or cyclic periodogram of a received signal as follows [75]:

$$S(f, \alpha) = \sum_{\tau=-\infty}^{\infty} R_Z^{\alpha}(\tau) e^{-j2\pi f \tau}, \tag{2.4}$$

where α is the cyclic frequency or frequency separation and $R_Z^{\alpha}(\tau)$ is the cyclic autocorrelation function of the received signal. The $R_Z^{\alpha}(\tau)$ can be expressed as

$$R_Z^{\alpha}(\tau) = \mathrm{E}[Z(t+\tau)Z^*(t-\tau)e^{j2\pi f\tau}]. \tag{2.5}$$

The cyclic spectral density function of the received signal given in (2.4) yields peaks when the cyclic frequency is equal to the fundamental frequency when the PUs transmit on that channel. Hence, the presence of PUs on a given channel can be detected by identifying peaks at fundamental frequency.

2.4.2 Cooperative Spectrum Sensing

The individual or non-cooperative spectrum sensing-based detection is highly vulnerable to uncertainties, channel fading, shadowing, and hidden terminal problem. It is possible for CRs to cooperate in order to achieve a higher sensing reliability than an individual CR does by mitigating the hidden PU problem that arises because of shadowing and multipath fading [74]. Cooperative spectrum sensing (CSS) schemes can be classified as either centralized or distributed CSS. The CSS techniques offer better accuracy in the detection of spectrum holes by exploiting the diversity gain provided by different CRs; however, at the cost of increased signalling/traffic overhead and increased complexity [76]. The required information in CSS is exchanged through a common control channel (CCC) which lies either in the licensed band or unlicensed band such as the ISM band. The level of signalling/traffic overhead in the CCC varies based on the type of the information exchange, i.e., some CSS algorithms require one bit decision from cooperating CRs whereas other CSS algorithms require multiple bits for the sensed information from cooperating CRs.

2.4.3 Fusion Techniques for Cooperative Spectrum Sensing

In cooperative spectrum sensing, individual sensing results are reported to a fusion centre to combine the sensing results. The commonly studied spectrum sensing fusing techniques are as follows: hard fusion, soft fusion, softened fusion, and learning-based fusion techniques. In the case of hard fusion, the CRs report only one-bit information to the fusion centre, which indicate whether the sensed spectrum result is above a particular threshold or not. For example, the AND-rule, the OR-rule and the M-out-of-N rule are commonly used for hard fusion-based cooperative spectrum sensing [78, 79]. In the soft fusion algorithms, the exact sensing results are reported to the fusion centre which then combines the individual sensing results using equal gain combining or maximum ratio combining techniques in such a way that yields PU detection decision [80, 81]. In learning-based fusion, the fusion centre adopts machine-learning techniques for fusing sensing information. Specifically, the learning-based fusion outperforms the affirmation fusion techniques due to its higher predictive power and adaptability to the environmental changes on-the-fly [54, 82].

Learning-based CSS can be classified as supervised and unsupervised learning-based CSS. Some of the learning-based fusion techniques used in the pattern recognition literature are K-nearest neighbour (KNN) and support vector machine (SVM) fusing whereas K-mean clustering and Gaussian mixture model (GMM) are examples for unsupervised learning based fusion. In learning-based fusion, prior to the online PU idle channel detection, the classifier has to go through a training phase where it learns from the CSS-based training results. Specifically, for the supervised learning techniques, the training results should be fed to the classifier with its label (i.e., $a^{(l)} = 1$ if l-th training sample for the PU active case, otherwise $a^{(l)} = -1$), whereas unsupervised learning does not need labels for its training samples. The main advantages of learning-based fusion over the traditional soft, hard, and softened fusions are as follows:

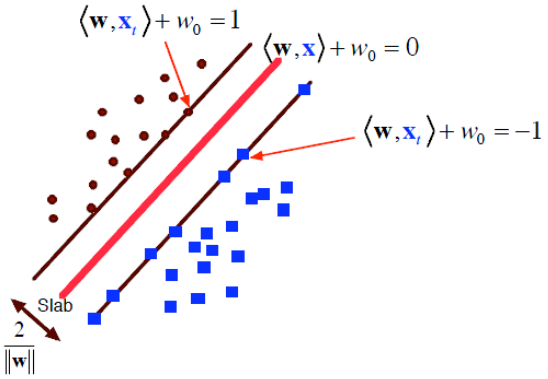

Figure 2.4: Perfectly separable hyperplane for two class training data, where $\mathbf{w}$ is the weighting vector and w_0 is the bias.

1. Learning based fusing techniques implicitly learns its radio environmental parameters (e.g., PU and CR network topology and channel gains) in an online fashion. Therefore, learning-based techniques are much more adaptive to environmental changes than the traditional fusion techniques.

2. Learning techniques obtain a more optimized decision region on spectrum sensing results than the traditional techniques can, by yielding better detection performance.

2.4.4 Pattern Classification Techniques for Cooperative Spectrum Sensing

Pattern recognition techniques such as the Support Vector Machine (SVM) and K-Nearest-Neighbor (KNN) techniques can be used for PU detection in CRNs.

Support Vector Machine (SVM) Approach

The SVM is a pattern classification method introduced in 1992 by Vapnik [83]. This approach is widely used in bioinformatics and image processing due to its higher accuracy and ability to deal with higher dimensional data.

The SVM classification involves in two main phases, namely, SVM training phase and

testing phase. In the training phase, the set of training data with the class label (target value) and the feature set (attributes or observed values) is fed into the classifier for classification. In this phase, we find optimal separating hyper plane that separates training data optimally into different classes. This is illustrated in Fig. 2.4 for a perfectly separable two class training data set.

For a given set of training data pairs $(\mathbf{x}_t, y_t)$, $t = 1, ..., N$ where $\mathbf{x}_t \in \mathbf{R}^N$ and $y_t \in \{-1, 1\}$, the SVM requires the solution of the following convex optimization problem [83]:

$$\text{Subject to} \begin{cases} \min \ \frac{1}{2}||\mathbf{w}||^2 + C\sum_{k=1}^{M} \delta_t \\ y_t[\mathbf{w}\phi(\mathbf{x}_t) + \ w_0] \geq 1 - \delta_t, \\ \delta_t \geq 0, \quad t = 1, 2, ..., M, \end{cases} \tag{2.6}$$

where $\mathbf{w}$ is the weighting vector, w_0 is the bias and δ_t is the slack variable, $\delta_t \geq 0$. $\phi(.)$ is the mapping function used to map training data into a linearly separable higher dimension and C is the penalty factor for error terms. Then, the optimization problem is solved by following the same procedure in [83] to obtain the support vectors α_t. Once we have obtained the support vectors, we can classify the test sample as follows [83]:

$$y(\mathbf{x}) = \text{sgn}\Big(\sum_{t}^{M} \alpha_t \ y_t \ K(\mathbf{x}, \mathbf{x}_t) + \ w_0\Big), \tag{2.7}$$

where $K(\mathbf{x}, \mathbf{x}_t) = \langle \phi(\mathbf{x})^T \phi(\mathbf{x}_t) \rangle$ which is known as the kernel function.

K-Nearest Neighbors (KNN) Approach

The KNN approach is a simple classification technique based on the majority voting of the neighbors. The neighbors are training points previously loaded into the KNN classifier in

the training phase. In the testing phase, the KNN classifier determines the distance between the test data and each training data. Then sort them in ascending order based on the distance between the test and the training data. Then count the label of the first K entries and assign the most frequent label to the test data [84].

2.4.5 Database Centric Approach for Spectrum Sensing

In the database-centric approach, the CRs acquire information about radio environment from a central database. Therefore, the CRs do not need the spectrum-sensing capability However, implementing an up-to-date and highly reliable central database for all geological locations is a daunting task. Therefore, researchers proposed an information grid-based approach to update the central database and calculate spectrum specific information for other locations based on the information obtained through the grid points. Furthermore, researchers proposed a combined approach for improving sensing performance by means of radio environmental maps (REM) [85–87]. The REM makes it possible to combine the spectrum-sensing system with the database centric approach by providing different mechanisms and algorithms to collect, process, store and retrieve different field measurements.

2.5 Resource Allocation in CRNs

In the literature, extensive research has been carried out to allocate resources for conventional wireless networks. However, those approaches cannot be directly applied to resource allocation in cognitive radio networks due to the added limitations such as mutual interference among PUs and CRs and imperfect spectrum sensing. In this context, inefficient utilization of the available spectrum and other wireless resources in CRNs degrade not only the performance of CRNs but also the performance of primary networks. Therefore, in order to optimize the performance of both networks, it is very important to manage the

mutual interference between CRs and avoid harmful interference at PUs. Hence, an efficient resource allocation algorithm should jointly consider the above aspects with spectrum management aspects [2, 4, 88–92].

2.5.1 Elements of Resource Allocation Problems in CRNs.

The main elements of resource allocation in CRNs are as follows:

- **Power allocation:** Efficient power allocation is a key problem in CRNs. The power allocation schemes which have been developed for traditional wireless networks cannot be used in CRNs due to the requirement that interference caused to the PUs has to be below a target threshold (i.e., acceptable interference limit).

- **Channel allocation:** Unlike those in traditional wireless networks, the channel allocation algorithms in CRNs are very tightly related to the PUs' channel activities on the considered channels. For channel allocation, the QoS requirements of the CRs as well as the interference constraints for the PUs need to be considered.

- **User scheduling:** An intelligent scheduling scheme in CRNs should select the best set of CRs at every time slot to maximize system throughput or achieve fairness among CRs. Therefore, the CR scheduling decision should be made by considering the CRs' channel conditions and their QoS requirements.

- **Quality-of-service (QoS):** Like other wireless networks, a CRN also needs to satisfy its users' QoS requirements (e.g., guarantee the minimum rate requirement, maximum packet error rate).

- **Fairness:** Fairness in CRNs can be defined as how equally the available resources are distributed among the CRs in the network. CRNs achieve fairness in terms of

different ways such as bandwidth fairness (equal number of spectrum to all CRs), power fairness (equal portion of power from the total budget in downlink transmission), or rate fairness (allocate resources in such a way that all the CRs can achieve same rate).

2.5.2 Resource Allocation Approaches in Cognitive Radio Networks

The general resource allocation problems for CRNs are shown in Table 2.2. The applicability of the input parameters, constraints and objective functions in resource allocation optimization problem is based on the cognitive radio network architecture, communication protocols, and transmission scenario (downlink/uplink transmission).

The input parameters and the constraints for resource allocation problem are generally set by the network operators or regulatory authorities. As an example, the number of CRs admitted to the CRNs is set by the network operators whereas the interference thresholds at the PUs are set by the regulatory authorities. The interference threshold levels allowed for underlay and overlay operational modes are not same and interference threshold for underlay operation is less than overlay operation due to the simultaneous opportunistic access in CRs in underlay operation. For resource allocation, perfect channel state information (CSI) at CRs is an important parameter and most of the resource allocation algorithms assume that perfect CSI information is available at CRs. However, in practical scenarios, this is not the case.

Optimization Objectives in CRNs

The objective functions in the CRNs can be mainly classified into three major categories such as minimization, maximization and fairness as illustrated in Table 2.2. In wireless communication systems, there is always a requirement to allocate the radio resources (i.e.,

Table 2.2: General resource optimization problems for CRNs [4]

Inputs/Given (any combination)	Number of CRs in CRN/cluster/cooperate Number of channel or spectrum bands sensed Number of PUs Number of relays Interference thresholds at PUs CSI, geographic location of PUs and SUs Protocol and the protocol-specific parameters CRN-specific custom inputs
Find/Decision variable (any combination)	Transmit power (CRs/CBS/relays) Allocation/assignment of spectrum bands (channels) and bandwidth User selection and scheduling Assignment/selection of relays CRN-specific custom decision variables
Constraints (any combination)	CBS/CR/cognitive relay specific power constraint Interference constraint at PUs Channel/bandwidth assignment constraint Relay selection/assignment constraint Fairness constraint Rate/delay constraint - QoS constraints Receiver sensitivity constraint CRN specific topology constraint Outage constraint Revenue specific constraint CRN-specific custom constraint
Objectives (any combination)	Minimize: Transmit power at CBS in downlink Per-CR transmit power in uplink transmission Generalized spectral footprints in CRNs (proposed in chapter 5) Outage probability of CRs, interference outage at PUs Bit-error rate in cognitive transmission End-to-end transmission delay Maximize: Sum rate in CRNs, weighted Sum rate in CRNs Energy efficiency in CRNs Utility in CRNs Max-min: Worst CRs capacity/SNR/utility Max/Min: CRN specific custom objectives

spectrum and power) in a way that satisfies the QoS requirements of the users by using minimum amount of resources. This is also required for CRNs. However, at the same time, harmful interference at the PUs also needs to be avoided [93]. The different optimization objectives are as follows:

Power minimization: For *downlink* transmission, the power minimization objective intends to mitigate harmful interference at the PUs while satisfying the QoS requirements for the CRs. The power minimization objective function for downlink transmission in a CRN can be expressed as follows:

$$\min_{X_{m,k},P_{m,k}} \sum_{m=1}^{\mathcal{M}} \sum_{k=1}^{\mathcal{K}} X_{m,k} P_{m,k} \tag{2.8}$$

The objective function in (2.8) shows the summation of total power allocated to all the PU idle subchannels. The iterative waterfilling algorithm [90] and Lagrangian-based dual decomposition algorithms are commonly used for solving power minimization optimization problems [94].

For *uplink* cognitive transmission, the power minimization objective has two different aims as follows: mitigate interference at the PUs and save battery power in the CR devices. An optimization problem with power minimization objective function utilizes as much bandwidth as possible to minimize power allocation to subchannels while satisfying cognitive transmission-specific constraints. The corresponding resource allocation scheme is generally known as a margin adaptive allocation scheme since it allocates power to subchannels until the QoS requirements of the CRs are satisfied [93].

Rate maximization: The optimization problems in CRNs with the objective of sum-rate maximization aims to maximize the total system throughput in CRNs under the interference (i.e., interference at the PUs) and total power constraints [95]. In the literature, this type of problems is known as rate-adaptive optimization problems. The sum-rate

maximization objective that maximizes the spectral efficiency in CRNs can be written as follows:

$$\max_{X_{m,k},P_{m,k}} R_T = \sum_{m=1}^{\mathcal{M}} \sum_{k=1}^{\mathcal{K}} X_{m,k} B \log\left(1 + \frac{P_{m,k} h_{m,k}}{\eta + \sum_{p\in\mathcal{P}} I_{p,m,k}}\right). \tag{2.9}$$

It is important to note that the sum-rate maximization problems in CRNs may not guarantee the satisfaction of individual CR's minimum rate requirement.

Utility maximization: Utility maximization-based resource allocation can consider both efficiency and fairness in resource allocation. Due to the high flexibility in defining a utility function, CRNs exploit the flexibility of defining utility function in such a way that can accomplish the unique requirements in CRNs. The utility functions, which are logarithmic, always guarantee both increment and marginal decrement by ensuring the fairness, concavity, optimality and uniqueness of the optimal solution [96]. However, selecting an appropriate logarithmic utility function to satisfy efficiency and fairness in CRNs is challenging and the utility function changes from application to application. Game theory is a very good tool for solving CRN-based utility optimization problem due to the capability of rational resource allocation among the CRs [97–100].

2.6 Medium Access Control for Cognitive Radio Networks

Cognitive MAC protocols should adopt a mechanism for exploiting the unlicensed spectrum to allow peaceful coexistence of CRs with the licensed users. Such a cognitive MAC protocol should achieve a higher overall spectrum efficiency by detecting all possible spectrum opportunities, spectrum sharing and accessing through adaptable control. The main functional requirements for a cognitive MAC protocol are as follows:

- **Interference avoidance and mitigation:** The MAC protocol is the entity that is

responsible for dynamic spectrum access based on the spectrum sensing information or up-to-date spectrum information in databases so that the collision with PUs and CRs is minimized. The transmission of the coexisting CRs in a spectrum band, which is licensed to the primary users, should not be harmful to the operation of primary networks.

- **Spectrum sharing:** The spectrum sharing strategies, which are implemented in cognitive MAC protocols, are responsible for choosing an optimal set of spectrum bands and transmission parameters to maximize the overall performance in CRNs while avoiding harmful interference at PUs.

- **Control signalling mechanism:** A reliable and secure control signalling mechanism has to be implemented in a cognitive MAC protocol.

The cognitive MAC protocols that support the above functional requirements can be classified, for example, according to the network architecture, control channel establishment method, spectrum sensing, spectrum access, spectrum sharing model, number of radios in cognitive device, and network coordination. The network architecture-based classification is the most frequently used classification technique for MAC protocols. Under this criterion, cognitive MAC protocols are categorized into centralized [68, 101] or distributed [102] protocols based on the location of the spectrum management entity. Based on the presence, scope and the characteristic of the common control channel (CCC), the cognitive MAC protocols are divided as local/global dedicated CCC [48] or dynamic CCC [68] based MAC protocols. The behaviour of the MAC protocols also varies with the degree of CRs' interaction for spectrum sensing, and accordingly, and the MAC protocols are classified as cooperative and non-cooperative-based MAC protocols [102]. In CRNs, the spectrum access techniques completely depend on the operational mode (i.e., underlay, overlay, and interweave) of CRs. Hence, to satisfy the different operational requirements

of CRs, the cognitive MAC protocols should behave differently. Therefore, the cognitive MAC protocols can also be identified as underlay, overlay, and interweave MAC protocols based on the CRs' operational modes [102]. The CRs, which are equipped with a single radio transceiver, access the spectrum by splitting time frame for spectrum sensing and accessing whereas the CRs equipped with multiple radios access the spectrum by allocating one/more radios for control signal exchange while utilizing the remaining radios for cognitive transmission. The MAC protocols developed for single radio spectrum access cannot be used for multi-radio CRNs. The optimization and learning-based MAC protocols learn the radio environment and optimally utilize the available spectrum whereas the other MAC protocols directly access the spectrum without adopting learning capabilities [103].

2.6.1 General Cognitive Medium Access Control (C-MAC) Cycle

To understand the operation of cognitive MAC protocols, it is very important to clearly identify the generic cognitive MAC functionalities, functionality-specific aspects and common aspects [48]. The generic cognitive MAC functionalities are radio environmental data acquisition (i.e., spectrum sensing and central database based data acquisition), spectrum sharing, and control channel management. The functionality-specific aspects are the issues encountered for solving in each generic cognitive function. Common aspects are referred to as the common techniques, features, approaches and mechanism that can be used to address cognitive functionality specific aspects. The general cognitive MAC protocol that supports functionality specific aspects and common aspects should satisfy the following requirements [48]:

- Clear understanding of the cognitive protocol stack and its impact on the CRN's performance.
- Extendibility in cognitive MAC design for new concepts and approaches. This flexi-

bility can be achieved through modularized designing.

- A general cognitive MAC design should provide a fundamental set of clearly-defined and standardized concepts which can be utilized as an individual or combined solution.

The cognitive MAC protocol taxonomy and standardization design that supports cognitive functionality and common aspects is referred to as C-MAC cycle as illustrated in Fig. 2.5.

General Functionality Aspects in C-MAC cycle

The identification and characterization of general functionalities in the C-MAC cycle is important in the cognitive MAC protocol design process. As illustrated in Fig.2.5, the general functionalities in C-MAC cycle are radio environmental data acquisition, spectrum sharing, and control channel management. The radio environmental information acquisition is a crucial function in cognitive MAC protocol design since all other functions' behaviour are based on this information. The radio environmental data acquisition techniques and relevant concerns were discussed in Sections 2.3.1 and 2.4. The spectrum-sharing functionality in C-MAC cycle exploits the radio environmental data for efficient utilization and management of PUs' idle spectrum. A detailed discussion on spectrum sharing was given in Section 2.3.3. The control channel management function is an integral function of the C-MAC cycle which allocates, establishes, and manages secure and reliable control signalling among the CRs in the network.

The common aspects which are used to address the functionality-specific aspects can be mainly divided into two types: operational common aspects and functionality-specific common aspects. The operational common aspects are the aspects that impact the cognitive MAC definition such as the number of radios per CR, number of antennas per CR, single/multi-band operation, synchronization vs. asynchronous operation and CR mobility.

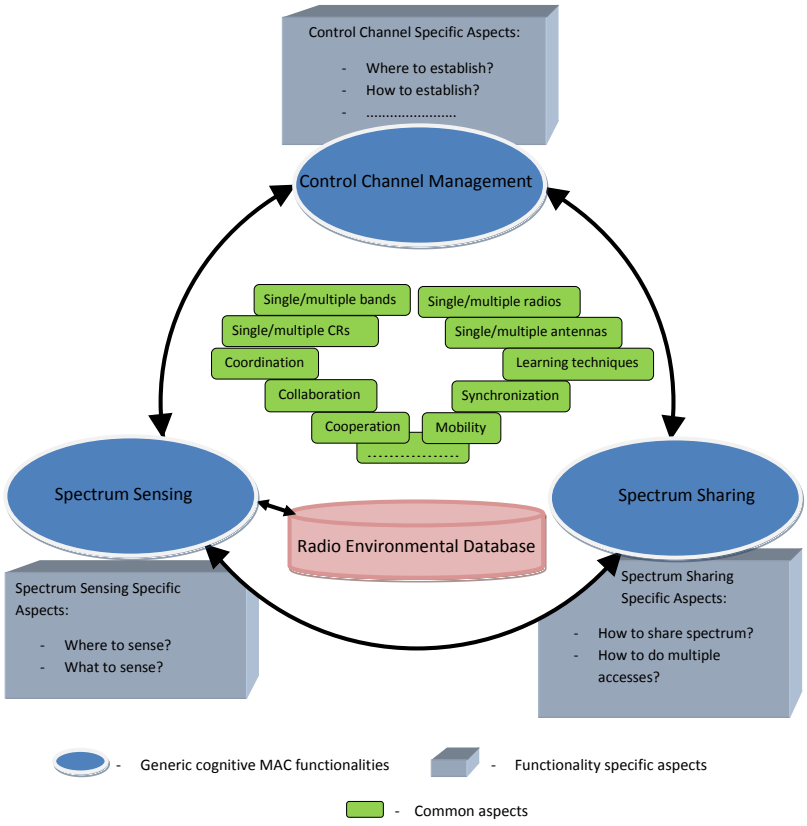

Figure 2.5: General cognitive MAC cycle.

The functionality-specific support aspects are the techniques, principles and solutions that can be implemented for addressing the functionality specific challenges such as cooperation, collaboration, coordination and learning mechanism.

Control Channel Management

Due to the heterogeneity of the available spectrum and dynamic spectrum access in CRNs, the control information exchange through common control channel is significantly diverse compared to traditional wireless networks. The control channel (CC) is responsible for providing its service to different CRN specific operational aspects such as network coordination, cooperation, collaboration, network self organization, flexible connection for data exchange and spectrum mobility [48]. To cater for the above mentioned operations, the CC carries different type of control information such as sensing results, spectrum sharing information, spectrum access decisions and system parameters. Therefore, the control channel which carries critical information in CRNs should be carefully established (i.e. where to establish and how to establish CC) and manage.

- **Where to establish:** In control channel management, deciding the spectral location to establish control channel is one of the key issues that is to be resolved in CRNs. The CC can be established as an in-band or out-of-band channel based on the cognitive application. If the control channel is established within the data transmission spectrum, such a control channel is known as an in-band control channel. This in-band CC can be a dedicated CC or a non-dedicated CC. On the other hand, if the control channel is established by physically separating it from the data transmission spectrum, such a CC is known as an out-of-band control channel.

- **How to establish:** The approaches for control channel establishment can be mainly divided in to two categories: dedicated control channel (DCC) or non-dedicated con-

trol channel (NDCC) establishment. In the dedicated control channel establishment-based approach, only the control information is exchanged in the channel whereas the non-dedicated CC establishment approach enables the exchange of both the control and data in the CC.

- **Dedicated control channel**: The dedicated CC can be either a global DCC or a local DCC. With a global DCC, all the CRs tune their radios to the global DCC to exchange control information since it is globally available to exchange control information. Since all the CRs tune to this channel, the global DCC is more susceptible to saturation. However, this approach provides a high level of network-wide coordination among CRs and is useful for centralized CRNs [104]. The local DCC-based approach is a very good solution for the control channel saturation problem at a cost of localized coordination among the CRs. In local DCC, the CRs in a cluster exchange control information with the help of locally available DCC. The selection of DCC within the cognitive network can be optimized by adopting a clustering mechanism [105]. In general, both the global and local DCC are allocated statistically for a long period of time. Therefore, both the approaches are more vulnerable to CC jamming and attacks.
- **Non-dedicated control channel:** Establishment of a non-dedicated control channel (NDCC) eliminates the requirement of a dedicated control channel; however, at the cost of transmission delay. Frequency hopping NDCC (FH-NDCC) and rendezvous NDCC (RNDCC) are the two different types of NDCC. Frequency hopping and rendezvous NDCC-based MAC protocols mainly differ in the hopping sequence adopted by the CRs in the networks. In the FHNDCC-based MAC protocols, the CRs hop across the spectrum bands or frequency channels according to a predefined hopping list [106, 107]. The hopping list

may be global and unique for the CRNs. The hopping list may have a local reference or it may dynamically adapt to the radio environment. In FHNDCC-based MAC protocols, the CRs exchange their control information and data once the communicating pair hop to a particular channel in the hopping list. The CRs in the network which follow the RNDCC-based approach for control information exchange adopt different hopping sequences that overlap at certain places [108]. Once the overlapping occurs, the CRs exchange their control information through the overlapped channel. The RNDCC-based MAC protocols are much simpler compared to the FHNDCC-based MAC protocols since they do not require network-wide synchronization. The transmission delay in RNDCC-based MAC protocols can be reduced further by properly designing the hopping sequence. Another solution for NDCC establishment is a hybrid scheme which exploits the advantages of frequency hopping and rendezvous approaches. Furthermore, the CRs can adopt rendezvous approach to find an overlap for initial control information exchange and should substitute a hopping list within this overlapping period. After that, the CRs can follow common hopping sequence for negotiation as in FHNDCC hopping.

Chapter 3

Machine Learning Techniques for Cooperative Spectrum Sensing in Cognitive Radio Networks

In this chapter, I use machine learning techniques to develop novel cooperative spectrum sensing (CSS) schemes for cognitive radio (CR) networks. In cognitive radio networks the secondary users (SUs) receive high signal strength from the primary users (PUs) in a particular band if PUs are active on that spectrum band and otherwise SUs receive only noise in that band. To differentiate PUs active channels from PUs inactive channels strong pattern recognition techniques can be utilized. Hence, in this chapter, I use machine learning techniques to develop novel cooperative spectrum sensing (CSS) schemes for cognitive radio (CR) networks. In this regard, unsupervised (e.g., K-means clustering and Gaussian mixture model (GMM)) and supervised (e.g., support vector machine (SVM) and weighted K-nearest-neighbor (KNN)) learning-based classification techniques are implemented for CSS. For a radio channel, the vector of the energy levels estimated at CR devices is treated as a feature vector and fed into a classifier to decide whether the channel is available or

not. Then, the classifier categorizes each feature vector into either of the two classes, namely, the ”channel available class” and the ”channel unavailable class”. Prior to the on-line classification, the classifier needs to go through a training phase. For classification, the K-means clustering algorithm partitions the training feature vectors into K clusters, where each cluster corresponds to a combined state of primary users (PUs) and then the classifier determines the class the test energy vector belongs to. The GMM obtains a mixture of Gaussian density functions that well describes the training feature vectors. In the case of the SVM, the support vectors (i.e., a subset of training vectors which fully specify the decision function) are obtained by maximizing the margin between the separating hyperplane and the training feature vectors. Furthermore, the weighted KNN classification technique is proposed for CSS for which the weight of each feature vector is calculated by evaluating the area under the receiver operating characteristic (ROC) curve of that feature vector. The performance of each classification technique is quantified in terms of the average training time, the sample classification delay, and the ROC curve. My comparative results clearly reveal that the proposed algorithms outperform the existing state-of-the-art CSS techniques.

3.1 Introduction

The concept of cognitive radio (CR) for designing wireless communications systems has emerged since last decade to mitigate the scarcity problem of limited radio spectrum by improving the utilization of the spectrum [11]. The CR refers to an intelligent wireless communications device, which senses its operational electromagnetic environment and can dynamically and autonomously adjust its radio operating parameters. In this context, opportunistic spectrum access (OSA) is a key concept, which allows a CR device to opportunistically access the frequency band allocated to a primary user (PU) when the PU trans-

mission is detected to be inactive [74, 109]. For OSA, the CR devices have to sense the radio spectrum licensed to the PUs by using its limited resources (e.g., energy and computational power), and subsequently utilize the available spectrum opportunities to maximize its performance objectives. Therefore, efficient spectrum sensing is crucial for OSA.

3.1.1 Related Work

Cooperative spectrum sensing (CSS) can be used when the CR devices are distributed in different locations. It is possible for the CR devices to cooperate in order to achieve higher sensing reliability than individual sensing does by yielding a better solution to the hidden PU problem that arises because of shadowing [110] and multi-path fading [111]. In cooperative sensing, the CR devices exchange the sensing results with the fusion center for decision making. With hard fusion algorithms, the CR devices exchange only one-bit information with the fusion center, which indicates whether the received energy is above a particular threshold. For example, the OR-rule [112], the AND-rule, the counting rule [79], and the linear quadratic combining rule [78] are commonly used for CSS. In [113], a softened hard fusion scheme with two-bit overhead for each CR device is considered. In soft decision algorithms [113, 114], the exact energy levels estimated at the CR devices are transmitted to the fusion center to make a better decision. In [115], the authors proposed an optimal linear fusion algorithm for spectrum sensing. Relay-based cooperative spectrum sensing schemes are studied in [116].

3.1.2 Motivation and Contribution

In CRNs the SUs receive high signal strength from the PUs if PUs are active on a particular spectrum band and otherwise, SUs receive only noise in that band. Therefore, to differentiate PUs active channels from PUs inactive channels the pattern recognition techniques can

be utilized. Further, the learning based techniques can describe more optimized decision region [1] on the feature space than the traditional CSS techniques (e.g., OR/AND-rule-based and linear fusion techniques) can, which results in better detection performance. Specially, the machine learning techniques are capable of implicitly learning the surrounding environment (e.g., the topology of the PU and the CR networks and the channel fading) in an online fashion. Therefore, the learning based techniques are much more adaptive than the traditional CSS techniques, which need prior knowledge about the environment for optimization. Hence, the affirmation advantages motive me to investigate the behaviour of machine learning techniques in CSS.

The machine learning techniques are often used for pattern classification, where a feature vector is extracted from a pattern and is fed into the classifier which categorizes the pattern into a certain class. In the context of CSS, I treat an ”energy vector”, each component of which is an energy level estimated at each CR device, as a feature vector. Then, the classifier categorizes the energy vector into one of two classes: the ”channel available class” (corresponding to the case that no PU is active) and the ”channel unavailable class” (corresponding to the case that at least one PU is active). Prior to online classification, the classifier has to go through a training phase where it learns from training feature vectors. According to which type of learning method is adopted, a classification algorithm can be categorized as unsupervised learning (e.g., K-means clustering and Gaussian mixture model (GMM)) or supervised learning (e.g., support vector machine (SVM) and K-nearest neighbor (KNN)) [83, 84, 117]. In supervised (resp., unsupervised) learning, a training feature vector is fed into the classifier with (resp., without) its label indicating the actual class the training feature vector belongs to.

The main contributions of this research can be listed as follows:

[1] The classifier categorizes a feature vector according to which decision region the feature vector falls in.

- I propose to use unsupervised learning approaches such as the K-means clustering and the GMM for CSS. The K-means clustering algorithm partitions the features into K clusters. Each cluster is mapped to either the channel available class or the channel unavailable class. On the other hand, in the GMM, I obtain a Gaussian mixture distribution from training feature vectors, where each Gaussian distribution in the mixture distribution corresponds to a cluster.

- Due to higher prediction capability in supervised learning, I also propose to use supervised learning approaches such as the SVM and the KNN for CSS. In the SVM, the support vectors (i.e., a subset of training vectors which fully specify the decision function) are obtained by maximizing the margin between separating hyperplanes and feature vectors. In addition, the weighted KNN classification technique is also investigated for CSS with different distance measures.

- The performance of each of the classification techniques is evaluated in terms of the training time, the classification delay, and the ROC curve. Specially, the effect of the number of the CR devices in cooperation is also quantified.

3.2 System Model and Assumptions

3.2.1 Cognitive Radio Network and Primary User Model

I consider a CR network which shares a frequency channel with PUs. Henceforth, a CR device in the CR network will be called a secondary user (SU). The CR network consists of N secondary users (SUs), each of which is indexed by $n = 1, \ldots, N$. SU n is located at the coordinate $\mathbf{c}_n^{\mathrm{SU}}$ in the two-dimensional space. For cooperative sensing, each SU estimates the energy level and reports it to cognitive base station which takes the role of a fusion center. The fusion center determines the channel availability based on the energy levels

reported by all SUs.

In this thesis, I adopt a very generalized PU model where multiple PUs alternate between active and inactive states. There are M PUs, each of which is indexed by $m = 1, \ldots, M$. Let $\mathbf{c}_m^{\text{PU}}$ denote the coordinate of PU m in the two-dimensional space. Let S_m indicate the state of PU m. I have $S_m = 1$ if PU m is in the active state (i.e., PU m transmits a signal); and $S_m = 0$ otherwise. Let $\mathbf{S} = (S_1, \ldots, S_M)^T$ be the vector of the states of all PUs, where the superscript T denotes the transpose operation. The probability that $\mathbf{S} = \mathbf{s}$ for given $\mathbf{s} = (s_1, \ldots, s_M)^T$ is denoted by

$$v(\mathbf{s}) = \Pr[\mathbf{S} = \mathbf{s}]. \tag{3.1}$$

If at least one PU is active (i.e., $S_m = 1$ for some m), the channel is considered as unavailable for the CR network to access. The channel is available only when there is no PU in the active state (i.e., $S_m = 0, \forall\, m$). If I let A denote the channel availability, I have

$$A = \begin{cases} -1, & \text{if } S_m = 1 \text{ for some } m \\ 1, & \text{if } S_m = 0 \text{ for all } m. \end{cases} \tag{3.2}$$

3.2.2 Energy Vector Model

To estimate the energy level, an SU performs energy detection for a time duration of τ. If I denote the bandwidth by B, the energy detector takes $B\tau$ baseband complex signal samples during τ. Let $Z_n(i)$ denote the ith signal sample taken by SU n. The signal samples consist of the summation of the signals from all PUs in the active state and the thermal noise, that

is,

$$Z_n(i) = \sum_{m=1}^{M} S_m h_{m,n} X_m(i) + N_n(i), \tag{3.3}$$

where $h_{m,n}$ denotes the channel gain from PU m to SU n, $X_m(i)$ is the signal transmitted by PU m, and $N_n(i)$ is the thermal noise at SU n. The transmission power of PU m is assumed to be fixed to $\rho_m = \sum_{i=1}^{B\tau} \mathrm{E}[|X_m(i)|^2]/\tau$ and the noise spectral density is denoted by $\eta = \mathrm{E}[|N_n(i)|^2]$. The energy detector of SU n estimates the energy level normalized by the noise spectral density, which is denoted by Y_n, from the signal samples as [82]

$$Y_n = \frac{2}{\eta} \sum_{i=1}^{B\tau} |Z_n(i)|^2. \tag{3.4}$$

All SUs report the estimated energy levels to the fusion center and the fusion center generates the "energy vector," which is defined as

$$\mathbf{Y} = (Y_1, \ldots, Y_N)^T. \tag{3.5}$$

Now, I investigate the distribution of the energy vector. It is known that, conditioned on $\mathbf{S} = \mathbf{s}$, the energy level Y_n follows a noncentral chi-squared distribution with the degree of freedom $q = 2w\tau$ and the non-centrality parameter,

$$\zeta_n = \frac{2\tau}{\eta} \sum_{m=1}^{M} s_m g_{m,n} \rho_m, \tag{3.6}$$

where $g_{m,n}$ is the power attenuation from PU m to SU n such that $g_{m,n} = |h_{m,n}|^2$. The power attenuation $g_{m,n}$ is given as

$$g_{m,n} = PL(\|\mathbf{c}_m^{\mathrm{PU}} - \mathbf{c}_n^{\mathrm{SU}}\|) \cdot \psi_{m,n} \cdot \nu_{m,n}, \tag{3.7}$$

where $\|\cdot\|$ is the Euclidean distance, $PL(d) = d^{-\alpha}$ is the path-loss component for relative distance d with the path-loss exponent α, $\psi_{m,n}$ is the shadow fading component, and $\nu_{m,n}$ is the multi-path fading component. I assume that PUs and SUs are immobile (e.g., the base station (BS), the consumer premise equipment (CPE), and the TV station in IEEE 802.22-based wireless regional area network (WRAN)). I assume that the shadow fading and the multi-path fading components are quasi-static during the time of interest.

3.3 Machine Learning-Based Cooperative Spectrum Sensing Framework

3.3.1 Operation of Proposed CSS Framework

The purpose of the proposed CSS techniques is to correctly determine the channel availability A based on the given energy vector $\mathbf{Y}$. In the context of the machine learning, this is equivalent to constructing a classifier to correctly map the energy vector $\mathbf{Y}$ to the channel availability A. Therefore, an energy vector in our problem is analogous to a feature in the machine learning terminology. To construct the classifier, the first step is to collect a sufficient number of training energy vectors. Let $\mathbf{y}^{(l)}$ denote the lth training energy vector and let $a^{(l)}$ denote the channel availability corresponding to $\mathbf{y}^{(l)}$. Then, the set of the training energy vectors, i.e., $\overline{\mathbf{y}} = \{\mathbf{y}^{(1)}, \ldots, \mathbf{y}^{(L)}\}$ (where L is the number of training samples), is fed into the classifier for training. In case of unsupervised learning, each of the training energy vectors does not need to be labeled with the corresponding channel availability. On the other hand, supervised learning requires to have the set of the channel availabilities, i.e., $\overline{a} = \{a^{(1)}, \ldots, a^{(L)}\}$, for training as well as the set of the training energy vectors.

Next, the classifier is trained by using the training energy vectors. The training procedure differs for each machine learning technique under consideration. For example, in case

of K-means clustering, the training involves partitioning the training energy vectors into K clusters and the centroid of each cluster is later used for classification. In another example, the SVM tries to find the maximum-margin hyperplane that splits the training energy vectors as clearly as possible.

Once the classifier is successfully trained, it is ready to receive the test energy vector for classification. Let $\mathbf{y}^*$ denote the test energy vector received by the classifier and let a^* denote the corresponding channel availability. In addition, let $\widehat{a}$ denote the channel availability determined by the classifier. The classifier categorizes the energy vector $\mathbf{y}^*$ into either "channel available class" (i.e., $\widehat{a} = 1$) or "channel unavailable class" (i.e., $\widehat{a} = -1$). If the energy vector is classified into the channel available class (resp., the channel unavailable class), it means that there is no PU (resp., at least one PU) in the active state and the channel is available (resp., unavailable) for the CR network to access. Therefore, the channel availability is correctly determined in the case that $\widehat{a} = a^*$, while misdetection (resp., false alarm) occurs in the case that $\widehat{a} = 1$ and $a^* = -1$ (resp., $\widehat{a} = -1$ and $a^* = 1$).

In Fig. 3.1, I illustrate the modular architecture of the proposed CSS framework, which consists of the training module and the classification module. In this architecture, the training and classification modules can operate independently. Whenever the CR network needs to find out the channel availability, the CR network generates the test energy vector and puts it into the classification module. The classification module determines the channel availability based on the test energy vector by using the classifier. Usually, finding the channel availability in the CR network requires very short delay. The classification delay of the proposed CSS techniques can meet this requirement due to low complexity.

The training module is responsible to train the classifier from the training energy samples and to provide the classification module with a trained classifier. The training module can be activated when the CR network is first deployed and when the radio environment

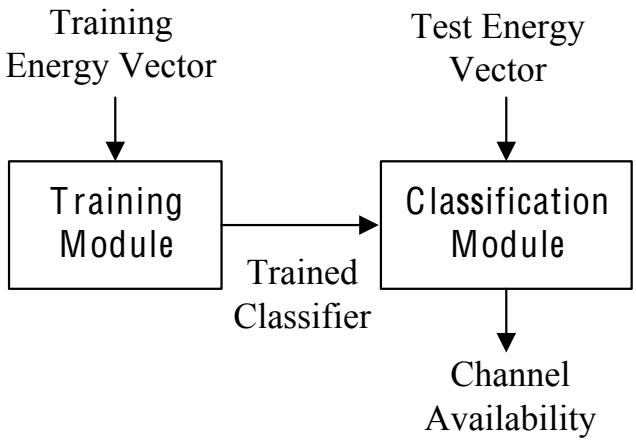

Figure 3.1: Modular architecture of the proposed CSS framework.

changes (e.g., when the PU network changes its configuration). In addition, the CR network can periodically activate the training module to catch up with the changing environment. The training procedure of machine learning techniques generally takes a long time. However, this is not a significant problem since the training module is activated only by the above-mentioned events. Moreover, the training procedure can be performed in the background while the classification module operates normally.

3.3.2 Advantages of Proposed CSS Framework

The advantage of the proposed machine learning-based CSS framework over the traditional CSS techniques is twofold.

- The proposed CSS techniques retain a learning ability since the optimized classifier is learnt from the training energy vectors, which makes the proposed CSS techniques adaptive to changing radio environment without human intervention. The training procedure is fully autonomous in that it does not require any prior information about the environment and does not involve any parameter setting. Moreover, the proposed CSS techniques can adapt themselves to the changing environment by retraining the

classifier periodically.

- The proposed CSS techniques can describe more optimized decision surface than the traditional CSS techniques can, which result in better performance in terms of the detection and the false alarm probabilities. The generalized multiple PU model in this thesis leads to very complex probability space of the energy vector, which cannot be handled by the traditional CSS techniques. However, the proposed CSS techniques can find the decision surface which efficiently classifies the energy vectors even in the multiple PU model.

In Fig. 3.3, I present example scatter plots of the energy vectors of two SUs in two different scenarios to highlight the advantages of the proposed CSS techniques. In Scenario I, there are two PUs whose locations are given in Fig. 3.2(a). The PUs in Scenario I are activated according to the probability of $v((0,0)^T) = 0.36$, $v((0,1)^T) = 0.24$, $v((1,0)^T) = 0.24$, and $v((1,1)^T) = 0.16$. In Scenario II, there is only one PU whose location is given in Fig. 3.2(b). In this scenario, the PU is activated with the probability of $v((1)) = 0.5$. In Figs. 3.3(a)–3.3(d)[2], the energy vectors as well as the decision surfaces of the proposed technique are plotted for each scenario. The decision surface divides the energy vectors into two decision regions - one for the channel available class and the other for the channel unavailable class. In these figures, one of the proposed techniques, the Gaussian mixture model (GMM) technique, is used to draw the decision surface. The GMM will be explained in detail in Section 3.4.3. The threshold for classification in the GMM (i.e., δ) is set to zero for Fig. 3.3. Figs. 3.3(a) and 3.3(b) are plotted for Scenarios I while Figs. 3.3(c) and 3.3(d) are plotted for Scenario II. The transmission power of each PU is 200 mW in Figs. 3.3(a) and 3.3(c), and is 80 mW in Figs. 3.3(b) and 3.3(d).

[2]The simulation parameter values for Fig. 3.3 are as follows: the bandwidth w is 5 MHz, the sensing duration τ is 100 μs, the noise spectral density η is -174 dBm, and the path-loss exponent α is 4. I assume that the shadow fading and the multi-path fading components are fixed as $\psi_{m,n} = 1$ and $\nu_{m,n} = 1$.

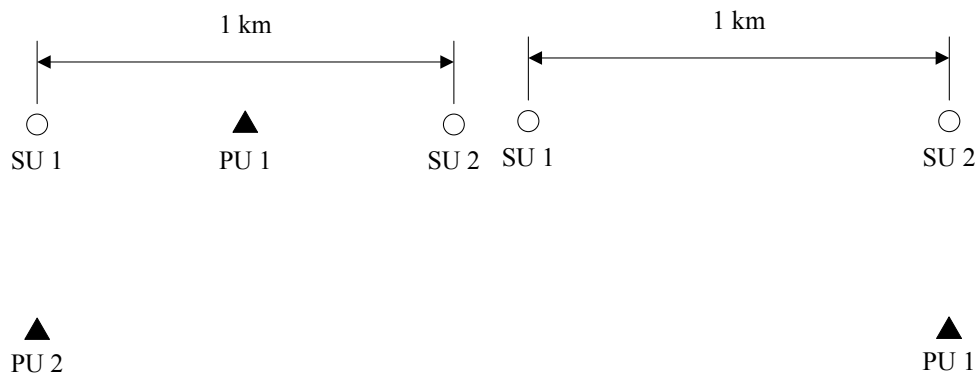

(a) Locations of PU and SU in Scenario I. (b) Locations of PU and SU in Scenario II.

Figure 3.2: Two scenarios of user locations.

From Fig. 3.3, we can notice the following advantages of the proposed machine learning-based CSS framework.

- We can see that the GMM technique is able to adaptively adjust the decision surface for different scenarios. Suppose that the CR network has the configuration in Scenario I and the transmission power of each PU is 200 mW. In this case, the CR network has the decision surface as shown in Fig. 3.3(a). Then, suppose that the PU network changes its configuration to Scenario II. The CR network can adapt to this change by gathering the energy vectors for a while and recalculate the decision surface as shown in Fig. 3.3(c). This process is autonomous and does not require any human intervention.

- We can see that the decision surface divides the energy vectors in each class as clearly as possible, which leads to improved detection performance. In Figs. 3.3(a) and 3.3(b), the decision surface, derived by the GMM technique, optimally separates the energy vectors. This decision surface takes a complex form, which cannot be described by any other existing CSS technique.

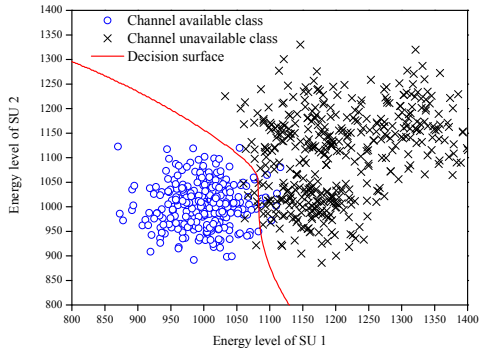

(a) Scatter plot of energy vectors in Scenario I when the transmit power of each PU is 200 mW.

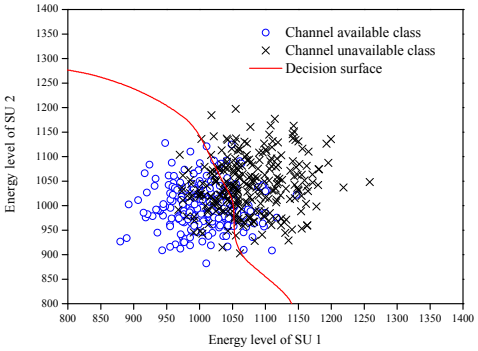

(b) Scatter plot of energy vectors in Scenario I when the transmit power of each PU is 80 mW.

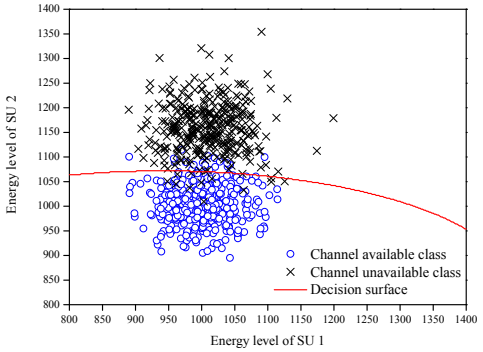

(c) Scatter plot of energy vectors in Scenario II when the transmit power of each PU is 200 mW.

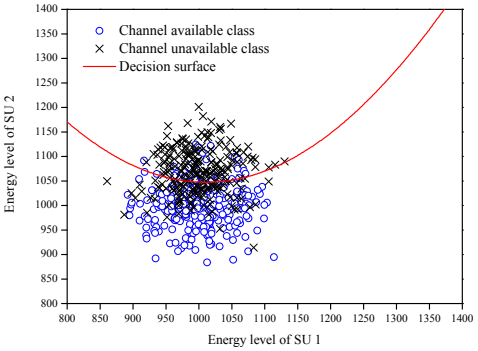

(d) Scatter plot of energy vectors in Scenario II when the transmit power of each PU is 80 mW.

Figure 3.3: Example scatter plots of energy vectors in two scenarios.

3.4 Unsupervised Learning for Cooperative Spectrum Sensing

3.4.1 Motivation for Unsupervised Learning

In this section, we propose unsupervised learning approaches for the proposed CSS framework. In case of unsupervised learning, only the training energy vectors (i.e., $\overline{\mathbf{y}} = \{\mathbf{y}^{(1)}, \ldots, \mathbf{y}^{(L)}\}$) are fed into the classifier for training. Unsupervised learning does not need the information regarding the channel availability corresponding to each training energy vector, i.e., $\overline{a} = \{a^{(1)}, \ldots, a^{(L)}\}$. Therefore, unsupervised learning can be easily implemented in a practical sense compared to the supervised learning which requires $\overline{a}$ for training.

Since there is no explicit teacher which helps training, unsupervised learning has to rely on the inherent clustering structure of the training energy vectors. Recall that the energy vector $\mathbf{Y}$ given $\mathbf{S} = \mathbf{s}$ follows a multivariate Gaussian distribution with the mean vector $\boldsymbol{\mu}_{\mathbf{Y}|\mathbf{S}=\mathbf{s}}$ and the covariance matrix $\boldsymbol{\Sigma}_{\mathbf{Y}|\mathbf{S}=\mathbf{s}}$. For each possible combination of the states of PUs, a cluster of the training energy vectors is formed according to the respective multivariate Gaussian distribution. In Fig. 3.3(a), we observe that four visible clusters are formed each of which respectively corresponds to the cases that $(S_1, S_2)^T$ is $(0, 0)^T$, $(0, 1)^T$, $(1, 0)^T$, and $(1, 1)^T$. If there are M PUs, the number of clusters can be calculated as $K = 2^M$. Each cluster is indexed by $k = 1, \ldots, K$.

More specifically, the training energy vectors are samples taken out of the Gaussian mixture distribution the pdf of which is as follows:

$$f(\mathbf{x}) = \sum_{\mathbf{s}} v(\mathbf{s}) \cdot \Phi(\mathbf{x}|\boldsymbol{\mu}_{\mathbf{Y}|\mathbf{S}=\mathbf{s}}, \boldsymbol{\Sigma}_{\mathbf{Y}|\mathbf{S}=\mathbf{s}}), \tag{3.8}$$

where $v(\mathbf{s})$ is the probability that $\mathbf{S} = \mathbf{s}$ (i.e., $v(\mathbf{s}) = \Pr[\mathbf{S} = \mathbf{s}]$) and $\Phi(\mathbf{x}|\boldsymbol{\mu}_{\mathbf{Y}|\mathbf{S}=\mathbf{s}}, \boldsymbol{\Sigma}_{\mathbf{Y}|\mathbf{S}=\mathbf{s}})$

is the pdf of the multivariate Gaussian distribution such that

$$\Phi(\mathbf{x}|\boldsymbol{\mu}_{\mathbf{Y}|\mathbf{S}=\mathbf{s}}, \boldsymbol{\Sigma}_{\mathbf{Y}|\mathbf{S}=\mathbf{s}}) = \frac{1}{(2\pi)^{N/2}|\boldsymbol{\Sigma}_{\mathbf{Y}|\mathbf{S}=\mathbf{s}}|^{1/2}} \exp\left\{-\frac{1}{2}(\mathbf{x}-\boldsymbol{\mu}_{\mathbf{Y}|\mathbf{S}=\mathbf{s}})^T \boldsymbol{\Sigma}_{\mathbf{Y}|\mathbf{S}=\mathbf{s}}^{-1}(\mathbf{x}-\boldsymbol{\mu}_{\mathbf{Y}|\mathbf{S}=\mathbf{s}})\right\}. \tag{3.9}$$

The samples from the Gaussian mixture distribution form discernible clusters as shown in Figs. 3.3(a) and 3.3(c) if the transmission power of each PU is high. However, clusters are not visually separable in Figs. 3.3(b) and 3.3(d) in the case that the transmission power of each PU is low. It is worth noting that, even in the case of low transmission power, the proposed CSS scheme is able to obtain the decision surface separating the channel available and channel unavailable classes as shown in Figs. 3.3(b) and 3.3(d).

Among all clusters, only one cluster corresponding to the case that no PU is in the active state (i.e., $\mathbf{S} = \mathbf{0}$ for the zero vector $\mathbf{0}$) can be mapped to the channel available class, while all the other clusters are mapped to the channel unavailable class. Without loss of generality, I designate the cluster corresponding to the case that $\mathbf{S} = \mathbf{0}$ as cluster 1. The CR network is aware of the parameters for the multivariate Gaussian distribution if and only if $\mathbf{S} = \mathbf{0}$ since the CR network does not know the power attenuation $g_{m,n}$. Therefore, cluster 1 can easily be identified by the mean vector $\boldsymbol{\mu}_{\mathbf{Y}|\mathbf{S}=\mathbf{0}}$ and the covariance matrix $\boldsymbol{\Sigma}_{\mathbf{Y}|\mathbf{S}=\mathbf{0}}$ while the other clusters should be blindly identified by unsupervised learning.

From now on, I will investigate the application of two representative unsupervised clustering algorithms, i.e., the K-means clustering and the GMM, to CSS. After training by using these clustering algorithms, each time the classifier receives the test energy vector for classification, the classifier finds out which cluster the test energy vector belongs to and classifies it as the channel available class if and only if the test energy vector belongs to cluster 1.

3.4.2 K-Means Clustering Algorithm

The unsupervised K-means clustering algorithm partitions a set of the training energy vectors (i.e., $\overline{\mathbf{y}} = \{\mathbf{y}^{(1)}, \ldots, \mathbf{y}^{(L)}\}$) into K disjoint clusters. Let $\mathcal{C}_k$ denote the set of the training energy vectors that belong to cluster k. Cluster k has a centroid $\boldsymbol{\alpha}_k$. Differently from the ordinary K-means clustering algorithm, I assume that the centroid of cluster 1 is fixed to the mean of $\mathbf{Y}$ conditioned on $\mathbf{S} = \mathbf{0}$, that is, $\boldsymbol{\alpha}_1 = \boldsymbol{\mu}_{\mathbf{Y}|\mathbf{S}=\mathbf{0}}$. For all other clusters, the centroid is defined as the mean of all training energy vectors in $\mathcal{C}_k$ such that $\boldsymbol{\alpha}_k = |\mathcal{C}_k|^{-1} \sum_{\mathbf{y}^{(l)} \in \mathcal{C}_k} \mathbf{y}^{(l)}$, $\forall k = 2, \ldots, K$, where $|\mathcal{X}|$ denotes the number of elements in the set $\mathcal{X}$. The K-means clustering algorithm aims to find out K clusters, $\mathcal{C}_1, \ldots, \mathcal{C}_K$, which minimize the within-cluster sum of squares as follows:

$$\underset{\mathcal{C}_1,\ldots,\mathcal{C}_K}{\operatorname{argmin}} \sum_{k=1}^{K} \sum_{\mathbf{y}^{(l)} \in \mathcal{C}_k} \left\| \mathbf{y}^{(l)} - \boldsymbol{\alpha}_k \right\|^2. \tag{3.10}$$

To find the clusters satisfying (3.10), I use an iterative suboptimal algorithm presented in **Algorithm 1**.

Algorithm 1 K-Means Clustering Algorithm for CSS

1: $\boldsymbol{\alpha}_1 \leftarrow \boldsymbol{\mu}_{\mathbf{Y}|\mathbf{S}=\mathbf{0}}$
2: $\boldsymbol{\alpha}_k$ is initialized, $\forall k = 2, \ldots, K$.
3: **while** $\mathcal{C}_k$ for some k is changed in the previous iteration **do**
4: $\quad \mathcal{C}_k \leftarrow \{\mathbf{y}^{(l)} | \|\mathbf{y}^{(l)} - \boldsymbol{\alpha}_k\| \leq \|\mathbf{y}^{(l)} - \boldsymbol{\alpha}_i\|,\ \forall i = 1, \ldots, K\}, \forall k = 1, \ldots, K$.
5: $\quad \boldsymbol{\alpha}_k \leftarrow |\mathcal{C}_k|^{-1} \sum_{\mathbf{y}^{(l)} \in \mathcal{C}_k} \mathbf{y}^{(l)}, \forall k = 2, \ldots, K$.
6: **end while**

In **Algorithm 1**, the centroid of cluster 1 is set to $\boldsymbol{\mu}_{\mathbf{Y}|\mathbf{S}=\mathbf{0}}$ in Line 1. The centroids for clusters except for cluster 1 are initialized in Line 2. The iteration begins from Line 3. In Line 4, each training energy vector is assigned to the cluster the centroid of which is closest to the training energy vector. In Line 5, the centroids of clusters except for cluster 1 are updated by taking the mean of all training energy vectors in each cluster. The iterations are

repeated until there is no change in the clusters. Finally, I have a suboptimal solution for (3.10) when the iteration is over. Let $\boldsymbol{\alpha}_k^*$ denote the centroid for cluster k obtained by the K-means clustering.

After the training is over, the classifier receives the test energy vector $\mathbf{y}^*$ for classification. The classifier determines if the test energy vector belongs to cluster 1 or the other classes, based on the distance from the test energy vector to the centroids. The classifier classifies $\mathbf{y}^*$ as the channel unavailable class (i.e., $\widehat{a} = -1$) if the following condition is met:

$$\frac{\|\mathbf{y}^* - \boldsymbol{\alpha}_1^*\|}{\min_{k=1,\ldots,K} \|\mathbf{y}^* - \boldsymbol{\alpha}_k^*\|} > \beta_{th}. \tag{3.11}$$

Otherwise, $\mathbf{y}^*$ is classified as the channel available class (i.e., $\widehat{a} = 1$). The parameter β_{th} is the threshold to control the tradeoff between the misdetection and the false alarm probabilities. If β becomes high, $\mathbf{y}^*$ is more likely to be classified as the channel available class, which in turn increases the misdetection probability while decreasing the false alarm probability.

3.4.3 Gaussian Mixture Model

A GMM is a weighted sum of multivariate Gaussian probability densities given by

$$f(\mathbf{x}|\boldsymbol{\theta}) = \sum_{k=1}^{K} v_k \cdot \Phi(\mathbf{x}|\boldsymbol{\mu}_k, \boldsymbol{\Sigma}_k), \tag{3.12}$$

where $\Phi(\mathbf{x}|\boldsymbol{\mu}_k, \boldsymbol{\Sigma}_k)$ is the Gaussian density such that

$$\Phi(\mathbf{x}|\boldsymbol{\mu}_k, \boldsymbol{\Sigma}_k) = \frac{1}{(2\pi)^{N/2}|\boldsymbol{\Sigma}_k|^{1/2}} \exp\left\{ -\frac{1}{2}(\mathbf{x} - \boldsymbol{\mu}_k)^T \boldsymbol{\Sigma}_k^{-1}(\mathbf{x} - \boldsymbol{\mu}_k) \right\}, \tag{3.13}$$

and $\boldsymbol{\theta}$ is the collection of all parameters for the GMM including v_k, $\boldsymbol{\mu}_k$, and $\boldsymbol{\Sigma}_k$ for all $k = 1, \ldots, K$. The GMM exactly matches our energy vector model where $\mathbf{Y}$ conditioned on $\mathbf{S} = \mathbf{s}$ follows the multivariate Gaussian distribution with the mean vector $\boldsymbol{\mu}_{\mathbf{Y}|\mathbf{S}=\mathbf{s}}$ and the covariance matrix $\boldsymbol{\Sigma}_{\mathbf{Y}|\mathbf{S}=\mathbf{s}}$. Let the kth Gaussian density $\Phi(\mathbf{x}|\boldsymbol{\mu}_k, \boldsymbol{\Sigma}_k)$ in the GMM approximate the density of the energy vectors belonging to cluster k. If cluster k corresponds to the case that $\mathbf{S} = \mathbf{s}$, the parameters for the kth Gaussian density, $\boldsymbol{\mu}_k$, $\boldsymbol{\Sigma}_k$, and v_k, correspond to $\boldsymbol{\mu}_{\mathbf{Y}|\mathbf{S}=\mathbf{s}}$, $\boldsymbol{\Sigma}_{\mathbf{Y}|\mathbf{S}=\mathbf{s}}$, and $v(\mathbf{s})$ in the energy vector model, respectively. Since cluster 1 corresponds to the case that $\mathbf{S} = \mathbf{0}$, I have $\boldsymbol{\mu}_1 = \boldsymbol{\mu}_{\mathbf{Y}|\mathbf{S}=\mathbf{0}}$ and $\boldsymbol{\Sigma}_1 = \boldsymbol{\Sigma}_{\mathbf{Y}|\mathbf{S}=\mathbf{0}}$, which are known to the CR network in advance. Moreover, I can restrict $\boldsymbol{\Sigma}_k$ to a diagonal matrix for all k since $\boldsymbol{\Sigma}_{\mathbf{Y}|\mathbf{S}=\mathbf{s}}$ is a diagonal matrix for all $\mathbf{s}$. The rest of the parameters in $\boldsymbol{\theta}$ are unknown and need to be estimated.

The parameters can be estimated by using the maximum-likelihood (ML) estimation given the set of the training energy vectors (i.e., $\overline{\mathbf{y}} = \{\mathbf{y}^{(1)}, \ldots, \mathbf{y}^{(L)}\}$). The log-likelihood of the set of the training energy vectors can be written as

$$\omega(\overline{\mathbf{y}}|\boldsymbol{\theta}) = \sum_{l=1}^{L} \ln \left(\sum_{k=1}^{K} v_k \cdot \Phi(\mathbf{y}^{(l)}|\boldsymbol{\mu}_k, \boldsymbol{\Sigma}_k) \right). \tag{3.14}$$

The ML estimator is the parameter that maximizes this log-likelihood function. Unfortunately, direct computation of the ML estimator is not possible due to latent information [84]. However, the parameters that maximize the log-likelihood can be obtained by using the expectation maximization (EM) algorithm [118].

The EM algorithm iteratively updates the parameter $\boldsymbol{\theta}$ by maximizing the following

function:

$$\begin{aligned} Q(\boldsymbol{\theta}'|\boldsymbol{\theta}) &= \mathrm{E}\left[\sum_{l=1}^{L} \ln\left(v'_{z^{(l)}} \cdot \Phi(\mathbf{y}^{(l)}|\boldsymbol{\mu}'_{z^{(l)}}, \boldsymbol{\Sigma}'_{z^{(l)}})\right) \middle| \overline{\mathbf{y}}, \boldsymbol{\theta}\right] \\ &= \sum_{l=1}^{L}\left\{\sum_{k=1}^{K} u_k^{(l)} \ln v'_k + \sum_{k=1}^{K} u_k^{(l)} \ln \Phi(\mathbf{y}^{(l)}|\boldsymbol{\mu}'_k, \boldsymbol{\Sigma}'_k)\right\}, \end{aligned} \tag{3.15}$$

where $z^{(l)}$ is a random variable which is the index of the cluster to which the lth training energy vector belongs to and $u_k^{(l)}$ is defined as

$$u_k^{(l)} = \Pr[z^{(l)} = k|\overline{\mathbf{y}}, \boldsymbol{\theta}] = \frac{v_k \cdot \Phi(\mathbf{y}^{(l)}|\boldsymbol{\mu}_k, \boldsymbol{\Sigma}_k)}{\sum_{i=1}^{K} v_i \cdot \Phi(\mathbf{y}^{(l)}|\boldsymbol{\mu}_i, \boldsymbol{\Sigma}_i)}. \tag{3.16}$$

Let us define $\boldsymbol{\theta}(j)$ as the estimated parameter at the jth iteration of the EM algorithm. At the jth iteration, the EM algorithm finds $\boldsymbol{\theta}(j+1)$ that satisfies

$$\boldsymbol{\theta}(j+1) = \underset{\boldsymbol{\theta}}{\operatorname{argmax}}\, Q(\boldsymbol{\theta}|\boldsymbol{\theta}(j)). \tag{3.17}$$

It is known that $\boldsymbol{\theta}(j)$ converges to a local optimal solution over iterations [118].

At each iteration, the EM algorithm first calculates $u_k^{(l)}$ from (3.16) in the expectation step, and then derives the solution of (3.17) in the maximization step. The solution of (3.17) can be evaluated by a basic optimization technique. In **Algorithm 2**, I present the EM algorithm for solving the GMM. In Line 1 of **Algorithm 2**, the mean $\boldsymbol{\mu}_1(1)$ and the covariance $\boldsymbol{\Sigma}_1(1)$ for cluster 1 are set to $\boldsymbol{\mu}_{\mathbf{Y}|\mathbf{S}=\mathbf{0}}$ and $\boldsymbol{\Sigma}_{\mathbf{Y}|\mathbf{S}=\mathbf{0}}$, respectively. In Line 2, all other parameters are initialized. In Lines 4–8, the expectation and the maximization steps are repeated until $\boldsymbol{\theta}(j)$ is converged. Note that $\boldsymbol{\mu}_1(j)$ and $\boldsymbol{\Sigma}_1(j)$ are not updated in the maximization step since $\boldsymbol{\mu}_1(j)$ and $\boldsymbol{\Sigma}_1(j)$ are fixed to $\boldsymbol{\mu}_{\mathbf{Y}|\mathbf{S}=\mathbf{0}}$ and $\boldsymbol{\Sigma}_{\mathbf{Y}|\mathbf{S}=\mathbf{0}}$, respectively. Let $\boldsymbol{\theta}^*$ denote the parameter obtained after the EM algorithm is over.

After obtaining the optimal parameter $\boldsymbol{\theta}^*$, the classifier receives the test energy vec-

Algorithm 2 EM Algorithm for GMM

1: $\boldsymbol{\mu}_1(1) \leftarrow \boldsymbol{\mu}_{\mathbf{Y}|\mathbf{S}=\mathbf{0}}$ and $\boldsymbol{\Sigma}_1(1) \leftarrow \boldsymbol{\Sigma}_{\mathbf{Y}|\mathbf{S}=\mathbf{0}}$
2: Initialize $v_k(1)$ for $k = 1, \ldots, K$ and $\boldsymbol{\mu}_k(1)$ and $\boldsymbol{\Sigma}_k(1)$ for $k = 2, \ldots, K$.
3: $j \leftarrow 1$
4: **repeat**
5: Expectation Step

$$u_k^{(l)} \leftarrow \frac{v_k(j) \cdot \Phi(\mathbf{y}^{(l)}|\boldsymbol{\mu}_k(j), \boldsymbol{\Sigma}_k(j))}{\sum_{i=1}^{K} v_i(j) \cdot \Phi(\mathbf{y}^{(l)}|\boldsymbol{\mu}_i(j), \boldsymbol{\Sigma}_i(j))},$$
$$\text{for } l = 1, \ldots, L \text{ and } k = 1, \ldots, K.$$

6: Maximization Step

$$v_k(j+1) \leftarrow \frac{\sum_{l=1}^{L} u_k^{(l)}}{L}, \quad \text{for } k = 1, \ldots, K.$$
$$\boldsymbol{\mu}_k(j+1) \leftarrow \frac{\sum_{l=1}^{L} u_k^{(l)} \mathbf{y}^{(l)}}{\sum_{l=1}^{L} u_k^{(l)}}, \quad \text{for } k = 2, \ldots, K.$$
$$\boldsymbol{\Sigma}_k(j+1) \leftarrow \frac{\sum_{l=1}^{L} u_k^{(l)} \{\mathrm{diag}(\mathbf{y}^{(l)} - \boldsymbol{\mu}_k(j+1))\}^2}{\sum_{l=1}^{L} u_k^{(l)}},$$
$$\text{for } k = 2, \ldots, K.$$

7: $j \leftarrow j + 1$
8: **until** $\boldsymbol{\theta}(j)$ converges.

tor $\mathbf{y}^*$ for classification. The classifier determines whether the test energy vector $\mathbf{y}^*$ belongs to cluster 1 or other clusters. The log-likelihood that $\mathbf{y}^*$ belongs to cluster 1 is $\ln(v_1^* \cdot \Phi(\mathbf{y}^*|\boldsymbol{\mu}_1^*, \boldsymbol{\Sigma}_1^*))$. Similarly, the log-likelihood that $\mathbf{y}^*$ belongs to the clusters other than cluster 1 is $\ln(\sum_{k=2}^{K} v_k^* \cdot \Phi(\mathbf{y}^*|\boldsymbol{\mu}_k^*, \boldsymbol{\Sigma}_k^*))$. Therefore, $\mathbf{y}^*$ is classified as the channel unavailable class (i.e., $\widehat{a} = -1$) if and only if

$$\ln\left(\sum_{k=2}^{K} v_k^* \cdot \Phi(\mathbf{y}^*|\boldsymbol{\mu}_k^*, \boldsymbol{\Sigma}_k^*)\right) - \ln(v_1^* \cdot \Phi(\mathbf{y}^*|\boldsymbol{\mu}_1^*, \boldsymbol{\Sigma}_1^*)) \geq \delta_{th}, \tag{3.18}$$

for a given threshold δ_{th}. I can decrease the false alarm probability at the expense of misdetection probability by increasing δ_{th} since $\mathbf{y}^*$ is more likely to be classified as the channel available class if the value of δ_{th} is high.

3.5 Supervised Learning for Cooperative Spectrum Sensing

3.5.1 Motivation for Supervised Learning

In this section, I propose the application of the supervised learning techniques, i.e., the support vector machine (SVM) and the weighted K-nearest-neighbor (KNN), to CSS in the CR networks. The main difference of the supervised learning from the unsupervised learning is that each training energy vector $\mathbf{y}^{(l)}$ is labeled with the corresponding channel availability $a^{(l)}$. Therefore, to implement supervised learning for CSS in practice, the PU should occasionally inform the CR network of the channel availabilities for some training energy vectors for the purpose of training. Since supervised learning can work with the explicit help from the PU, it is more difficult to implement than the unsupervised learning. However, supervised learning tends to show better performance due to the extra information on the channel availability. I assume that the training energy vectors (i.e., $\overline{\mathbf{y}} = \{\mathbf{y}^{(1)}, \ldots, \mathbf{y}^{(L)}\}$) and the channel availability corresponding to each training energy

vector (i.e., $\overline{a} = \{a^{(1)}, \ldots, a^{(L)}\}$) are fed into the classifier for training.

3.5.2 Support Vector Machine

The SVM tries to find a linearly separable hyperplane, with the help of support vectors (i.e., energy vectors that lie closest to the decision surface), by maximizing the margin of the classifier while minimizing the sum of errors. However, the training energy vectors may not be linearly separable. Therefore, I try to map the training energy vectors into a higher dimensional feature space by a non-linear mapping function, denoted by ϕ, to make the training samples linearly separable [83, 119]. Hence, the classifier should satisfy the following condition for all $l = 1, \ldots, L$:

$$\begin{aligned} &\mathbf{w} \cdot \phi(\mathbf{y}^{(l)}) + w_0 \geq 1, \text{ if } a^{(l)} = 1, \\ &\mathbf{w} \cdot \phi(\mathbf{y}^{(l)}) + w_0 \leq -1, \text{ if } a^{(l)} = -1, \end{aligned} \tag{3.19}$$

where $\mathbf{w}$ is the weighting vector and w_0 is the bias. The bias is used for shifting the hyperplane away from the origin.

Although I map the training energy vectors into a higher dimensional feature space, practically I cannot achieve a perfect linearly separable hyperplane that satisfies the condition in (3.19) for each $\mathbf{y}^{(l)}$. Hence, I modify condition (3.19) by introducing a slack variable $\delta^{(l)}$ for possible classification errors as follows:

$$a^{(l)}[\mathbf{w} \cdot \phi(\mathbf{y}^{(l)}) + w_0] \geq 1 - \delta^{(l)}, \tag{3.20}$$

where $\delta^{(l)} \geq 0$ for $l = 1, \ldots, L$. For marginal classification errors, the slack variable lies in $0 \leq \delta^{(l)} \leq 1$, whereas $\delta^{(l)} > 1$ for misclassification. Hence, the optimization problem for maximizing the margin of classifier while minimizing the sum of errors can be written

as follows [83]:

$$\text{minimize} \quad \frac{1}{2}\|\mathbf{w}\|^2 + \xi \sum_{l=1}^{L} I_{\{\delta^{(l)}>1\}} \tag{3.21}$$

$$\text{subject to} \quad a^{(l)}[\mathbf{w} \cdot \phi(\mathbf{y}^{(l)}) + w_0] \geq 1 - \delta^{(l)}, \tag{3.22}$$

$$\text{for } l = 1, \ldots, L, \tag{3.23}$$

$$\delta^{(l)} \geq 0, \quad \text{for } l = 1, \ldots, L, \tag{3.24}$$

where $\|\mathbf{w}\|^2 = \mathbf{w} \cdot \mathbf{w}$, ξ is a soft margin constant [83], and $I_{\{X\}}$ is the indicator function which is one if X is true; and is zero, otherwise.

The optimization problem defined in (3.21)–(3.24) is non-convex due to $I_{\{\delta^{(l)}>1\}}$ in the objective function. Since $\delta^{(l)} > 1$ for misclassification, $\sum_{l=1}^{L} \delta^{(l)}$ gives a bound on the number of the misclassified training energy vectors. Therefore, $\sum_{l=1}^{L} \delta^{(l)}$ can be used to measure the number of the training energy vectors which are misclassified by the decision surface $\mathbf{w} \cdot \phi(\mathbf{y}^{(l)}) + w_0 = 0$ as well as the number of the training energy vectors that are correctly classified but they lie in the slab $-1 < \mathbf{w} \cdot \phi(\mathbf{y}^{(l)}) + w_0 < 1$. Hence, I can rewrite the optimization problem as a convex optimization problem as follows:

$$\text{minimize} \quad \frac{1}{2}\|\mathbf{w}\|^2 + \xi \sum_{l=1}^{L} \delta^{(l)} \tag{3.25}$$

$$\text{subject to} \quad a^{(l)}[\mathbf{w} \cdot \phi(\mathbf{y}^{(l)}) + w_0] \geq 1 - \delta^{(l)}, \tag{3.26}$$

$$\text{for } l = 1, \ldots, L, \tag{3.27}$$

$$\delta^{(l)} \geq 0, \quad \text{for } l = 1, \ldots, L. \tag{3.28}$$

The Lagrangian of (3.25)–(3.28) can be written as

$$\Lambda(\mathbf{w}, w_0, \boldsymbol{\delta}; \boldsymbol{\lambda}, \boldsymbol{\gamma}) = \frac{1}{2}\|\mathbf{w}\|^2 + \xi \sum_{l=1}^{L} \delta^{(l)} - \sum_{l=1}^{L} \lambda^{(l)} \left\{ a^{(l)}[\mathbf{w} \cdot \phi(\mathbf{y}^{(l)}) + w_0] - 1 + \delta^{(l)} \right\} - \sum_{l=1}^{L} \gamma^{(l)} \delta^{(l)}, \tag{3.29}$$

where $\lambda^{(l)}$ and $\gamma^{(l)}$ are Lagrangian multipliers. By applying the Karush-Kuhn-Tucker (KKT) conditions, I can obtain

$$\mathbf{w} = \sum_{l=1}^{L} \lambda^{(l)} a^{(l)} \phi(\mathbf{y}^{(l)}) \tag{3.30}$$

$$\sum_{l=1}^{L} \lambda^{(l)} a^{(l)} = 0 \tag{3.31}$$

$$\lambda^{(l)} = \xi - \gamma^{(l)}. \tag{3.32}$$

It is noticeable that $\gamma^{(l)} \geq 0$ and $0 \leq \lambda^{(l)} \leq \xi$. The vector of $\lambda^{(l)}$'s is known as a support vector. Hence, I can obtain the dual problem in terms of the support vector as follows [83]:

$$\text{maximize} \quad \sum_{l=1}^{L} \lambda^{(l)} - \frac{1}{2} \sum_{i=1}^{L} \sum_{j=1}^{L} \lambda^{(i)} \lambda^{(j)} a^{(i)} a^{(j)} \{ \phi(\mathbf{y}^{(i)}) \cdot \phi(\mathbf{y}^{(j)}) \} \tag{3.33}$$

$$\text{subject to} \quad \sum_{l=1}^{L} \lambda^{(l)} a^{(l)} = 0 \tag{3.34}$$

$$0 \leq \lambda^{(l)} \leq \xi, \quad \text{for } l = 1, \ldots, L. \tag{3.35}$$

The KKT conditions uniquely characterize the solution of the primal problem as (3.30)–(3.32), and the dual problem as two active constraints $\lambda^{(l)} \left\{ a^{(l)}[\mathbf{w} \cdot \phi(\mathbf{y}^{(l)}) + w_0] - 1 + \delta^{(l)} \right\} = 0$ and $\gamma^{(l)} \delta^{(l)} = (\xi - \lambda^{(l)}) \delta^{(l)} = 0$. I can solve the optimization problem in (3.33)–(3.35) by using standard techniques to solve a quadratic program. Let $\widetilde{\lambda}^{(l)}$ denote the solution of

(3.33)–(3.35).

Finally, the nonlinear decision function can be obtained as

$$d(\mathbf{x}) = \mathrm{sgn}\left(\sum_{l=1}^{L} \widetilde{\lambda}^{(l)} a^{(l)} \kappa(\mathbf{x}, \mathbf{y}^{(l)}) + w_0\right), \tag{3.36}$$

where sgn is the sign function and $\kappa(\mathbf{x}, \mathbf{y}) = \phi(\mathbf{x}) \cdot \phi(\mathbf{y})$ is the kernel function. Some of the commonly used kernel functions are linear, polynomial, and Gaussian radial basis functions [83]. After the classifier obtains the decision function, the classifier can categorize the test energy vector $\mathbf{y}^*$ as

$$\widehat{a} = d(\mathbf{y}^*). \tag{3.37}$$

Note that the bias w_0 can be derived by solving the optimization problem (3.25)–(3.28) after finding the optimal $\mathbf{w}$.

Remark: If L denotes the the number of training energy vectors and L_s denotes the the total number of support vectors, then the expected error rate is bounded by $\mathrm{E}[error] \leq \mathrm{E}[L_s]/L$ [84]. The expectation is taken over the training set generated from the distribution of energy vectors. Note that this bound is independent of the dimension of the feature space that is determined by ϕ. Furthermore, if I can map the original feature space to the higher dimensional feature space (i.e., the feature space of ϕ) so that it separates the training energy vectors by using a small number of support vectors, the expected error becomes lower. Hence, it is important to select a kernel function which reduces the number of support vectors.

3.5.3 Weighted K-Nearest-Neighbor

The weighted K-nearest-neighbor (KNN) is a classification technique based on the majority voting of neighbors. For a given test energy vector $\mathbf{y}^*$, the KNN classifier finds K neighboring training energy vectors among $\overline{\mathbf{y}} = \{\mathbf{y}^{(1)}, \ldots, \mathbf{y}^{(L)}\}$ based on a particular distance measure. I define $\Delta(\mathbf{x}, \mathbf{y})$ as a distance between the energy vectors $\mathbf{x}$ and $\mathbf{y}$. To find the neighboring training energy vectors, the KNN classifier calculates $\Delta(\mathbf{y}^*, \mathbf{y}^{(l)})$ for all $\mathbf{y}^{(l)}$'s and sorts the training energy vectors in the ascending order of $\Delta(\mathbf{y}^*, \mathbf{y}^{(l)})$. Then, the KNN classifier selects the first K training energy vectors as neighbors. Let $\Phi(\mathbf{y}^*, \overline{\mathbf{y}})$ denote the set of neighbors of $\mathbf{y}^*$ among $\overline{\mathbf{y}}$. To determine the class of $\mathbf{y}^*$, I count the number of neighbors that belong to the channel available class and the channel unavailable class, respectively. The number of the neighbors in the channel available class ($a = 1$) and the channel unavailable class ($a = -1$) is defined as

$$\nu(a; \mathbf{y}^*, \overline{\mathbf{y}}) = |\{l = 1, \ldots, L | a^{(l)} = a, y^{(l)} \in \Phi(\mathbf{y}^*, \overline{\mathbf{y}})\}|. \tag{3.38}$$

The KNN classifier categorizes $\mathbf{y}^*$ as the channel unavailable class (i.e., $\widehat{a} = -1$) if and only if

$$\frac{\nu(-1; \mathbf{y}^*, \overline{\mathbf{y}})}{\nu(1; \mathbf{y}^*, \overline{\mathbf{y}})} \geq \varphi, \tag{3.39}$$

where φ is a constant that controls the tradeoff between the false alarm and the misdetection probabilities.

The distance $\Delta(\mathbf{x}, \mathbf{y})$ can be calculated in various ways. In this dissertation, I adopt a weighted distance measure where each component of the energy vector is weighted by a certain weight factor. The weight factor for the nth component of the energy vector is denoted by ω_n. To calculate ω_n, I draw an ROC curve by using the nth components of

the training energy vectors (i.e., $y_n^{(1)}, \ldots, y_n^{(L)}$) and the corresponding channel availabilities (i.e., $a_n^{(1)}, \ldots, a_n^{(L)}$). Then, the weight factor ω_n is equal to the area-under-the-ROC-curve (AUC) of the nth components of the training energy vectors. If I consider the squared Euclidean distance, the distance measure is given as

$$\Delta(\mathbf{x}, \mathbf{y}) = \sum_{n=1}^{N} \{\omega_n (x_n - y_n)\}^2. \tag{3.40}$$

On the other hand, if I adopt the city block distance, we have

$$\Delta(\mathbf{x}, \mathbf{y}) = \sum_{n=1}^{N} |\omega_n (x_n - y_n)|. \tag{3.41}$$

Remark: If the number of neighbors (i.e., K) is fixed and the number of training energy vectors approaches infinity, then all the K neighbors converge to $\mathbf{y}^*$. Hence, the label of each of the K-nearest-neighbors is a random variable which takes the value of a with probability $\Pr[A = a|\mathbf{Y} = \mathbf{y}^*]$ [84]. When the number of neighbors, K, increases, the proportion of each label of the neighbors approaches the Bayesian a posteriori probability. Hence, the error probability of the KNN classifier becomes closer to that of the Bayesian classifier with increasing K. In practice, I can have only a limited number of training energy vectors. On the other hand, I want to reduce errors by increasing the number of training energy vectors. This tradeoff forces us to select a reasonable value for K.

3.6 Performance Evaluation and Discussion

3.6.1 Simulation Parameters

In this study, unless otherwise specified, I consider that the SUs participating in cooperative spectrum sensing (CSS) are located in a 5-by-5 (25 SUs) grid topology in a 4000 m $\times$ 4000

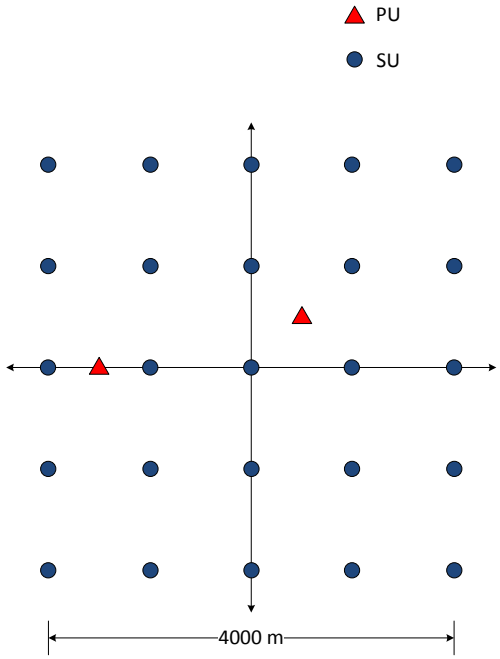

Figure 3.4: The CR network topology used for simulation.

m area as shown in Fig. 3.4. The values of important simulation parameters are as follows: the bandwidth B is 5 MHz, the sensing duration τ is 100 μs, the noise spectral density η is -174 dBm, and the path-loss exponent α is 4. I assume that the standard deviation of shadowing is 8 dB. The transmit power of each PU is 200 mW. I consider two PUs having fixed locations with coordinates (500 m, 500 m) and (-1500 m, 0 m). The probability that a PU is in the active state is 0.5 and the state of each PU is independent of that of the other PU. The proposed algorithms are implemented by using Matlab 7.10.0 (R2010a) in a 64-bit computer with a core i7 processor (clock speed of 2.8 GHz) and 4 GB RAM.

3.6.2 Training Duration for Different Classifiers

The average training durations for different classifiers according to the size of training energy vectors are shown in Table 3.1. The GMM shows relatively high training dura-

Table 3.1: Average training duration (in Seconds) for different classifiers (5×5 SUs)

Classification Methods	**Number of Training Samples**					
	100	**200**	**300**	**400**	**500**	**1000**
Fisher	0.01001	0.01035	0.01067	0.01091	0.01144	0.01346
K-means	0.09202	0.09319	0.09363	0.09455	0.09536	0.11704
GMM	0.0309	0.06621	0.17373	0.24281	0.35527	1.12796
SVM-Linear	0.01114	0.01426	0.01792	0.02114	0.0268	0.06289
SVM-Poly.	0.04986	0.31983	0.46806	0.85701	1.03886	1.65817

Table 3.2: Average classification delay (in Seconds) for different classifiers (5×5 SUs)

Classification Methods	**Number of Training Samples**					
	100	**200**	**300**	**400**	**500**	**1000**
Fisher	5.3×10^{-6}	5.3×10^{-6}	5.3×10^{-6}	5.3×10^{-6}	5.3×10^{-6}	5.3×10^{-6}
K-means	1.9×10^{-5}	1.9×10^{-5}	1.9×10^{-5}	1.9×10^{-5}	1.9×10^{-5}	1.9×10^{-5}
GMM	3.8×10^{-5}	3.8×10^{-5}	3.8×10^{-5}	3.8×10^{-5}	3.8×10^{-5}	3.8×10^{-5}
SVM-Linear	1.92×10^{-5}	3.24×10^{-5}	3.87×10^{-5}	4.45×10^{-5}	4.86×10^{-5}	5.67×10^{-5}
SVM-Polynomial	1.02×10^{-5}	1.12×10^{-5}	1.25×10^{-5}	1.32×10^{-5}	1.53×10^{-5}	2.81×10^{-5}
KNN-Euclidean	4.68×10^{-5}	5.82×10^{-5}	7.72×10^{-5}	8.73×10^{-5}	1.17×10^{-4}	2.98×10^{-4}
KNN-Cityblock	4.62×10^{-5}	5.73×10^{-5}	7.63×10^{-5}	8.57×10^{-5}	1.16×10^{-4}	2.84×10^{-4}

tion (1.12796 seconds for 1000 samples) among the unsupervised classifiers whereas the supervised SVM classifier with the polynomial kernel takes the highest training duration (1.65817 seconds for 1000 samples) among all classifiers. The average training time for the KNN classifier is measured as the uploading time of the training energy vectors to the classifier and it is approximately 50 μs for 1000 energy vectors. Hence, the KNN classification has the capability of changing the training energy vectors more promptly as compared to all other classifiers.

3.6.3 Average Classification Delay for Different Classifiers

Table 3.2 shows the time taken for deciding the channel availability for different classifiers. The classification delay of Fisher linear discriminant, K-means clustering, and GMM classifiers does not change with different batch of training energy vectors. More specifically, the number of decision parameters do not change with the number of training energy vectors even though the values of the decision parameters change slightly with the number of

training energy vectors. Table 3.2 clearly shows that the K-means classifier has the capability to detect channel availability more promptly in comparison to other unsupervised learning approach (i.e., GMM). For supervised learning, the Fisher linear discriminant shows the lowest classification delay. It is important to note that, for the KNN classifier, the classification delay is relatively high even though its training time is found to be the lowest.

3.6.4 Detection Probability for Different Classifiers

Fig. 3.5 compares the performance of different proposed CSS schemes in terms of receiver operating characteristic (ROC) curves for different sets of cooperating SUs when there is only a single PU at (500 m, 500 m). In particular, Figs. 3.5(a) and 3.5(b) show the ROC curves when 3×3 SUs (i.e., 9 SUs) and 5×5 SUs (i.e., 25 SUs) participate in CSS, respectively. These figures clearly reveal that the performances of the proposed classifiers improve with the increasing number of SUs. It is important to notice that all the proposed CSS schemes outperform the existing CSS techniques such as those based on the Fisher linear discriminant analysis, AND-rule, and OR-rule. Fig. 3.5 depicts that the SVM with the linear kernel outperforms the other CSS schemes. The SVM-Linear classifier achieves high detection probability by mapping a feature space to a higher dimension with the help of the linear kernel. Interestingly, Fig. 3.5 clearly shows that the unsupervised K-means classifier achieves the performance comparable to the SVM-Linear classifier. The simple weighted KNN scheme achieves comparatively higher detection probability than the existing CSS techniques due to the exploitation of localized information.

Fig. 3.6 shows the performance of different CSS schemes in terms of the ROC curve when there are two PUs at (500 m, 500 m) and (-1500 m, 0 m). This figure clearly depicts that the SVM classifier with the linear kernel outperforms the other supervised and unsupervised CSS schemes. The computational complexity of the SVM-Linear classifier

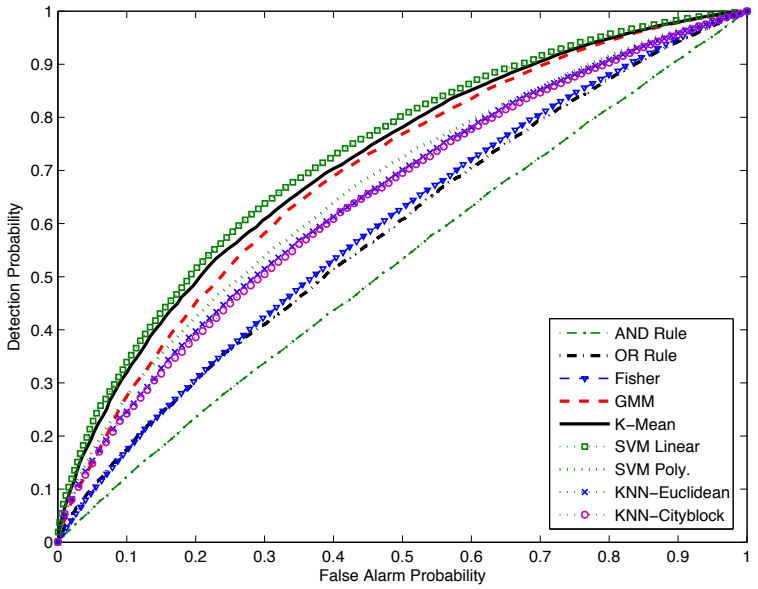

(a) ROC curve for 3-by-3 SU cooperation.

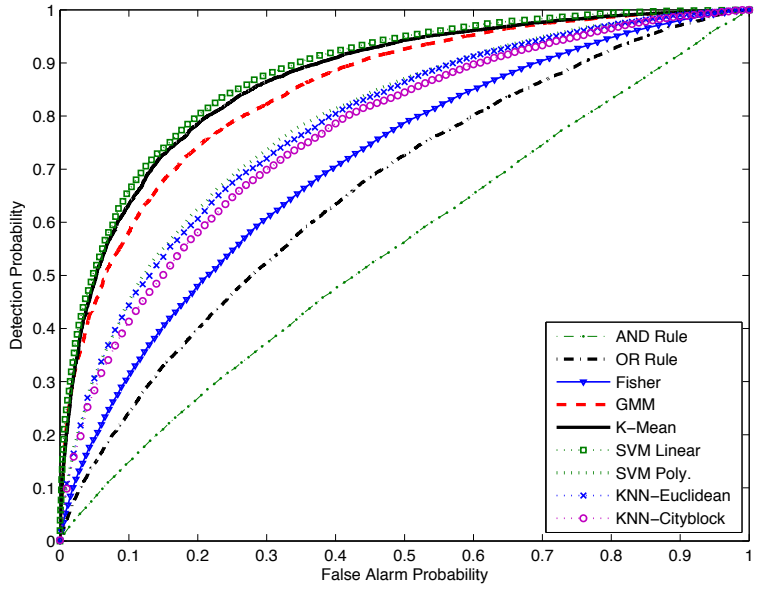

(b) ROC curve for 5-by-5 SU cooperation.

Figure 3.5: The ROC curves when a single PU is present. I use 500 training energy vectors to train each classifier.

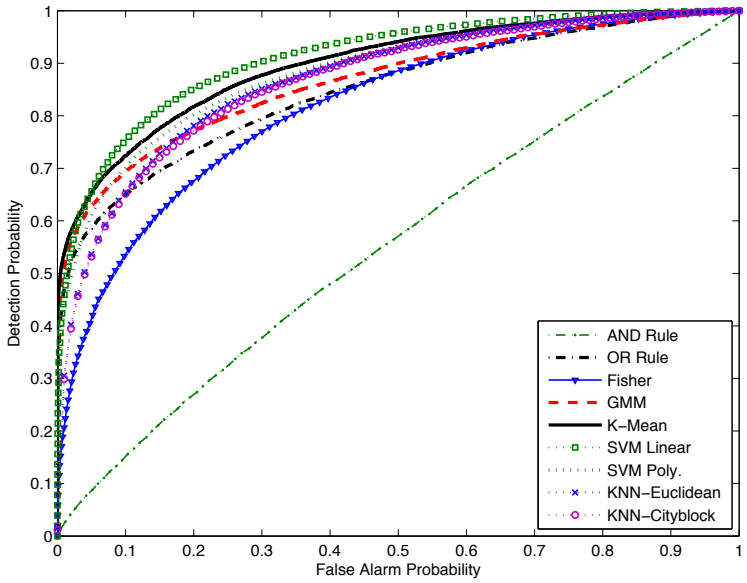

Figure 3.6: The ROC curves when there are two PUs. I use 500 training energy vectors to train each classifier.

can be compensated by its high detection capability and comparatively low training and classification delay. Hence, the SVM classifier with the linear kernel is well-suited for CSS requiring high accuracy. Further, this figure reveals that the K-means clustering scheme outperforms the other unsupervised CSS schemes even in the multiple PU case.

In Fig. 3.7, the detection probabilities for the different CSS schemes are plotted against the transmission power of a PU. The results are obtained for a target false alarm probability of 0.1 when there is a single PU at (500 m, 500 m). This figure shows that all the proposed CSS schemes outperform the existing CSS schemes in all range of the transmission power of a PU. Especially, it is worth noting that the unsupervised learning schemes (i.e., K-means and GMM) achieve performance which is comparable to that of the supervised learning schemes even when the transmission power of a PU is very low.

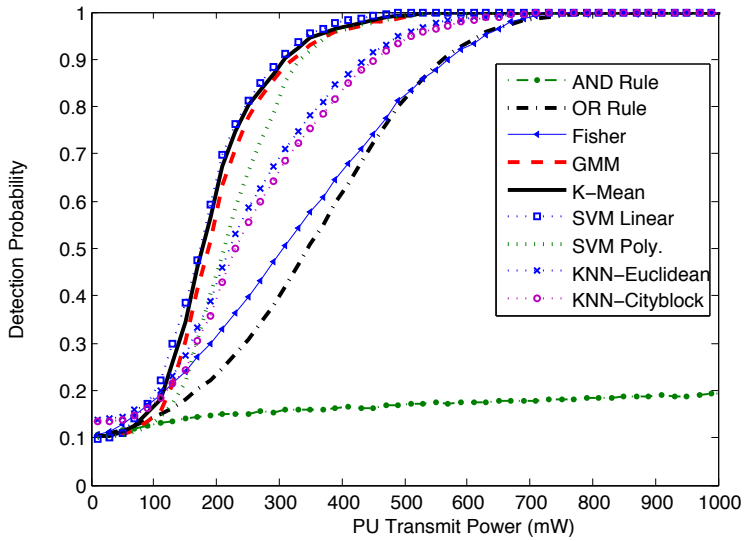

Figure 3.7: The detection probability according to the transmission power of a PU when the false alarm probability is 0.1 and there are 25 (5×5) SUs.

3.6.5 Summary of Results

The main results of the analysis can be summarized as follows:

- The unsupervised K-means clustering is a promising approach for CSS due to its higher PU detection capability and lower training and classification delay. Moreover, its detection probability is very close to the best performing classifier, i.e., the SVM-Linear classifier.

- Compared to all other classifiers, the supervised SVM classifier with the linear kernel performs well in terms of the detection probability. The computational complexity of the SVM-Linear classifier is compensated by its higher detection capability and comparatively lower training and classification delay.

- In terms of updating the training energy vectors on-the-fly, the KNN performs extremely well (training duration for 1000 sample is approximately 50 μs). However, its classification delay is relatively higher than other classifiers.

Table 3.3: Comparison among different CSS classifiers

Classification Methods	**Training Duration**	**Classification Delay**	**ROC Performance**
Fisher Linear Discriminant	Low	Normal	Low
K-Means	Normal	Low	High
GMM	High	Low	High
SVM-Linear	Low	Normal	High
SVM-Poly.	High	Low	Normal
KNN-Euclidean	Low	High	Normal
KNN-Cityblock	Low	High	Normal

A qualitative comparison among the different classifiers is shown in Table 3.3.

3.7 Conclusion

In this chapter, I have designed cooperative spectrum sensing (CSS) mechanisms for cognitive radio networks by utilizing pattern recognition techniques. Specially, I have implemented unsupervised (i.e. K-mean clustering and Gaussian mixture model) and supervised (i.e. support vector machine and K-nearest-neighbour) based learning for cooperative spectrum sensing. The proposed SVM classifier achieves the highest detection performance compared to the other CSS algorithms by mapping the feature space into the higher dimensional space with the help of kernel functions. Further, the unsupervised K-means clustering scheme achieves the performance very close to the supervised SVM-Linear classifier in terms of the ROC performance. In particular, the weighted KNN cognitive classifier requires very small amount of time for training the classifier. Hence, the weighted KNN classifier is well suited for CSS which requires to update training energy vectors on-the-fly.

Chapter 4

A Dynamic Common Control Channel-Based MAC Protocol for Cellular CRNs

In the previous chapter, I have only proposed a cooperative spectrum sensing scheme for cognitive radio networks. However, there should have a mechanism for sending sensing information to the cognitive base station and inform primary user idle channels to the cognitive users. Therefore, in this chapter I propose a novel dynamic common control channel-based medium access control (DCCC-MAC) protocol for cellular cognitive radio networks. Specifically, unlike the traditional dedicated control channel-based MAC protocols, the proposed MAC protocol eliminates the requirement of a dedicated channel for control information exchange. During a given transmission frame, the common control channel (CCC) is selected by a cooperating set of secondary users (SUs) by using support vector machine (SVM)-based learning technique. In the DCCC-MAC protocol, the frame duration is divided into four main phases as follows: spectrum sensing phase, CCC selection phase, data transmission phase, and beaconing phase. The SUs who participate in

the common control channel selection process are allocated channels for data transmission during a frame interval using a scheduling process, while the other SUs have to contend for accessing the channels. I present an analytical approach to calculate the minimum required number of mini-slots in the transmission frame for a given number of SUs in the CCC selection process. The saturation throughput of the proposed MAC protocol is analyzed in closed-form. To this end, the numerical and simulation results are presented to quantify the performance of the proposed DCCC-MAC protocol. I also compare the performance of the DCCC-MAC protocol with that of two other state-of-the-art cognitive radio MAC protocols which use common control channels.

4.1 Introduction

Cognitive radio (CR) is a promising technology for designing wireless communications systems to mitigate the spectrum scarcity problem by improving the utilization of the spectrum. A CR device is an intelligent wireless communication device, which senses its operational electromagnetic environment and can dynamically and autonomously adjust its radio operating parameters. In this context, opportunistic spectrum access (OSA) is a key concept, which allows a CR device to opportunistically access the frequency band allocated to a primary user (PU) when the primary user transmission is detected to be absent [74, 120, 121]. Designing efficient medium access control (MAC) protocols for OSA while limiting the interference imposed on the primary network is a key to the deployment of practical CRNs.

4.1.1 Related Work

The existing MAC protocols for traditional wireless networks cannot be directly applied in CRNs. The authors in [122–124] discuss the main difference of existing multichannel

MAC protocols and cognitive MAC protocols. Specifically, in traditional MAC protocols, the number of channels available for access is fixed whereas the number of channels available for secondary users in a CRN varies with time and space. The different aspects of multichannel cognitive MAC protocols, their functionalities and challenges in their implementations are reviewed in [48, 103, 125]. According to their principle of operation, the existing cognitive MAC protocols in the literature can be categorized dedicated and non-dedicated control channel based MAC protocols.

In [2], the authors propose an opportunistic spectrum access MAC protocol for CRNs assuming that a dedicated CCC is available (which is owned by the cognitive radio network operator) all the time. This approach exploits CCC for data transmission after the ATIM (Ad-Hoc Traffic Indicator Message) window. The authors in [3] propose a cognitive MAC protocol based on CSMA/CA technique by considering the mobility support. A CCC-driven dynamic open spectrum sharing MAC scheme for ad hoc wireless networks is studied in [126]. In [5], an energy-efficient multichannel distributed MAC protocol for multihop CRNs is proposed by dividing the time frame into control phase and data transmission phase. The authors in [127] propose a splitting-based MAC protocol to mitigate the hidden terminal problem in multichannel cognitive networks by using temporal synchronization. A single transceiver-based channel (frequency) hopping protocol is proposed in [127] and the performance of the proposed MAC protocol is evaluated analytically by using a Markov chain. The switching penalty in frequency hopping-based cognitive MAC protocols significantly impacts the performance of such networks.

4.1.2 Motivation and Contribution

In general, since the amount of control information required to broadcast in CRNs is comparatively larger than in conventional wireless networks, the efficiency of the medium ac-

cess control method can be improved by using a CCC. Most of the studies in the literature assume that there exists a dedicated CCC owned by the cognitive operator. This assumption itself challenges the definition of cognitive radios. Further, the fixed and dedicated CCC-based MAC protocols are vulnerable to jamming. This motivates us to design a dynamic CCC-based MAC (DCCC-MAC) protocol for CRNs.

In this protocol, the frame duration is divided into four main phases as follows: spectrum sensing phase, CCC selection phase, data transmission phase, and beaconing phase. In the spectrum sensing phase, the secondary users, who want to transmit, perform spectrum sensing on a subset of all the available channels. In the CCC selection phase, the SUs select the best idle channel based on their own sensing results in the spectrum sensing phase. Then, these SUs send their sensing results through their sensed idle channels to the cognitive radio base station (CR-BS) to decide on the CCC for that frame. The CR-BS decides on the CCC based on the outcome of a support vector machine (SVM) [54, 83, 84], and the decision is broadcast over all the idle channels. In the data transmission phase, all the SUs, who participate in the CCC selection process, are allocated channels directly without any contention process while the other SUs have to follow a contention process for channel access. The beaconing phase is used for synchronizing the CRN.

To the best of my knowledge, the proposed DCCC-MAC protocol would be the first cognitive MAC protocol in the literature that utilizes a dynamically changing in-band CCC. The main contributions of the research can be summarized as follows.

- I propose a dynamic common control channel-based MAC (DCCC-MAC) protocol for CRNs. Specifically, for a set of cooperating SUs, the common control channel during a given frame is selected by employing an SVM-based learning technique. The sensing results of the cooperating SUs are fed into a SVM classifier to determine the activity of PUs on the channels. Then, the one-dimensional decision values of the

SVM are processed for selecting the control channel. As an incentive, the SUs who participate in the CCC selection process are prioritized during the data transmission phase. This prioritization is achieved by scheduling the SUs in the channels without a contention process while the other SUs (who do not participate in the CCC selection process) contend for channel access.

- The proposed DCCC-MAC protocol is capable of implicitly learning the surrounding environment cooperatively in an online fashion. Since the CCC is selected based on the learning decision, the proposed MAC protocol eliminates the requirement of dedicated channel for control information exchange. Also, due to the dynamic nature of the CCC, the proposed DCCC-MAC protocol is able to withstand against control channel jamming problem. Further, this protocol is much more adaptive than the traditional cognitive MAC protocols, which needs prior knowledge about the environment for optimization.

- The effect of multiple channel hidden terminal problem in the existing MAC protocols with single transceiver is mitigated in the proposed MAC protocol by prioritizing the channel access of scheduled SUs. This MAC protocol mitigates not only the multichannel hidden terminal problem but also the PU hidden terminal problem due to the cooperative PUs idle channels detection.

- An analytical approach is proposed to calculate the minimum required number of minislots for a given number of SUs participating in the control channel selection process. Further, the saturation throughput of the proposed MAC protocol is analyzed in closed-form.

4.2 System Model and Assumptions

I consider a CRN consisting of a CR-BS and N cognitive users. Henceforth, a cognitive user in the CRN is called as an SU and the SUs are indexed by $n = 1, \ldots, N$. I assume that every SU is equipped with a single half-duplex transceiver and it is capable of switching channels as required. I assume that due to the hardware constraints, the SUs can sense only $\bar{\mathcal{K}}$ channels out of $\mathcal{K}$ channels. The set of channels considered and the set of channels sensed at a given frame are denoted by $\boldsymbol{\mathcal{K}}$ and $\bar{\boldsymbol{\mathcal{K}}}$, respectively. The control information is exchanged by using a CCC and the index of this channel varies from frame to frame. For selection of the CCC, at the beginning of every frame, each SU estimates the received energy level on a chosen set of channels ($\bar{\boldsymbol{\mathcal{K}}}$) and reports it to the CR-BS via the best predicted (based on individual sensing) idle channel. The processes of reporting the sensing results and selecting the CCC are discussed in Section 4.3.2.

In this thesis, I adopt a generalized PU activity model where multiple PUs alternate between active and inactive states. There are M PUs, each of which is indexed by $m = 1, \ldots, M$. Let $S_{m,k}$ indicate the state of m-th PU's activity on k-th channel. I have $S_{m,k} = 1$ if the m-th PU is in the active state on k-th channel (i.e., PU m transmits a signal on the k-th channel); and $S_{m,k} = 0$ otherwise. Let $\mathbf{S}_k = (S_{1,k}, \ldots, S_{M,k})^T$ denote the vector of the states of all PUs on the k-th channel, where the superscript T denotes the transpose operation. If at least one PU is active on the k-th channel (i.e., $\mathbf{S}_k = 1$), then the k-th channel is considered to be unavailable for the SUs to access. The channel is available for cognitive transmission only when there is no PU in the active state (i.e., $\mathbf{S}_k = 0$). Hence, the availability of k-th channel can be denoted as follows:

$$A_k = \begin{cases} 1, & \text{if } S_{m,k} = 1 \text{ for some } m \\ -1, & \text{if } S_{m,k} = 0 \text{ for all } m. \end{cases} \tag{4.1}$$

Table 4.1: List of notations

N	Total number of SUs in the cognitive network
$\overline{N}$	Number of SUs expected to cooperate for spectrum sensing
N_i	Number of SUs transmitting their sensing results to CR-BS in the i-th mini-slot
$\overline{N}_i$	Average number of SUs successfully transmitting their sensing results in the i mini-slot
N_b	Minimum number of mini-slots required to send the sensing results from N SUs to CR-BS
$\overline{N}_{N_b}$	Number of SUs transmit their sensing results within N_b mini-slots or number of SUs participate for cooperative spectrum sensing or number of SUs scheduled for data transmission
M	Total number of PUs
$\overline{\mathcal{K}}$	Number of channels sensed at a given frame
$\mathcal{K}$	Total number of channels available for sensing
$\overline{\boldsymbol{\mathcal{K}}}$	Set of channels sensed
$\boldsymbol{\mathcal{K}}$	Set of channels available for sensing
τ	Sensing duration
B	Bandwidth of a channel
P_s	Transmission probability of an SU within a mini-slot in the CCC selection phase if the SU has not successfully transmitted in the previous mini-slot
P_b	Probability that a PU is active in a given channel
$\overline{\kappa}$	Average number of idle channels available for cognitive transmission
$\overline{\mathbf{y}}$	Training energy vector for SVM
$\overline{a}$	Channel availability (idle/busy) vector corresponding to a training an energy vector
ϕ	Non-linear mapping function
$\mathbf{w}$	Weighting vector of ϕ
w_0	Bias value used in the SVM to determine the classification hyperplane
$\delta^{(l)}$	Slack variable, $l = 1, \ldots, L$
ξ	Soft margin constant
L	Number of training samples for SVM
W	Maximum size of contention window
t	Number of times the algorithm executes
T_k	Number of times the k-th channel is sensed
Γ	Number of SUs contending for channel access
$\mathbf{S}_k$	Vector of the states of all PUs on k-th channel
$S_{m,k}$	State of m-th PU's activity on k-th channel
$\mathbf{P}_{\boldsymbol{\Theta}}$	Relative channel idle probability w.r.t. the CCC
T_S	Total time for spectrum sensing
T_{SCCC}	Time duration for the CCC selection phase
T_D	Time duration for the data transmission phase
T_B	Time duration for the beaconing phase
t_{IB}	Time to select the best idle channel based on individual sensing
t_{SSR}	Time duration to send sensing results to the CR-BS
t_{SSR-ms}	Mini-slot duration in the CCC selection phase
t_{D-ms}	Mini-slot duration in the data transmission phase
$t_{S_{ccc}}$	Time required to execute the CCC selection process based on SVM
$t_{I_{ccc}}$	Time required to inform the CCC to the SUs
t_{D-TS}	Time to transmit $Transmission\_Setup$ message

4.3 Dynamic CCC-Based Medium Access Control Protocol

In this section, I propose a dynamic CCC-based MAC protocol for opportunistic spectrum access in CRNs and refer to this as the DCCC-MAC in the sequel.

In the DCCC-MAC protocol, I assume that all the SUs exchange their control information through the selected CCC and the CR-BS transmits a periodic beacon in all of the idle channels to synchronize the SUs. The beacon period (frame duration) is divided into four phases as shown in Fig. 4.1 and these phases are referred to as sensing phase, CCC selection phase, data transmission phase, and synchronization phase. The operational flow of each phase is illustrated in the block diagram in Fig. 4.2.

In the sensing phase, the SUs perform fast sensing in a given set of channels. The set of channels required to be sensed in the next frame is informed by the beacon at the end of the beacon period. Henceforth, the beacon period is referred to as the frame duration. At the beginning of the CCC selection phase, every SU informs its sensing result to the CR-BS through the best idle channel. Then, an SVM [54, 83, 84]-based algorithm is used to select the CCC for the current frame. The information about the CCC and the list of idle channels are broadcast to the SUs by using all the channels in which PUs are absent. The data transmission phase is utilized by the SUs for cognitive communications while the synchronization of secondary communication is achieved by broadcasting a beacon in the synchronization phase. The detailed descriptions of the phases in the DCCC-MAC protocol are presented below.

4.3.1 Spectrum Sensing Phase

I assume that out of $\mathcal{K}$ channels only $\bar{\mathcal{K}}$ channels are selected for sensing at a given frame duration. At the beginning of the spectrum sensing phase, I assume that every SU knows the list of channels that need to be sensed in the current frame. This information is broadcast

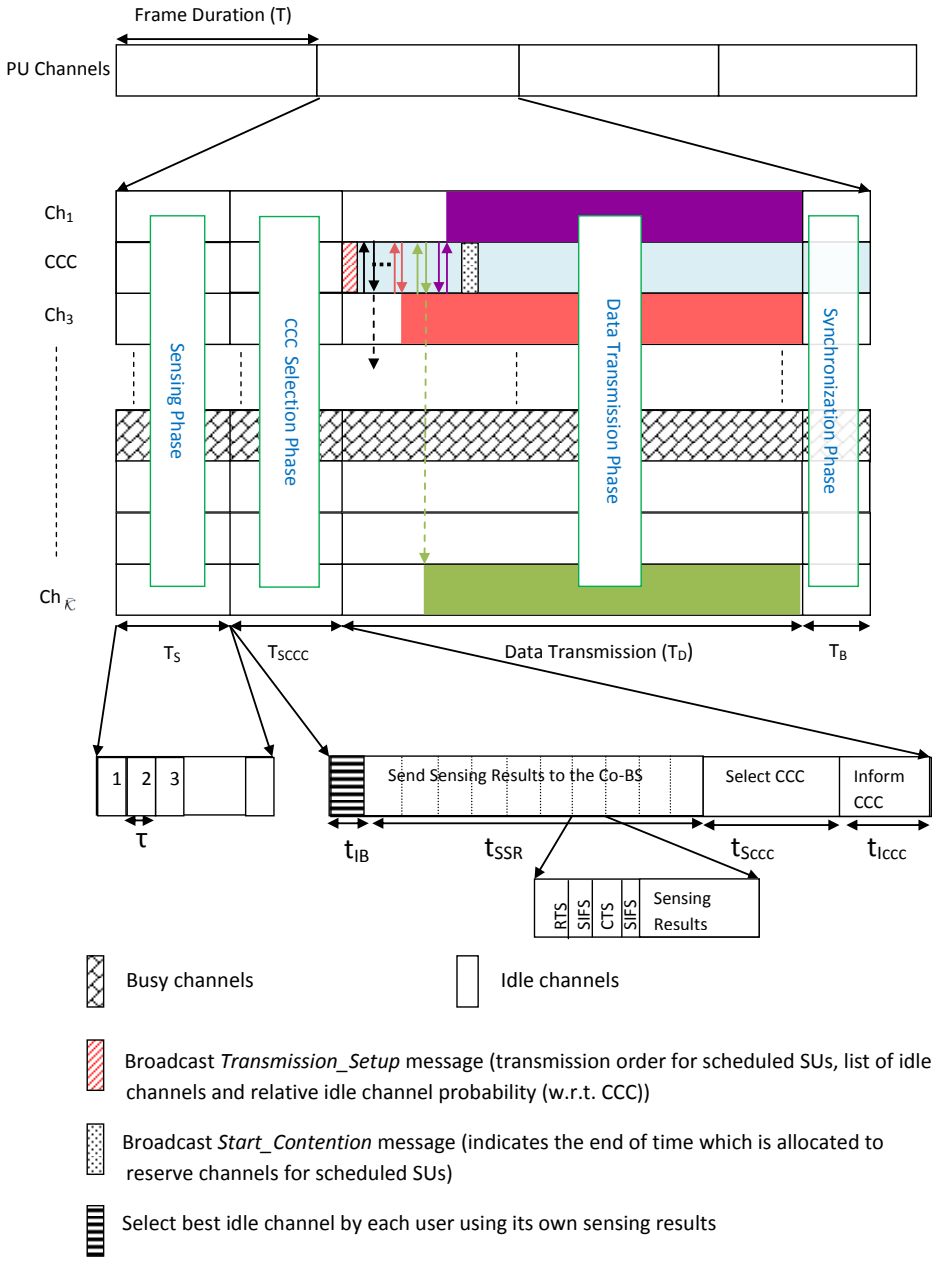

Figure 4.1: Frame structure of the DCCC-MAC protocol.

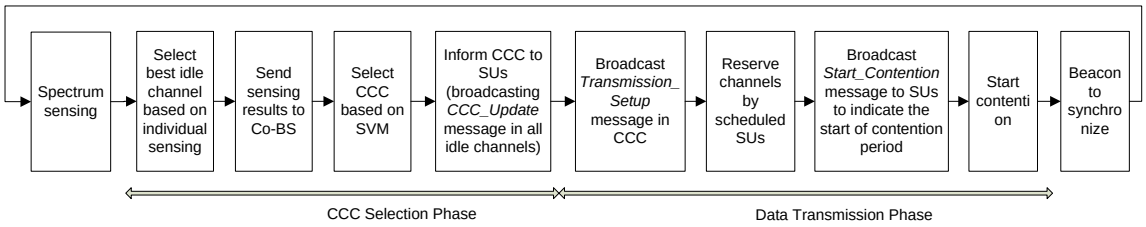

Figure 4.2: The operation of the DCCC-MAC protocol.

by the CR-BS with the beacon at the end of previous frame during the synchronization phase. The details of the algorithm which updates the list of the channels to be sensed is shown in **Algorithm** 3 in Section 4.3.4. In case of a loss of the sensing list update message, a particular SU selects a random set of $\bar{K}$ channels and does spectrum sensing. Every listed channel is sensed in sequence by the SUs for a time duration of τ and the total time period for spectrum sensing can be expressed as

$$T_S = \tau \bar{K}. \tag{4.2}$$

The received normalized energy within τ duration at n-th SU on k-th channel is given by (3.4).

4.3.2 CCC Selection Phase

The CCC selection phase is the core of the proposed DCCC-MAC protocol. Four main functionalities are executed during the CCC selection phase the duration of which is T_{SCCC}. At the beginning of the CCC selection phase, every SU selects the best idle channel based on the individual sensing and then informs the sensing result to the CR-BS via the selected best channel. Then, the CR-BS selects the CCC channel for that frame duration based on an SVM-based approach to be described in Section 4.4.2. Finally, the CR-BS informs (broadcasts) the information about the selected CCC and the list of idle channels to the SUs

via the idle channels.

Select the best idle channel based on individual sensing

Since the SUs do not have any dedicated channel for sending the sensing results to the CR-BS without interfering the PUs, each SU needs to find a channel. Every SU selects the channel, which has the minimum received normalized energy, as the candidate channel for sending the sensing results to the CR-BS. The candidate channel for the n-th SU can be selected as follows:

$$Ch_{n,best} = \arg\min\{Y_{n,k}\}, \quad \forall k. \tag{4.3}$$

Although $Ch_{n,best}$ is a candidate channel for transmitting the sensing results, I cannot guarantee that there is no PU activity on that channel. Therefore, I protect the PUs from the harmful interference only by transmitting sensing results if the received energy of the $Ch_{n,best}$ is less than a predefined value δ (i.e., $\min\{Y_{n,k}\} < \delta$). If $\min\{Y_{n,k}\} \geq \delta$, that particular SU does not transmit its sensing result to the CR-BS. Let us denote by t_{IB} the time to select the best idle channel based on individual sensing.

Inform the sensing results to the CR-BS

Let t_{SSR} denote the time duration to send the sensing results of the SUs to the CR-BS. Every SU sends the *log* value of its sensing result to the CR-BS using its best channel ($Ch_{n,best}$). The reliability of the selection of CCC and the selection of idle channel increases with the increasing number of cooperating SUs.

Let us assume that the number of SUs expected to participate in the decision making process is $\bar{N}$. That is, the CR-BS needs the sensing results at least from $\bar{N}$ SUs. I assume

that the transmission period for the sensing results is divided into mini-slots and the duration of each mini-slot is t_{SSR-ms}. The transmission probability of a particular SU in a given mini-slot during the CCC selection phase is P_s if that SU has not successfully transmitted its sensing result in one of the previous mini-slots. During the CCC selection phase, the successfully transmitted SUs do not contend in the forthcoming mini-slots. At the beginning of each mini-slot during the CCC selection phase, the SUs transmit request-to-send (RTS) packets with probability P_s. If the CR-BS receives that RTS without collision, then the CR-BS sends a clear-to-send (CTS) packet on that channel. Upon reception of the CTS packet that particular SU sends its sensing results to the CR-BS and receives acknowledgement (ACK) within the mini-slot. The transmission of sensing result within a mini-slot is illustrated in Fig. 4.1. In case of RTS collision, the SUs wait for the next mini-slot to transmit the sensing results until t_{SSR} duration is spent.

The time duration allocated for t_{SSR} varies from frame to frame based on the number of mini-slots required to send the sensing results from $\bar{N}$ SUs to the CR-BS. The number of mini-slots varies based on the number of SUs and the number of idle channels in the network. The time duration to send results from $\bar{N}$ SUs to the CR-BS can be expressed as

$$t_{SSR} = N_b t_{SSR-ms} \tag{4.4}$$

where N_b is the minimum number of mini-slots required to send the sensing results from $\bar{N}$ SUs to the CR-BS. The value of N_b is broadcast to all of the SUs by the CR-BS with the beacon. The calculation of N_b will be shown in Section 4.4.2.

Select CCC

Out of all the idle channels, the channel which is likely to be the most reliable idle channel is selected as the CCC. For this, the SVM-based classification [54, 83, 84] is used, which

is a learning tool with high predictive power. In this approach, not only the CCC is selected but also the idle channels (i.e., channels in which there is no PU activity) are also detected cooperatively. Therefore, the proposed approach mitigates the hidden terminal problem in spectrum sensing. The details of the proposed SVM-based method are given in Section 4.4.2. Let $t_{S_{ccc}}$ denote the time required to execute CCC selection base on SVM.

Inform the CCC to the SUs

After the duration of t_{SSR} for updating the sensing results during the CCC selection phase, the synchronized SUs keep listening to their best idle channels with the hope of receiving the CCC_Update message. Meanwhile, the CR-BS executes the CCC selection process. After deciding on the CCC, the CR-BS broadcasts a CCC_Update message to all the SUs in all the idle channels. The CCC_Update mesaage only contains the index of the channel which is selected as the CCC for the current frame. All the SUs which receive the CCC_Update message tune to the CCC for exchanging control information to obtain channel reservation. Let $t_{I_{ccc}}$ denote the time required to inform the CCC to the SUs.

In this proposed DCCC-MAC protocol, the RTS message contains one bit additional field compared to the traditional RTS message. This additional bit field is used to indicate whether the SUs have information about the CCC or not. If a particular SU does not know about the CCC, it obviously does not know about the idle channels determined during the CCC selection phase, the relative channel idle probability, and the channel allocations for SUs. Let us denote this indicator bit field as $cccIndicator$. When a particular user knows about the CCC, $cccIndicator$ is set to 1. Otherwise, $cccIndicator$ is set to 0. This additional bit field is used to improve the scalability and robustness of the proposed MAC protocol as will be described in section 4.6.1.

4.3.3 Data Transmission Phase

Throughout the data transmission phase, the CCC is utilized only for exchanging control information and this period is divided into mini-slots with the size of t_{D-ms}. The mini-slot duration in the data transmission phase is good enough to send and receive the RTS and CTS messages, respectively. At the beginning of a data transmission phase, in the CCC, the CR-BS broadcasts a $Transmission\_Setup$ message containing the list of the scheduled SUs, channel reservation order for scheduled SUs, indices of the idle channels, and the relative channel idle probability with respect to the CCC ($\mathbf{P_{\Theta}}$). The $Transmission\_Setup$ message is transmitted within t_{D-TS} duration and I assume that the size of this message is an integer multiple of t_{D-ms} for the convenience of implementation. Let $t_{D-TS} = \nu t_{D-ms}$, where ν denotes the number of mini-slots required to transmit the $Transmission\_Setup$ message. The SUs, which send their sensing results to the CR-BS for cooperative decision making, are treated as scheduled SUs. The relative channel idle probability, $\mathbf{P_{\Theta}}$, can be calculated as illustrated in **Algorithm** 3. The channel reservation order for the scheduled SUs is a vendor specific function. In this thesis, I assume that the scheduled SUs are ordered in an ascending order based on SUs' indices and the one which has a lower SU index gets the chance to reserve a channel first.

The SUs which receive the $Transmission\_Setup$ message know their channel reservation order and send the reservation requests in sequence. Every scheduled SU sends an RTS message with the index of its best available channel to the CR-BS and the CR-BS sends a CTS message confirming the reservation. I assume that each of the SUs in the CRN maintains a possible-channel-allocation list based on its channel quality metric and selects the best available channel from the possible-channel-allocation list for its reservation. I assume that the possible-channel-allocation list is updated based on the relative channel idle probability ($\mathbf{P_{\Theta}}$) and the channel which has the highest relative probability is

treated as the best channel for SUs. With an allocation of a channel, every SU updates its possible-channel-allocation list by removing the index of the allocated channel from the list. This is possible since all the SUs can decode the RTS and CTS messages in the CRN. Therefore, the SUs know the list of channels currently available for possible allocation. This process continues until the end of scheduled channel reservation period ($\bar{N}_{N_b} t_{D-ms}$) or all the idle channels have been allocated. Here, $\bar{N}_{N_b}$ is the number of SUs participating in the cooperative decision making process (or in other words, the number of SUs which have successfully transmitted their sensing results to the CR-BS within N_b mini-slots).

At the end of the channel reservation period for scheduled SUs or when all the idle channels have been allocated, the CR-BS broadcasts a $Start\_Contention$ message indicating the start of contention for the remaining SUs in the network. The $Start\_Contention$ message is broadcast within a single mini-slot. Then, the SUs which receive information about the CCC but are not scheduled (i.e., the SUs which did not participate in the CCC selection process) start to contend for a channel. Note that, if all the idle channels are allocated among the schedule users, then all the SUs who receive information about the CCC but are not allocated channels for data transmission have to wait until the next beacon since no more allocation is possible.

At first, the remaining synchronized SUs choose a random backoff value from a closed window $[0, W-1]$, where W is the maximum size of the contention window. The remaining data transmission period in a frame may consist of more than one contention windows since the value of W is predefined. Specifically, a single mini-slot duration (t_{D-ms}) is considered as a single backoff period and the SUs decrement their backoff timer values by one after every mini-slot duration. Until its backoff counter expires, an SU listens to the CCC with the intention of updating the list of channels it may possibly access. Once its backoff timer reaches zero, the SU starts the channel reservation process by transmitting an RTS packet

with its best channel index. Right after receiving the CTS from the CR-BS, the SU starts its transmission on the reserved channel until the next beacon is received. If the RTS packet collides with another packet, that SU has to wait for the next backoff window or next data transmission phase for transmitting its data.

4.3.4 Beacon Phase

All the synchronized SUs (i.e., those SUs who do not get reservation in the current frame) know their remaining time for next beacon since the time stamp for next beacon is transmitted with the channel reservation CTS. Therefore, all the synchronized SUs get ready to receive beacon on their current reserved channel or the best idle channel. The CR-BS broadcasts its beacon in all the idle channels. In the beacon, the CR-BS transmits the list of channels to be sensed in the next frame and the minimum number of mini-slots (N_b) required for at least $\bar{N}$ SUs participating in the cooperative decision making process (i.e., to select the CCC channel and detect the idle channels). The number of mini-slots required for $\bar{N}$ SUs particpating in the CCC selection process will be calculated in Section 4.4.1. The list of channels to be sensed in the next time slot is updated offline by using **Algorithm** 3, which is presented in Section 4.4.3.

4.4 Cooperative Spectrum Sensing and Selection of CCC

In this section, I calculate the minimum number of mini-slots required for at least $\bar{N}$ SUs to cooperating in spectrum sensing. Then, I present an SVM-based method to determine the CCC as well as estimate the availability of the channels. To this end, I present an algorithm for selecting the channels to be sensed by the SUs.

4.4.1 Calculation of the Minimum Number of Mini-Slots Required for at least $\bar{N}$ SUs to cooperate in spectrum sensing, N_b

At the beginning of every frame the exact number of synchronized SUs in the network and the number of idle channels in the network are unknown. Therefore, N_b is calculated based on the average number of idle channels and the number of SUs in the previous frame. Since the number of SUs in a network does not change drastically from one frame to another, it is reasonable to calculate N_b based on the number of SUs in the previous frame.

Let $\bar{\kappa}$ $(1 \leq \bar{\kappa} \leq K)$ be the average number of idle channels available for cognitive transmission and P_p be the probability that a PU is active in a given channel. Hence, the average number of idle channels available for cognitive transmission in a given frame can be expressed as

$$\bar{\kappa} = \bar{\mathcal{K}}(1 - P_p)^{\mathcal{M}}. \tag{4.5}$$

Assuming that each idle channel has equal probability ($\frac{1}{\bar{\kappa}}$) to be the best idle channel sensed by an individual SU, the probability that r SUs select a given channel (P_r) can be written as

$$P_r = \binom{N}{r} \left(\frac{1}{\bar{\kappa}}\right)^r \left(1 - \frac{1}{\bar{\kappa}}\right)^{(N-r)}. \tag{4.6}$$

The probability of successful transmission of a packet in a mini-slot, given that r SUs contend for transmission, can be expressed as

$$P_{(S|r)} = rP_s(1 - P_s)^{(r-1)} \tag{4.7}$$

where P_s is the average SU transmission probability in a given mini-slot during the CCC

selection phase. Hence, the average transmission probability in a given channel at first mini-slot ($P_{1,ccc}$) in the CCC selection phase can be expressed by using (4.6) and (4.7) as follows:

$$\begin{aligned} P^0_{1,ccc} &= \sum_{r=1}^{N_1} P_r P_{(S|r)} \\ &= \sum_{r=1}^{N_1} \binom{N_1}{r} r P_s (1-P_s)^{(r-1)} \Big(\frac{1}{\bar{\kappa}}\Big)^r \Big(1-\frac{1}{\bar{\kappa}}\Big)^{(N_1-r)} \end{aligned} \tag{4.8}$$

where $N_1 = N$. Notice that every SU selects its best idle channel for transmitting the sensing results to the CR-BS based on its individual sensing result and the selected idle channel may not be idle due to the hidden terminal problem. Hence, by taking into account the effect of errors in the selection of the best idle channel, I can rewrite the successful transmission probability in the first mini-slot as follows:

$$P_{1,ccc} = \sum_{r=1}^{N_1} \binom{N_1}{r} r P_b P_s (1-P_s)^{(r-1)} \Big(\frac{1}{\bar{\kappa}}\Big)^r \Big(1-\frac{1}{\bar{\kappa}}\Big)^{(N_1-r)} \tag{4.9}$$

where P_b is the probability that the selected channel is idle. Hence, the average number of SUs successfully transmitting in the first mini-slot can be expressed as

$$\bar{N_1} = \Big\lfloor \bar{\kappa} P_{1,ccc} \Big\rfloor. \tag{4.10}$$

Hence, the average number of SUs left for transmitting their sensing results in the second mini-slot is $N_2 = N - \lfloor \bar{\kappa} P_{1,ccc} \rfloor$. Then, the average number of SUs successfully transmitting within the first and second mini-slots can be written as follows:

$$\bar{N_2} = \lfloor \bar{\kappa} \sum_{j=1}^{2} P_{j,ccc} \rfloor \tag{4.11}$$

where

$$P_{2,ccc} = \sum_{r=1}^{N_2} \binom{N_2}{r} \binom{r}{1} P_b P_s (1-P_s)^{(r-1)} \left(\frac{1}{\bar{\kappa}}\right)^r \left(1-\frac{1}{\bar{\kappa}}\right)^{(N_2-r)}. \tag{4.12}$$

Similarly, the successful transmission probability in the i-th mini-slot and the number of SUs successfully transmitting within i mini-slots can be expressed in closed-form as in (4.13) and (4.14), respectively, as follows:

$$P_{i,ccc} = \sum_{r=1}^{N_i} \binom{N_i}{r} r P_b P_s (1-P_s)^{(r-1)} \left(\frac{1}{\bar{\kappa}}\right)^r \left(1-\frac{1}{\bar{\kappa}}\right)^{(N_i-r)} \tag{4.13}$$

$$\bar{N}_i = \lfloor \bar{\kappa} \sum_{j=1}^{i} P_{j,ccc} \rfloor. \tag{4.14}$$

Note that, in (4.13), N_i ($= N - \left\lfloor \bar{\kappa} \sum_{j=1}^{i-1} P_{j,ccc} \right\rfloor$) is the number of SUs transmitting their sensing results to the CR-BS in the i-th mini-slot. Therefore, the minimum number of mini-slots (N_b) required to successfully send at least $\bar{N}$ samples (i.e., from N SUs) can be obtained as

$$N_b = \sum_i I(\bar{N}_i \leq \bar{N}). \tag{4.15}$$

where

$$I(\bar{N}_i \leq \bar{N}) = \begin{cases} 1, & \text{if } \bar{N}_i \leq \bar{N} \\ 0, & \text{otherwise.} \end{cases} \tag{4.16}$$

The number of SUs successfully sends their sensing results within N_b mini-slots is ex-

pressed as $\bar{N}_{N_b}$.

4.4.2 SVM-Based Method for Selection of the CCC

The CCC is selected based on the decision which is given by the optimization problem in (3.33). Hence, I can write the decision function as follows:

$$F(\mathbf{x}_k) = \sum_{l=1}^{L} \widetilde{\lambda}^{(l)} a^{(l)} \kappa(\mathbf{x}_k, \mathbf{y}^{(l)}) + w_0 \tag{4.17}$$

where $\mathbf{x}_k$ is the collected sensing results or energy vector for the k-th channel received from different SUs for selecting the CCC. $\kappa(\mathbf{x}, \mathbf{y}) = \phi(\mathbf{x}) \cdot \phi(\mathbf{y})$ is the kernel function used to map the low dimensional energy vector to a higher dimensional space. Some of the commonly used kernel functions are linear, polynomial, and Gaussian radial basis functions [83]. Hence, I can select the common control channel as follows:

$$\text{Ch}_{CCC} = \arg\min_{k \in \bar{\mathbf{K}}} \left\{ \sum_{l=1}^{L} \widetilde{\lambda}^{(l)} a^{(l)} \kappa(\mathbf{x}_k, \mathbf{y}^{(l)}) + w_0 \right\} \tag{4.18}$$

At the same time, I can make an estimate for the availability of the k-th channel for cognitive transmission as follows:

$$\widehat{a}_k = \text{sgn} \left\{ \sum_{l=1}^{L} \widetilde{\lambda}^{(l)} a^{(l)} \kappa(\mathbf{x}_k, \mathbf{y}^{(l)}) + w_0 \right\} \tag{4.19}$$

where sgn is the sign function. If $\widehat{a}_k = 1$, then the PUs are active on the k-th channel. Otherwise, the PUs are idle on that channel and hence can be allocated to the SUs. Since the estimates $\widehat{a}_k$ are based on cooperative spectrum sensing, they are more reliable than the individual sensing-based estimates.

4.4.3 Selection of Channels for Spectrum Sensing

The list of channels to be sensed in the next time frame is updated offline using **Algorithm 3** below, where t is the number of times the algorithm is executed and T_k is the number of times the k-th channel sensed.

Algorithm 3 Algorithm to select the channels to be sensed

1: **Input:** $\{\lambda_l\}, \{a_l\}, \{\mathbf{x}_k\}, \{\mathbf{y}^{(l)}\}, \omega_0$
2: Estimate relative channel idle probability
$\Theta_L \leftarrow \min_{k\in\boldsymbol{\mathcal{K}}}\left\{ \sum_{l=1}^{L} \widetilde{\lambda}^{(l)} a^{(l)} \kappa(\mathbf{x}_k, \mathbf{y}^{(l)}) + w_0 \right\}$
If $\Theta_L < 0$ **then**
$\boldsymbol{\Theta} \leftarrow \sum_{l=1}^{L} \widetilde{\lambda}^{(l)} a^{(l)} \kappa(\mathbf{x}_k, \mathbf{y}^{(l)}) + w_0 + |\Theta_L|, \quad \forall k, k \in \boldsymbol{\mathcal{K}}$
Else
$\boldsymbol{\Theta} \leftarrow \sum_{l=1}^{L} \widetilde{\lambda}^{(l)} a^{(l)} \kappa(\mathbf{x}_k, \mathbf{y}^{(l)}) + w_0, \quad \forall k, k \in \boldsymbol{\mathcal{K}}$
End If
$\Theta_M^0 \leftarrow \max\{\boldsymbol{\Theta}\}$
$\boldsymbol{\Theta} \leftarrow \{\Theta_M^0 - \boldsymbol{\Theta}\}$
$\Theta_M \leftarrow \max\{\boldsymbol{\Theta}\}$
$\mathbf{P}_{\boldsymbol{\Theta}} \leftarrow \frac{\boldsymbol{\Theta}}{\Theta_M}$
3: Select set of channels for sensing in the next time slot
$\bar{\boldsymbol{\mathcal{K}}} \leftarrow \arg\max_{1\le k\le \bar{\mathcal{K}}} \left\{ \mathbf{P}_{\{\Theta_k\}} + \sqrt{\frac{2\ln(t-1)}{T_k}} \right\}, \quad \forall k, k \in \boldsymbol{\mathcal{K}}$

4.5 Saturation Throughput Analysis of the DCCC-MAC Protocol

In this section, the average system throughput for the proposed DCCC-MAC protocol is analyzed in closed-form under the assumption that the SUs always have data to transmit. At a given time frame, I categorize the SUs into two different sets of SUs based on the way they are allocated channels for data transmission. One set of SUs has a reserved mini-slot to obtain channel allocation for data transmission while the other SUs have to contend to obtain channel allocation for their data transmissions. The SUs belonging to these two sets are not fixed and vary from frame to frame. Therefore, the total average throughput of the network is the combination of the average throughputs of these two different types of SUs.

In the proposed DCCC-MAC protocol, one channel is allocated to only a single SU within any given frame duration. Therefore, the maximum number of SUs that can be supported by the DCCC-MAC protocol is $\bar{\kappa} - 1$ since one idle channel is assigned as the CCC. Hence, the average number of SUs ($\mathcal{I}$) transmit within a frame duration can be expressed as follows:

$$\mathcal{I} = \begin{cases} \bar{\kappa} - 1, & \text{if } \alpha N \geq (\bar{\kappa} - 1) \\ \alpha N, & \text{otherwise} \end{cases} \tag{4.20}$$

where α is the percentage of the SUs synchronized in a given frame and can be defined as the average number of synchronized SUs divided by the total number of SUs in the network. Hence, the average number of SUs that can be satisfied through contention ($\mathcal{I}_C$) can be expressed as

$$\mathcal{I}_c = \mathcal{I} - \bar{N}_{N_b} \tag{4.21}$$

where $\bar{N}_{N_b}$ is the number of scheduled SUs or the number of SUs which successfully send their sensing results to the CR-BS within N_b mini-slots during the CCC selection phase and can be obtained as follows:

$$\bar{N}_{N_b} = \left\lfloor \bar{\kappa} \sum_{j=1}^{N_b} P_{j,ccc} \right\rfloor. \tag{4.22}$$

Hence, the total average time for the scheduled SUs to transmit their data (T_{avgS}) can be calculated as follows:

$$T_{avgS} = \bar{N}_{N_b}(T - T_S - T_{SCCC} - t_{D-TS} - T_B) - \frac{\bar{N}_{N_b}(\bar{N}_{N_b}+1)t_{D-ms}}{2} \tag{4.23}$$

where $T_{SCCC} = t_{IB} + t_{SSR} + t_{S_{ccc}} + t_{I_{ccc}}$ and the term $\frac{\bar{N}_{N_b}(\bar{N}_{N_b}+1)t_{D-ms}}{2}$ denotes the average delay in $\bar{N}_{N_b}$ channels due to channel reservation for $\bar{N}_{N_b}$ scheduled SUs. Hence, the total

average time remaining (i.e., summation of average remaining time in each idle channels) for the contending SUs (T_{avgRC}) to transmit their data can be expressed as

$$T_{avgRC} = \mathcal{I}_c(T - T_S - T_{SCCC} - t_{D-TS} - T_B - (\bar{N}_{N_b}+1)t_{D-ms}) \tag{4.24}$$

where $(\bar{N}_{N_b} + 1)t_{D-ms}$ indicates the silence duration of a remaining idle channel (i.e., not assigned to any SU but to be assigned through a contention process) due to the $\bar{N}_{N_b}$ number of scheduled SUs' channel reservation and the $Start\_Contention$ message.

Let $\Gamma = \alpha N - \bar{N}_{N_b}$ denote the number of SUs to be allocated at the beginning of the contention period. The maximum number of mini-slots in the remaining contention period is β which can be expressed as: $\beta = \frac{T_{avgRC}}{\mathcal{I}_c . t_{D-ms}}$. Hence, the average number of contention windows for the remaining data transmission duration can be calculated as

$$\lambda = \Big\lfloor \frac{\beta}{W} \Big\rfloor. \tag{4.25}$$

The average number of successful transmissions (C_i) within i-th contention window can be expressed as in (4.26) below since the SUs transmit RTS to the CR-BS after a chosen random backoff value from a closed window $[0, W-1]$:

$$\begin{aligned} C_i &= W\Gamma_i\Big(\frac{1}{W}\Big)\Big(1-\frac{1}{W}\Big)^{\Gamma_i - 1} \\ &= \Gamma_i\Big(1-\frac{1}{W}\Big)^{\Gamma_i - 1} \end{aligned} \tag{4.26}$$

where Γ_i denotes the number of SUs in the i-th contention window for contention and $\Gamma_{i+1} = \Gamma_i - C_i$. Hence, the total average delay for data transmission due to contention can be expressed as

$$T_{avgC} = \sum_{i=1}^{\lambda} \mathcal{Q}(I_{c_i}, C_i, W) \tag{4.27}$$

where $\mathcal{Q}(.,.,.)$ can be defined as follows:

$$\mathcal{Q}(I_{c_i}, C_i, W) = \begin{cases} (I_{c_i} - C_i)W + \frac{C_i W}{2}, & \text{if } I_{c_i} - C_i \geq 0 \\ \frac{C_i W}{2}, & \text{if } I_{c_i} - C_i < 0 \text{ and } I_{c_{i-1}} - C_{i-1} > 0 \\ 0, & \text{otherwise} \end{cases} \tag{4.28}$$

in which $I_{c_1} = I_c$ and $I_{c_i} = I_{c_{i-1}} - C_i$

I assume that the SVM-based cooperative decision making mechanism makes an accurate channel idle decision. The accuracy of the decision in SVM improves with the increasing number of SUs participating in the cooperative decision making process. Considering the imperfectness in the decision making process by the SVM, the average system throughput (T_{avg}) can be calculated as follows:

$$T_{avg} = (T_{avgS} + T_{avgRC} - T_{avgC})(1 - p_{f,svm}) \tag{4.29}$$

where $p_{f,svm}$ denotes the false-alarm probability of the SVM classifier when $\bar{N}_{N_b}$ number of SUs cooperate to make decision.

4.6 Robustness and Scalability of DCCC-MAC protocol

In this section, I focus on the robustness and scalability of the proposed DCCC-MAC protocol. The scalability of the DCCC-MAC protocol is defined as the ability to handle an increasing number of SUs in the network whereas the robustness is defined as the ability to withstand against the SUs' irregular operation (i.e., loss of synchronization and control information) and the capability to bring them back to the normal operation.

4.6.1 A new SU appears in the CRN or an SU is not synchronized with beacon

Since a newcomer and an SU unsynchronized with the beacon act in a similar way, I treat these two different types of SUs in a similar manner. The newcomer does not have any idea about the CCC as well as the current phase (i.e., sensing, CCC selection, or data transmission phase) of the frame. Therefore, every newcomer has to select a predefined number of channels ($\mathcal{K}$) randomly to perform energy sensing. With the intention of identifying the CCC, the newcomer tries to decode the sensed signal. If the newcomer finds the CTS message, that particular channel is the CCC in the current transmission cycle. Hence, the newcomer transmits an RTS packet in the CCC after a random backoff if the CCC is sensed idle. Since the newcomer does not know about the idle channels in the network, the relative channel idle probability and the channel allocated to SUs so far (by now some of the channels might have been allocated to SUs and only the left over channels can be allocated to the remaining SUs), the newcomer sets the $cccIndicator$ field in the RTS packet to 0. Following a successful reception of the RTS packet, the CR-BS checks the $cccIndicator$ bit in the RTS packet. Since the $cccIndicator$ bit is set to 0, the CR-BS transmits the $Transmission\_Setup$ message again containing the indices of the remaining idle channels, relative channel idle probabilities, and timing span for the next beacon. Hence, the newcomer selects the best channel for its data transmission from the list of currently available idle channels. Then, the newcomer sends an RTS packet by setting the $cccIndicator$ bit to 1 if there is enough time for transmitting at least a single data packet. Otherwise, it remains silent for the next beacon. This procedure continues until the newcomer tunes to a dynamic CCC.

4.6.2 Participate in the CCC selection process but does not receive the CCC information

As an incentive for participating in the CCC selection process, all the participating SUs receive channel reservation and this information is broadcast using the $Transmission\_Setup$ message (at the beginning of the data transmission phase) using the CCC. A particular SU may fail to spot the $Transmission\_Setup$ message since it did not tune to the CCC due to the fact that it failed to spot the CCC_Update message. However, this SU is scheduled by the CR-BS since it participated in the CCC selection process and reserved a mini-slot for the RTS/CTS handshake to obtain a channel allocation for its data transmission. Such an SU will not send any RTS on that mini-slot. However, by this time the SU knows that data transmission has already started and it failed to detect the CCC_Update message. Hence, this SU starts to listen to the idle channel (in which it sent its sensing results) with the hope of receiving CTS or the next beacon signal. Meanwhile, the CR-BS knows that it did not receive the RTS packet for a scheduled SU in the reserved mini-slot. Therefore, the CR-BS broadcasts the CCC_Update message again in the channel in which the scheduled SU sends its sensing results to the CR-BS if and only if that particular channel is idle and that channel is not allocated to any SU at the time it tries to send the CCC_Update message. Since this SU is listening to the best idle channel, it will receive the CCC information and tune its receiver to the CCC. It is important to note that another mini-slot is not scheduled for this SU even though the CR-BS sends the CCC_Update message to bring that SU to transmission mode. This SU has to contend for a channel upon reception of the $Start\_Contention$ message which is broadcast after the scheduled SUs' reservation period is over.

Note that all the synchronized SUs know the exact time span for next beaconing or the duration for data transmission in the current frame. At the end of data transmission period,

the synchronized SUs tune their receivers to the CCC or their best idle channels for the next beacon. The SUs who receive the beacon obtain the list of channels for sensing in the next time frame and others select a random set of channels for sensing in the next time frame.

4.6.3 The selected CCC may be occupied by PUs

The CCC could be occupied by PUs (e.g., due to sensing error and subsequent error in the selection of CCC or sudden PU appearance in the CCC). However, since we adopt cooperative spectrum sensing for detection of PUs' idle channels and select the most reliable channel out of all detected PUs' idle channels as the CCC, the effect of PU misdetection on the CCC would be negligible in the proposed scheme when the number of PUs' idle channels is comparatively large. We discuss the two scenarios below when the selected CCC might be occupied by PUs.

- *The selected CCC is actually occupied by PUs*: The CCC unavailability can be detected by SUs based on the individual sensing. To select another available channel as the CCC, the SUs should inform the CCC unavailability to Co-BS. For this, instead of transmitting RTS packets to the Co-BS at the beginning of data transmission phase, the scheduled SUs keep silent during their scheduled periods. If the Co-BS does not receive scheduling requests from more than the half of the scheduled SUs, then the Co-BS assumes that there is a problem with the selected CCC. However, to take this decision Co-BS has to wait until the end of time duration which is allocated for scheduling. At the end of the scheduled allocation period, instead of transmitting $Start\_Contention$ message, the Co-BS broadcasts a special message called $Chirping$ message to inform the new CCC. The next available best channel is selected as the CCC. Then, the SUs who want to get allocated channel start contention on the new CCC. Note that an SU, who has already started communication,

does not want CCC information because it can receive the next beacon in the current communication channel at the start of the beacon period. This is possible since the beacon is broadcast by the Co-BS in all the PUs' idle channels. If there is no other candidate channel for CCC, then the Co-BS sets the CCC index field to 0 in the $Chirping$ message. With the reception of 0 in the CCC index field in the $Chirping$ message, the SUs start to freeze until the next beacon period starts. If the Co-BS does not transmit any $Chirping$ message while a particular SU detects that the CCC is not available for SU transmission, then that particular SU needs to keep silent for the current frame and should wait for the next beacon in its best PUs' idle channel.

- *Sudden PU appearance in the CCC*: The appearance of a PU in a channel is not visible to the SUs and the Co-BS after the spectrum sensing period since both the SUs and the Co-BS follow half-duplex communication. In this situation, there is no way to stop interference at the PU until the end of the current transmission frame. However, if we assume that the Co-BS has full-duplex communication capability, then the Co-BS can do simultaneous spectrum sensing and transmission. In such a scenario, the Co-BS will be able to detect the collision with PU and it can use the aforementioned procedure to shift the CCC.

4.6.4 Adaptation of the protocol for downlink transmission

Let us assume that the Co-BS wants to start downlink transmission to the SUs. Then, the indexes of the SUs, who will be receiving data from the Co-BS, are informed by Co-BS with the beacon. Note that this information is reachable to all the SUs since all the SUs registered in the CRN listen to the CCC and synchronize with the beacon irrespective of their transmission status. However, the SUs who want to do communication (i.e., uplink or downlink communication) with the Co-BS try to send their sensing information to the Co-

BS and try to obtain a channel allocation for transmission. Once a channel is allocated to an SU, that SU can use the allocated channel for either uplink or downlink communication.

4.7 Performance Evaluation Results and Discussions

4.7.1 Simulation Parameters

In this study, unless otherwise specified, I consider that the SUs are located randomly in a 500 m $\times$ 500 m area. The important simulation parameter values are as follows: the bandwidth of a channel B is 5 MHz, the sensing duration τ is 100 μs, the noise spectral density η is -174 dBm, and the path-loss exponent α is 4. I assume that the standard deviation of shadowing is 8 dB. The transmit power of each PU is 300 mW and the frame duration is 100 ms. I consider three PUs having fixed locations with coordinates (5000m, 1500m), (-1500m, -2000m), and (1000m, 2000m). The probability that a PU is in the active state is 0.3 and the state of each PU is independent of that of any other PU. The false alarm probability of SVM-based cooperative spectrum sensing ($p_{f,svm}$) is set to 0.1. The packet-specific simulation parameters for the MAC protocol are listed in Table 4.2 [5,6]. The total number of channels available for communication is $\mathcal{K} = 64$, and $\bar{\mathcal{K}} = 32$ channels are sensed at a given frame. Two bytes are used to represent the $\log$ value of energy level in a given channel at any SU, where the first and the second bytes represent the integer and decimal component of the *log* value of energy, respectively. Therefore, each user should allocate $16 \times \bar{\mathcal{K}}$ bits for sensing payload. Further, the indices for the SUs and channels are represented by 8 bits.

I compare the performance of the proposed DCCC-MAC protocol with that of two other cognitive radio MAC protocols, namely, the OSA-MAC protocol and the CM-MAC protcol from the exisiting literature. Both of these protocols use common control channels for distributed channel access.

Table 4.2: Simulation parameters [5, 6]

Channel bit rate	1 Mbps
MAC header	272 bits
PHY header	128 bits
ACK	112 bits + PHY header
RTS	160 bits + PHY header
CTS	112 bits + PHY header
SIFS	28μs

4.7.2 Results

Results for the CCC selection process

Fig. 4.3 depicts the minimum number of mini-slots (N_b) required when at least 4 or more SUs participate in the CCC selection process. It is evident that N_b neither significantly increases with the number of channels sensed nor the number of SUs when $P_s = 0.4$.

Fig. 4.4 shows the number of SUs ($\bar{N}_{N_b}$) participating in the CCC selection process by sending their sensing results to the CR-BS using N_b mini-slots. I can clearly observe that the number of SUs participate for CCC selection is most of the times greater than the expected number of SUs ($\bar{N}$) even the minimum number of mini-slots is utilized for cooperation. This fact is revealed by comparing the curves in Fig. 4.3 and Fig. 4.4. Note that, the number of SUs ($\bar{N}_{N_b}$) participate in the CCC selection is scheduled for data transmission at the start of data transmission phase as an incentive. Hence, the increasing number of schedule SUs increases the system throughput in two ways: i) the schedule SUs start their transmission at the most possible time instant in the data transmission phase. ii) due to the schedule allocation no waste in contention and at the same time it reduces the number of SUs left for contention. This phenomena reduces the possible collision at contention based allocation. In particular, most of the times the gap between the expected number of cooperating SUs ($\bar{N}$) and the number of SUs actually participating in cooperative spectrum sensing ($\bar{N}_{N_b}$) for CCC selection is significant when the number of channels sensed is in-

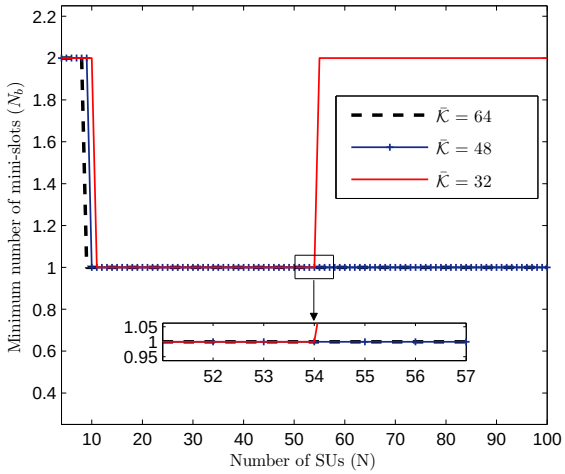

Figure 4.3: Minimum number of mini-slots (N_b) required for at least 4 or more SUs participating in the cooperative decision making process when $P_s = 0.4$ and $W_{max} = 16$.

creased. In fact, this is due to the increase of number of idle channels in the CRN with the increasing number of channels sensed (see equation (4.22)).

Table 4.3 shows the effect of channel access probability (P_S), during the CCC selection phase, on the minimum number of mini-slots (N_b) required for at least four SUs cooperating in the decision making process. This table reveals that N_b increases when both the number of SUs in the network and the channel access probability (P_S) increase. This is due to the increased number of collisions among the SUs and increased channel access probability. It is important to note that the minimum number of mini-slots required to send at least four SUs sensing results is not high (i.e., maximum $N_b = 4$).

Performance of SVM-based cooperative spectrum sensing

Fig. 4.5 shows the performance of the proposed SVM-based cooperative decision making scheme in terms of receiver operating characteristic (ROC). This figure clearly depicts that the correctness of the decision (channel idle or busy) improves with the increasing number of SUs participating in the decision making process. However, the relative improvement of

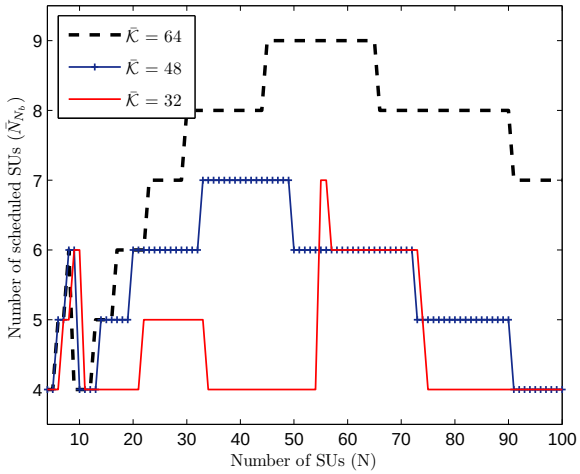

Figure 4.4: Number of SUs participating ($\bar{N}_{N_b}$) in the cooperative decision making process within N_b mini-slots when $P_s = 0.4$ and $W_{max} = 16$.

Table 4.3: Effect of P_s on minimum number of mini-slots (N_b) required for at least 4 or more SUs participating in cooperative decision making process when $W_{max} = 16$ and $\bar{\mathcal{K}} = 32$

P_s	**Minimum number of mini-slots (N_b)**				
	N=4	**N=25**	**N=50**	**N=75**	**N=100**
0.1	4	2	1	1	1
0.2	4	1	1	1	1
0.3	3	1	1	2	2
0.4	2	1	1	2	2
0.5	2	1	2	2	4
0.6	2	1	2	4	4
0.7	2	1	2	4	4
0.8	2	1	4	4	4
0.9	2	2	4	4	4
1	1	2	4	4	4

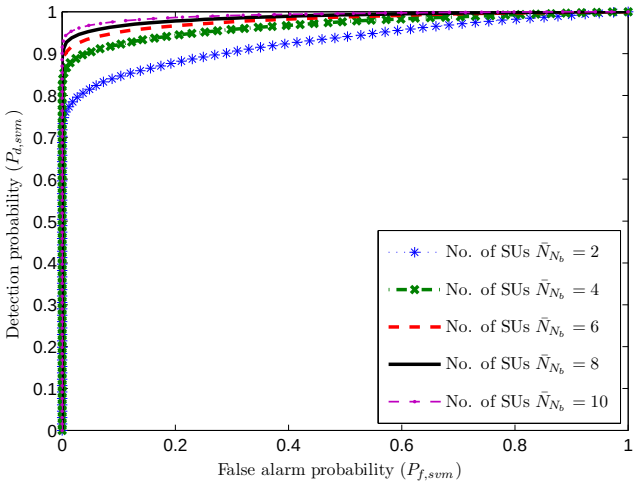

Figure 4.5: The ROC performance for different combination of SUs' cooperation when there are three PUs and the SVM classifier with linear kernel is used.

the correctness of the decision with additional SU reduces when the number of cooperating SUs is relatively high. I observe that even with two cooperating SUs, the probability of detection of PU activity is quite high. That is, the CCC selection and idle channel selection scheme based SVM perform well even with a small number of cooperating SUs.

Fig. 4.6 compares the effect of sensing duration on the performance of cooperative decision making process in terms of receiver operating characteristic. This figure clearly depicts that the increasing duration of sensing time increases the system performance in terms of idle channel detection. However, the level of system performance improvement decreases with respect to the increasing sensing duration. Note that, the proposed SVM-based decision making scheme performs well even with a lower sensing duration.

Throughput performance of DCCC-MAC protocol

The performance of the proposed dynamic common control channel-based MAC protocol is presented in Fig. 4.7. Specially, the system throughput is plotted against the number of SUs in the network. As expected, the system throughput increases with the increasing

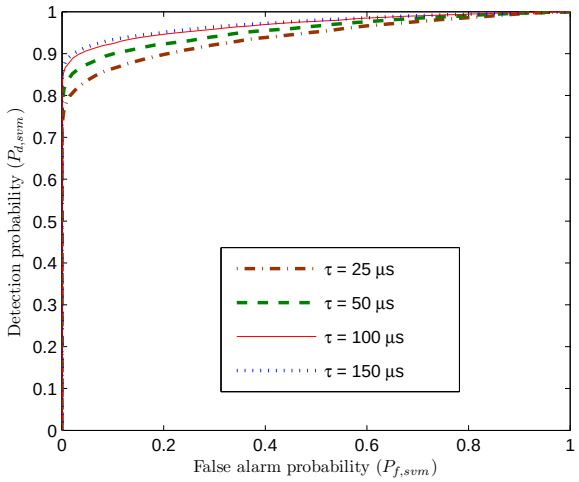

Figure 4.6: Effect of sensing duration (τ) on the performance of cooperative decision making process when there are three PUs, four SUs and a linear kernel is used in SVM classifier.

number of channels sensed ($\bar{\mathcal{K}}$). This performance gain is achieved due to the increased number of idle channels with the increasing number of channels sensed. However, the system performance deteriorates with the increasing number of SUs in the network due to the saturation effect of the selected CCC. This performance degradation is significant when $\bar{\mathcal{K}}$ is high. Interestingly, all the system throughput curves approximately coincide when the number of SUs are less than or equal to the number of idle channels. This is due to the fact that the CCC is not saturated when the number of SUs is small. In this figure, the performance of proposed DCCC-MAC is compared with the OSA-MAC [2] and CM-MAC [3] protocols in term of system throughput. Note that, due to the greedy allocation of channels [1] in the CM-MAC, the CM-MAC outperforms the proposed DCCC-MAC when the number of SUs in the network is comparatively large. Note that the system throughput for the OSA-MAC [2] and CM-MAC [3] protocols are evaluated using the given closed-formed expressions. Further, the simulation results coincide with the analytical curves

[1]The SU who wins the contention in CCC utilizes all the idle channels for its data transmission. At this point, all other SUs keep silent until the next beacon.

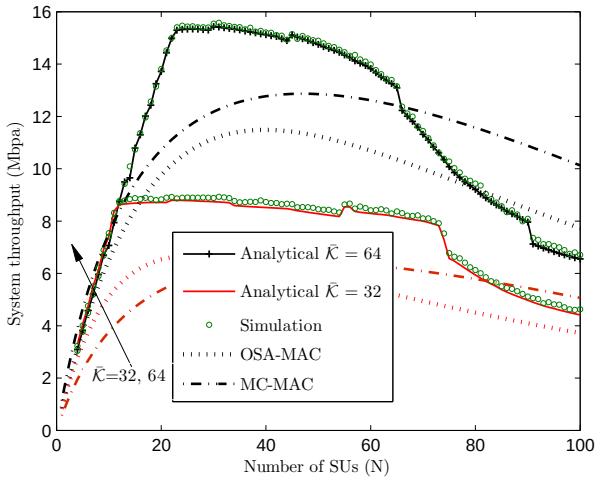

Figure 4.7: System throughput variation with respect to the number of SUs when $P_s = 0.4$ and $W_{max} = 16$. The overhead of the OSA-MAC protocol is assumed to be 25% [2] and average time for mobility support in CM-MAC protocol is assumed to be 3 ms [3].

validating our analysis.

Fig. 4.8 shows the impact of contention window on the performance of system throughput when the number of channels sensed is $\bar{\mathcal{K}} = 32$. With small contention windows (i.e., $W_{max} = 8, 16, 24$), the throughput is high when the number of SUs is relatively low (i.e., 10-30 SUs). At the same time, with small contention widows, as the number of SUs increases, the throughput performance degrades drastically due to the increase in collision possibilities. On the other hand, the performance does not degrade significantly with the increasing number of SUs when the contention window is relatively large (i.e., $W_{max} = 64$ and $W_{max} = 128$). This is due to the reduced possibilities of collision. However, larger contention windows degrade the system performance when there is a small number of SUs in the network. The throughput curves in Fig. 4.8 show peaks (avalanches) due to the sudden increment (decrement) of the number of SUs involved in cooperative decision making within N_b mini-slots (see Fig. 4.4). The cooperating SUs obtain the channel allocations without going through the contention process which leads to peaks at those points.

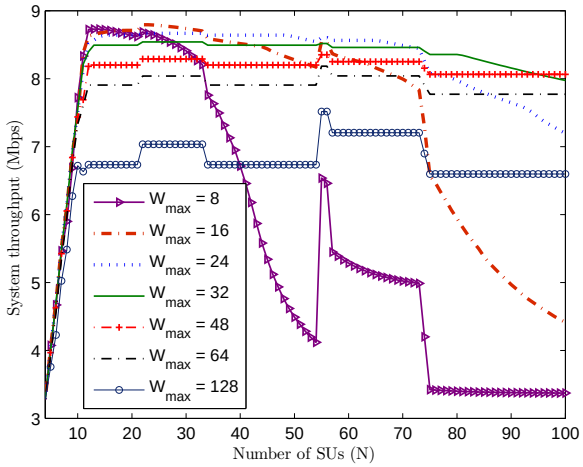

Figure 4.8: System throughput variation with respect to contention window (W_{max}) when $P_s = 0.4$ and $\bar{\mathcal{K}} = 32$.

Fig. 4.9 shows the effect of sensing duration on system throughput. The system performance degrades with the increasing sensing duration although the probability of idle channel detection increases with the sensing time. This means that the performance loss due to the increased sensing duration is significant compared to the performance gain due to improved idle channel detection probability. However, the sensing time cannot be chosen to be very small due to the requirement of protecting the PUs from possible interference due to misdetection. Further, I can observe peaks (e.g., at $N = 55$) and avalanches (e.g., at $N = 75$) in throughput curves due to the sudden increment and decrement of schedule SUs in data transmission phase, respectively. This fact is revealed by the curve corresponding to $\bar{\mathcal{K}} = 32$ in Fig. 4.4.

A qualitative comparison among the exisiting distributed cognitive MAC protocols is presented in Table 4.4.

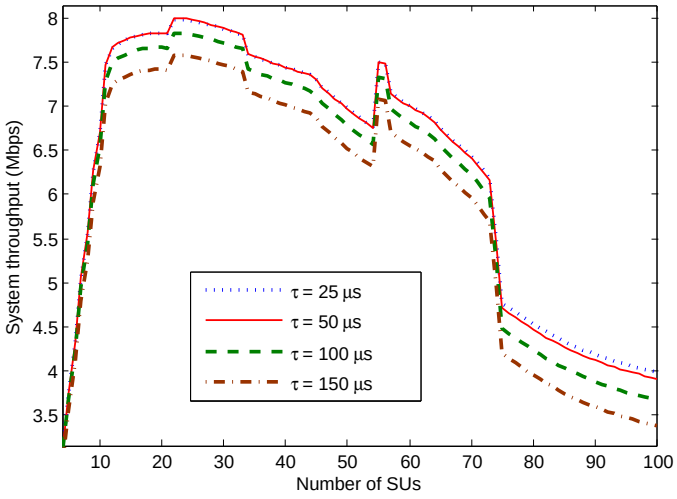

Figure 4.9: Effect of sensing duration (τ) on the performance of system throughput when $W_{max} = 16$, $\bar{\mathcal{K}} = 32$ and the frame duration is 50 ms).

Table 4.4: Quantitative comparison among distributed cognitive MAC protocols

MAC protocol	No. of transceivers	Hidden node problem	CCC	Synchronization	Signaling	Access method
DCCC-MAC (proposed)	Single	Yes	Dynamic CCC	Yes	In band	Hybrid
OSA-MAC [128]	Single	No	Dedicated CCC	Yes	In band	Contention-based
CM-MAC [3]	Single	No	Dedicated CCC	No	Out of band	Contention-based
DOSS-MAC [126]	Three	No	Dedicated CCC	No	Out of band	Contention-based
C-MAC [129]	Single	Yes	Dedicated CCC	Yes	Out of band	Coordination-based
ECR-MAC [130]	Single	Yes	Dedicated CCC	Yes	Out of Band	Contention-Based
HC-MAC [131]	Single	Yes	Dedicated CCC	No	Out of band	Contention-based
OS-MAC [132]	Single	No	Dedicated CCC	Yes	Out of band	Coordination-based
SCA-MAC [133]	Single	No	Dedicated CCC	No	Out of band	Contention-based

4.8 Conclusion

I have presented a solution to the common control channel selection problem in cellular cognitive radio networks. The common control channel for a given frame is selected using a support vector machine-based approach. Specially, the common control channel selection scheme gives a set of idle channels in the network as a by product of the cooperative spectrum sensing process. In the proposed dynamic common control channel MAC protocol, the secondary users who participate in the control channel selection process are scheduled for data transmission while the other SUs contend for channel access. The proposed dynamic common control channel-based MAC protocol achieves a higher performance compared to the OSA-MAC [2] and MC-MAC [3] protocols over a wide range of values of secondary users in a cell. The system throughput has been analyzed in closed-form and simulation results have validated the correctness of our analysis.

Chapter 5

Generalized Spectral Footprint Minimization for OFDMA-Based CRNs

In CRNs, due to the scarcity of radio resources (e.g., channel and power), efficient utilization of these resources is critical. In this chapter, I consider the problem of joint subchannel and power allocation for an orthogonal frequency division multiple access (OFDMA)-based cellular CRNs. Note that the medium access control method proposed in the previous chapter did not consider any specific radio transmission technology, while this chapter specifically considers the OFDMA technology which is used in the current 4G cellular networks. I formulate the downlink resource allocation problem as a generalized spectral-footprint (bandwidth-power product) minimization problem under the interference threshold at the primary users, as well as total power and quality of service constraints. A cognitive base station solves this non-convex mixed-integer programming problem iteratively by dividing it into a subchannel allocation master problem and a power allocation subproblem. The subchannel assignment problem for secondary users is solved by applying a modified Hungarian algorithm while the power allocation subproblem is solved by using Lagrangian technique. Specifically, I propose a low-complexity modified Hungarian algorithm for subchannel allocation which exploits the local information in the cost matrix. To apply the modified Hungarian algorithm, it is require to know the exact number

of subchannel requirement of each user in every iteration. Hence, I develop an algorithm to update the number of subchannels required by each user in each iteration based on the spectral footprint difference of each user. An asymptotic analysis is carried out for the single secondary user case and a closed-form expression is derived for the optimal number of subchannels which minimizes the spectral footprint. The performance of our generalized spectral-footprint minimization technique is compared with the power minimization and a scheme based on brute-force search. Also, several applications of the proposed algorithms are outlined.

5.1 Introduction

Cognitive radio based on dynamic spectrum access has emerged as a promising technology to improve the utilization of the radio spectrum and thereby mitigate the spectrum scarcity problem to some extent. With respect to the radio environment, the distinctive feature of cognitive radio networks is the availability of spectral resources in the time, frequency, and spatial domains. In this context, opportunistic spectrum access is a key concept, which allows a SUs to opportunistically access the frequency band allocated to a PU when the PU transmission is detected to be absent in a given geographical area (spectrum overlay paradigm). Further, in cognitive radio systems, SUs can use the licensed spectrum if and only if they guarantee no harmful interference to primary user networks (spectrum underlay paradigm). In this context, inefficient utilization of the available spectrum and power in cognitive networks degrades the performance of both the cognitive and the primary networks. Studying the efficient allocation of scarce bandwidth and power (spectral footprint) for CRNs is of significant interest.

5.1.1 Related Work

Extensive researches have been carried out on subchannel and power allocation in conventional wireless networks [134, 135] and a survey of different adaptive power and bandwidth allocation algorithms for the downlink multiuser OFDMA networks is presented in [93]. However, those algorithms cannot be directly used for resource allocation in CRNs due to the added limitations such as mutual interference between primary user and secondary users [136] and imperfect spectrum sensing [56]. The authors in [90] propose an efficient algorithm based on iterative water-filling to overcome such limitations. In [137], a power allocation scheme for OFDM-based CRNs is investigated by taking the effect of imperfect spectrum sensing. In [2], the authors propose a joint power/rate allocation scheme for CRNs with proportional and max-min fairness criteria. The queue length-aware channel and power allocation schemes for CRNs are studied in [91]. The authors in [138] propose a technique for subchannel and power allocation in multi-cell CRNs. In [139], the heterogeneity of spectral footprint of wireless networks is shown as a key to maximizing coverage in a particular area. The authors in [140] use spectral footprint as the optimization function to regulate spectrum sharing in CRNs.

5.1.2 Motivation and Contribution

The traditional resource allocation techniques in CRNs try to utilize as much bandwidth as possible to minimize the transmit power and interference caused to the PU receivers [90]. However, it is reasonable to allow the cognitive radio transmitters to keep transmitting until the interference caused by them reaches a predefined interference threshold. Thus, instead of utilizing all the available bands for transmitting the cognitive users can save some spectrum bands for other cognitive applications. This is a trade off between the allocation of power and spectrum band. The spectral footprint (SF) minimization facilitates reducing

the number of channels used to satisfy the required quality-of-service (QoS) at the expense of higher transmission power while maintaining the given interference threshold at the PU receivers. Moreover, for CRNs, a generalized spectral footprint based allocation paves the way to optimally and opportunistically utilize the available radio resources (spectrum and power) depending on the network operators' objectives. On the other hand, the authors in [141] extend the work in [140] by utilizing the bandwidth-power product, by giving equal weight for bandwidth and power, as a minimization objective for allocating power and subcarriers in CRNs. The authors in [141–143] propose an iterative algorithm based on the Hungarian algorithm for subchannel allocation in CRNs where at each iteration the algorithm is applied without exploiting the available local information. As a result, the complexity of each iteration remains the same until the convergence is reached. However, the complexity of the subchannel allocation can be reduced from the second iteration onwards by utilizing the local information in the subchannels assignment cost matrix. The affirmation facts motivate me for this study.

In the above context, I investigate the problem of designing lower-complexity joint subchannel and power allocation for multiuser OFDMA-based cognitive radio networks for generalized spctral footprint minimization. The main contributions of this study can be listed as follows:

- I formulate the resource allocation problem for multiuser OFDMA-based CRNs as a generalized spectral footprint minimization problem under the required rate, total power and interference constraints. The objective function of the resource allocation optimization problem is formulated by weighting the bandwidth-footprint and power-footprint. The weighting parameters provide more flexibility to adjust the radio resources as required and can also reflect the scarcity of the resources. The formulated optimization problem is a non-convex mixed-integer programming problem.

Therefore, I solve this optimization problem by dividing the original problem into a subchannel allocation master problem and a power allocation subproblem.

- I propose a lower-complexity Hungarian-based subchannel assignment algorithm by exploiting the local information in the available subchannel assignment cost-table, which is used for subchannel assignment. Moreover, to apply the Hungarian-based modified algorithm, I need to know the exact number of subchannels required for each user. Therefore, I propose an algorithm for updating the number of subchannels allocated to each user in each iteration.

- Through an asymptotic analysis of the resource allocation scheme in a single user case, I derive a closed-form expression for the number of subchannels required to satisfy a given QoS requirement.

5.2 System Model and Problem Formulation

5.2.1 System Model

I consider downlink transmission in an OFDMA-based system multiuser CRN as illustrated in Fig 5.1. The number of SUs in the CRN is denoted by N. The considered CRN coexists with a primary network which is denoted by $\mathcal{P}$. I assume that the downlink transmissions by the cognitive radio base station (CR-BS) in the CRN are synchronized with the uplink transmissions in the primary network [141, 144, 145]. Further, this assumption does not limit the analysis but it reduces the complexity of resource allocation due to the reduction of interference possibilities. The PUs transmit in the uplink and the primary base stations are the primary receivers.

The total available band in the CRN is divided into $\mathcal{K}$ equal independent subchannels each with bandwidth B. I assume that the channel realization from any transmitter (PU transmitter/CR-BS) to any receiver (PU-BS/SUs) is quasi-static for one frame duration,

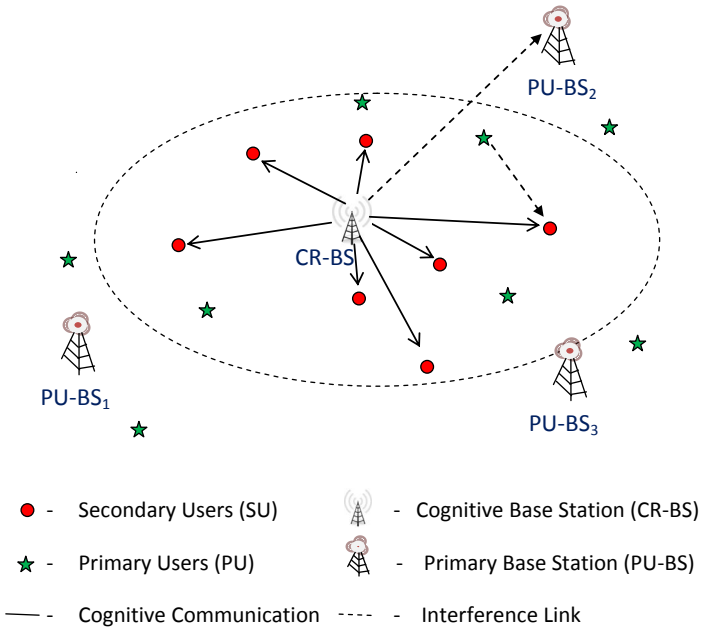

Figure 5.1: System model.

and independent and identically distributed (i.i.d.) over different frames. The channel gains between the CR-BS and the cognitive users are characterized by long-term path-loss, shadowing, and short-term fading whereas the channel gain between the PUs and cognitive users are characterized by long term fading and shadowing. The location information of the BSs and PUs in the primary network can be obtained from the radio environment map (REM) [141, 144, 145]. Further, the waveform of the PU signal is unknown at the cognitive user on a given subchannel. Hence, the interference at cognitive user is calculated by assuming power spectral density of that subchannel as given in [141, II.B]. I assume that at the beginning of every frame, the CR-BS obtains information such as the channel state information (CSI) and aggregate interference at the SUs caused by the PUs.

5.2.2 Problem Formulation for Joint Subchannel and Power Allocation

In this section, I formulate the joint subchannel and power allocation problem as a generalized spectral-footprint minimization problem for OFDMA-based CRNs with the rate,

Table 5.1: Notations used in the optimization problem formulation

Notation	Definition
$\{X_{n,k}\} \in \{1, 0\}$	1 if k-th subchannel is assigned to the n-th user; 0, otherwise
$\{P_{n,k}\}$	Transmit power allocated on k-th subchannel to n-th user
$\{SF_n\}$	Spectral footprint of n-th user
$\{\phi_n\}$	Minimum rate requirement of n-th user
$\mathcal{K}$	Total number of available subchannels
$\{\mathcal{K}_n\}$	Number of subchannels assigned to n-th user
$\omega_k, (0 \leq \omega_k \leq 1)$	Primary users' activity factor on k-th subchannel
ω_{th}	Threshold activity factor

total power, and interference constraints. The symbols and notations used for the problem formulation are shown in Table 5.1.

The spectral footprint is defined as a product of the bandwidth-footprint $\left(F_B = \sum_{n=1}^{N} \sum_{k=1}^{\mathcal{K}} \frac{BX_{n,k}}{(1-\omega_k)}\right)$ and the power-footprint ($F_P = \sum_{n=1}^{N} \sum_{k=1}^{\mathcal{K}} P_{n,k}$) [94, 141]. Here ω_k is incorporated in the objective function to capture the spectrum activity of PU [62] in the optimization process. Further, a given subchannel is allocated to a cognitive user if and only if its activity factor is less than the threshold activity (w_{th}). Intuitively, I try to allocate the subchannels with lower PU activity to SUs while avoiding the subchannels with higher PU activity in the allocation process so that the spectral footprint (SF) is minimized. I set $X_{n,k} = 1$ if the k-th subchannel is allocated to the n-th user, otherwise $X_{n,k} = 0$. Note that $P_{n,k}$ denotes the transmit power of the CR-BS on the k-th subchannel assigned to the n-th user.

The optimization problem for minimizing the generalized spectral footprint for the cognitive radio network can be stated as follows:

$$\min \Big[\sum_{n=1}^{N}\sum_{k=1}^{\mathcal{K}} \frac{BX_{n,k}}{(1-\omega_k)}\Big]^{\alpha}\Big[\sum_{n=1}^{N}\sum_{k=1}^{\mathcal{K}} P_{n,k}\Big]^{\beta} \tag{5.1}$$

$$\text{s.t.} \sum_{k=1}^{\mathcal{K}} X_{n,k} B\log\left(1+\frac{P_{n,k}h_{n,k}}{\eta+\sum_{p\in\mathcal{P}} I_{p,n,k}}\right) \geq \phi_n, \forall n \tag{1.1}$$

$$\sum_{n=1}^{N} X_{n,k} \leq 1 \tag{1.2}$$

$$g_{p,k}P_{n,k} \leq I_{th,k}^{p},\ \ \forall\, \omega_k \leq \omega_{th}, p \in \mathcal{P}, \forall k \tag{1.3}$$

$$\sum_{n=1}^{N}\sum_{k=1}^{\mathcal{K}} P_{n,k} \leq P^{max} \tag{1.4}$$

$$P_{n,k}h_{n,k} \geq \Gamma_n, \forall n, \forall k \tag{1.5}$$

$$X_{n,k} \in \{0,1\},\ P_{n,k} \geq 0, \forall n, k \tag{1.6}$$

where $X_{n,k}$ and $P_{n,k}$ are the decision variables to be optimized. The weighting parameters for the bandwidth-footprint and the power-footprint are α (≥ 0) and β (≥ 0), respectively. The footprint weighting parameters provide flexibility to adjust the radio resources as required and can also reflect the scarcity of resources. Note that the case with $\alpha = 0$ and $\beta = 1$ case is the known power minimization problem. The constraint in (1.1) is the rate constraint which ensures that the n-th SU achieves its minimum rate requirement of ϕ_n where η denotes the noise power, $I_{p,n,k}$ denotes the interference caused by the primary user $p \in \mathcal{P}$ at the n-th SU on the k-th subchannel, and $h_{n,k}$ is the channel power gain from CR-BS to the n-th user on subchannel k. The constraint in (1.2) ensures that the k-th subchannel is not allocated to more than one user in the cognitive network. The third constraint guarantees that the interference caused at the p-th primary receiver on the k-th subchannel is always below the interference threshold $I_{th,k}^{p}$ and $g_{p,k}$ is the channel power gain from the CR-BS to the PU-BS. The constraint in (1.4) enforces the limit on the total transmit power budget of the CR-BS and the constraint in (1.5) ensures that the received signal on the k-th subchannel is greater than the sensitivity threshold (Γ_n) of the SUs.

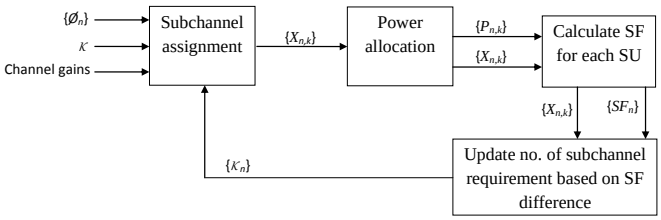

Figure 5.2: Block diagram of the resource allocation process.

I notice that the generalized spectral footprint minimization problem in (5.1) is a collection of two separable subproblems where one depends on the subchannel allocation and the other depends on the power allocation only. Hence, by applying the decomposition technique [146] I can convert (5.1) into subchannel and power allocation subproblems. These subproblems can be coupled through an appropriate coupling constraint. In fact, the coupling constraint is the rate constraint defined in (1.1). In this study, I decompose our original optimization problem in (5.1) into a subchannel allocation master problem and a power allocation subproblem and solve them iteratively as will be discussed in Section 5.3.1 and Section 5.3.2, respectively. The block diagram of the proposed resource allocation algorithm, which is executed at the CR-BS, is shown in Fig. 5.2.

5.3 Solutions of the Subchannel and Power Allocation Problems

5.3.1 Subchannel Allocation Problem

First I fix the transmission power to a feasible value $P^*_{n,k}$ and solve for a feasible subchannel allocation pattern. For a given feasible $P^*_{n,k}$, the subchannel allocation problem is bounded by the rate constraint and PUs' activity. Hence, the subchannel allocation problem can be written as:

$$\begin{aligned} \min \ & \Big[\sum_{n=1}^{N}\sum_{k=1}^{\mathcal{K}} \frac{BX_{n,k}}{(1-\omega_k)}\Big]^{\alpha} \\ \text{s.t.} \ & \sum_{k=1}^{\mathcal{K}} X_{n,k} B\log\left(1+\frac{P^*_{n,k}h_{n,k}}{\eta+\sum_{p\in\mathcal{P}} I_{p,n,k}}\right) \geq \phi_n, \forall n \\ & \sum_{n=1}^{N} X_{n,k} \leq 1 \\ & X_{n,k} \in \{0,1\}, \forall n,k. \end{aligned} \tag{5.2}$$

The binary integer programing problem in (5.2) can be solved by using the traditional Hungarian algorithm [141–143, 147–149]. However, the Hungarian based subchannel assignment algorithms do not exploit the local cost information to reduce the complexity in each iteration. For this reason, I propose a novel low-complexity modified Hungarian-based subchannel assignment algorithm which exploits the available local cost information to reduce the complexity after the first iteration. The step-by-step implementation procedure of the proposed subchannel assignment algorithm is given in **Algorithm** 4 so that the interested readers can implement the algorithm easily.

The total number of subchannels ($\mathcal{K}^*$) required to obtain a feasible solution is calculated in line 2 of **Algorithm** 4. The flag F_0 indicates whether the algorithm requires to exploit the subchannel assignment information in the previous iteration or not. Specially, from the second iteration onward, F_0 is set to *False* for exploiting the assignment information from the previous iteration. In this algorithm, subchannels are assigned to SUs based on the cost. The cost associated with PU's activity and channel to interference and noise ratio (CINR) is calculated as: $c_{n,k} = \frac{\eta+\sum_{p\in\mathcal{P}} I_{p,n,k}}{(1-\omega_k)Bh_{n,k}}$, where $c_{n,k}$ is the cost for assigning the k-th subchannel to the n-th SU. Hence, the CR-BS constructs an $N \times \mathcal{K}$ cost matrix (**C**) for all possible subchannel allocations and $c_{n,k}$ is the element of cost matrix **C**.

For each user in the CR-BS, I select the best $\mathcal{K}^* \leq \mathcal{K}$ subchannels from the cost matrix

Algorithm 4 Subchannel Assignment Algorithm

Input: $\{\mathcal{K}_n\}, \{h_{n,k}\}, \{I_{p,n,k}\}, \{\omega_k\}, \eta, \mathcal{K}, N, F_0 \leftarrow$ True
$\mathcal{K}^* = \sum_{n=1}^{N} K_n$
if $N > \mathcal{K}^*$ **then**
  return $\{\mathbf{X}_{n,k}\} \leftarrow \{0\}$
else
  if $F_0 =$ True **then**
    $\mathbf{C}[n,k] \leftarrow \frac{\eta + \sum_{p \in \mathcal{P}} I_{p,n,k}}{(1-\omega_k) B h_{n,k}}, \forall n, k$
    $[\mathbf{C}_{srt}, \mathbf{D}] \leftarrow$ sort $(\mathbf{C}, \mathcal{K}^*,$ 'Ascend')
    $[\mathbf{X}_{n,k}, \mathcal{K}_n, \mathbf{D}] \leftarrow$ DirChAssign $(\mathbf{D}, N, \{\mathcal{K}_n\})$
    if $\sum_{n=1}^{N} \mathcal{K}_n \neq 0$ **then**
      $\mathbf{T} \leftarrow \mathbf{C}[\forall n, k \in \mathbf{D}]$
      Duplicate each user's row in $\mathbf{T}$ by $\mathcal{K}_n$ times
      d $\leftarrow$ no. of subchannels in $\mathbf{D}$
      Add dummy rows with a Big-M value in row entries to balance no. of rows and no. of columns in $\mathbf{T}$
      Assign index of dummy rows to set $\mathbf{A}$
      $[\mathbf{X}^*_{n,k}, \mathbf{T}, \mathbf{U}, \mathbf{V}] \leftarrow$ Hungarian Method $(\mathbf{T})$
    end if
    $\mathbf{D}_0 \leftarrow \mathbf{D}, \{K_{0,n}\} \leftarrow \{K_n\}, F_0 \leftarrow$ False
  else
    $[\mathbf{C}_{srt}, \mathbf{D}] \leftarrow$ sort $(\mathbf{C}, \mathcal{K}^*,$ 'Ascend')
    $[\mathbf{X}_{n,k}, \mathcal{K}_n, \mathbf{D}] \leftarrow$ DirChAssign $(\mathbf{D}, N, \{\mathcal{K}_n\})$
    for $n = 1$ **to** N **do**
      $\{t_{\mathcal{K}_n}\} \leftarrow \{\mathcal{K}_{0,n} - \mathcal{K}_n\}$
      if $t_{\mathcal{K}_n} > 0$ **then**
        $I_{rem} \leftarrow \{n, t_{\mathcal{K}_n}\}$
        for $i = 1$ **to** $t_{\mathcal{K}_n}$ **do**
          $a_t \leftarrow$ arg max $\{\mathbf{C}[\forall$ rows of n-th user, $\mathbf{X}^*_{n,k}]\}$
          Change the row cost at a_t to a Big-M in $\mathbf{T}$
          Assign a_t to the set $\mathbf{A}$
          $\mathbf{U}(a_t) \leftarrow \min_j \{\mathbf{T}(a_t, j) - \mathbf{V}(j)\}$
        end for
      else
        $I_{add} \leftarrow \{n, -t_{\mathcal{K}_n}\}$
      end if
    end for
    for $\forall\, i \in I_{add}(:, 1)$ **do**
      if $|\mathbf{A}| \neq 0$ **then**
        Replace row $a_t \in \mathbf{A}$ of $\mathbf{T}$ by candidate row
        Remove the edge $(a_t, \text{mate}(a_t))$ from $\mathbf{X}^*_{n,k}$ if $\mathbf{X}^*_{n,k}(a_t, \text{mate}(a_t))$ is matched
        $\mathbf{U}(a_t) \leftarrow \min_j \{\mathbf{T}(a_t, j) - \mathbf{V}((j))\}$
        Remove a_t from $\mathbf{A}$
      else
        Duplicate row of $I_{add}(i, 1)$ at the end of $\mathbf{T}$
      end if
    end for
    $t_c \leftarrow$(no. of subchannels in $\mathbf{D}$)$-$(no. of subchannels in $\mathbf{D}_0$)
    if $t_c > 0$ **then**
      r $\leftarrow$ (no. of subchannels in $\mathbf{D}_0$)
      $\mathbf{T} \leftarrow$ Add new cost columns of new candidate subchannels in $\mathbf{D}$ to the end of $\mathbf{T}$
      d $\leftarrow$ no. of columns in $\mathbf{T}$, $p \leftarrow$ no. of rows in $\mathbf{T}$
      if d $\neq$ p **then**
        Add $(d - p)$ no. of dummy rows at the end of $\mathbf{T}$
        Assign indices of dummy rows to the set $\mathbf{A}$
      end if
      Calculate $\mathbf{V}$(q) and $\mathbf{U}$(q) one-by-one starting from $q = r + 1, q = r + 1, r + 2, \cdots, d$
      $\mathbf{V}(q) = \min\{\min_{1 \leq i \leq (q-1)} \{\mathbf{T}(i, q) - U(i)\}, \mathbf{T}(q, q)\}$
      $\mathbf{U}(q) = \min_{1 \leq i \leq q} \{\mathbf{T}(q, i) - \mathbf{V}(i)\}$
    end if
    t $\leftarrow \max\{|\text{sum}(I_{rem}(:, 2)) - \text{sum}(I_{add}(:, 2))| + t_c, \text{sum}\,(I_{rem}(:, 2)), \text{sum}(I_{add}(:, 2))\}$
    $[\mathbf{X}^*_{n,k}, \mathbf{T}, \mathbf{U}, \mathbf{V}] \leftarrow$ Perform t iteration of stages of the basic Hungarian algorithm
    $\mathbf{D}_0 \leftarrow \mathbf{D}, \{\mathcal{K}_{0,n} \leftarrow \{\mathcal{K}_n\}\}$
  end if
end if

even though the required number of subchannels for the n-th user is $\mathcal{K}_n$. I need to obtain the best $\mathcal{K}^*$ subchannels for each user to be able to completely resolve the overlapping problem. Hence, the costs of sorted best $\mathcal{K}^*$ subchannels of each user and the corresponding indices of subchannels are stored in the sorted matrix $\mathbf{C}_{srt}$ and the index matrix $\mathbf{D}$, respectively. With the intention of reducing the complexity of the Hungarian algorithm, the non-overlapping subchannels are directly allocated to the corresponding users (in line 9 of **Algorithm** 4) using the direct subchannel assignment algorithm in **Algorithm** 5. If there is any remaining subchannels ($\mathcal{K}_n \neq 0$), I construct the assignment-cost-table $\mathbf{T}$ by duplicating the cost of n-th user $\mathcal{K}_n$ times. If the numbers of rows and columns in $\mathbf{T}$ are not equal, I balance number of rows and columns in $\mathbf{T}$ by adding dummy rows at the end with a Big-M (Big-M $>$ max($\mathbf{T}$)) value in the row entries (illustrated in lines 13-15 of **Algorithm** 4). The indices of the dummy rows are stored in the set $\mathbf{A}$ for future usage. It is important to note that the number of rows in $\mathbf{T}$ should not be greater than the number of columns since the total number of required subchannels cannot be greater than the total number of candidate subchannels in a feasible situation. At the end, the optimal matching $\mathbf{X}^*_{n,k}$ in the first iteration is obtained along with its dual variables ($\mathbf{U}$, $\mathbf{V}$) and the labels of assignment-cost-table ($\mathbf{T}$) by using Hungarian algorithm [147, 148, 150, 151]. The corresponding dual variables of the rows and columns in the assignment-cost-table are the elements of vectors $\mathbf{U}$ and $\mathbf{V}$, respectively.

From the second iteration onward, the subchannel assignment steps are illustrated in the lines 19-60 of **Algorithm** 4. Since I use the Hungarian algorithm based approach for subchannel allocation, I need to know the exact number of subchannels required by each user in every iteration. Hence, I update the number of subchannel requirement of each user based on the spectral footprint difference which minimizes the total spectral footprint in the CRN. The algorithm to update the number of subchannel requirement is presented by a flow

chart in Fig. 5.3 which will be described later in this section. In each iteration, new candidate subchannels will be added to or removed from the previous assignment-cost-table $\mathbf{T}_0$ until the resource allocation algorithm converges. Then, I traverse user by user by checking whether any subchannel/subchannels should be added to or removed from that user's assignment. If a particular subchannel, which is assigned in the previous assignment, should be removed from a particular user then I remove the matching $(a_t, \text{mate}(a_t))$ from $\mathbf{X}^*_{n,k}$ and assign a Big-M value to the corresponding entire row a_t in $\mathbf{T}$. Due to this assignment, the dual variable corresponding to that row is changed. Therefore, I update the corresponding dual variable as follows:

$$\mathbf{U}(a_t) = \min_j \{\mathbf{T}(a_t, j) - \mathbf{V}(j)\}. \tag{5.3}$$

Algorithm 5 DirChAssign Algorithm

```
1: Input: D, N, {K_n}
2: for ∀n ∈ N do
3:     R ← D[all users except n, ∀k]
4:     for k = 1 to K_n do
5:         k_ind ← D[n, k]
6:         if k_ind ∉ R then
7:             X_{n,k} ← 1, K_n ← K_n − 1
8:             Remove k_ind from D
9:         end if
10:    end for
11: end for
```

The removed row index, a_t, is stored in the set $\mathbf{A}$ for future usage. The row removal process due to the decrement of demand for number of subchannels is illustrated in lines 24-32.

After removing the mismatches from the assignment due to the reduction in the number of subchannels of users, I duplicate each user's cost row in $\mathbf{T}$ by the number of increment of subchannels compared to the previous iteration. If the set $\mathbf{A}$ is not empty then select a row from $\mathbf{A}$ and replace the corresponding user's cost for all subchannels. The binding dual

variable for this scenario can be updated using equation (5.3). This is continued until the set **A** becomes empty or all the duplication of cost row corresponding to the increased demand is completed. The process of duplicating rows for the increased subchannel demand of each user is illustrated in lines 36–45.

In the case that the number of subchannels in **D** is greater than the number of subchannels in $\mathbf{D}_0$, I should add new candidate subchannels with their corresponding cost columns at the end of **T**. Where $\mathbf{D}_0$ is the index matrix which stores the indices of subchannels used in the previous iteration (described in lines 18 and 59). Note that to apply the proposed algorithm, the number of rows and columns in **T** should be equal. When the number of rows and columns are unequal I add dummy rows with a Big-M value at the end of **T**. In general, if new subchannels appear in **D** for possible assignment then I have to calculate new dual variables for the corresponding columns as well as the corresponding rows which have the same row indices. Hence, the dual variables for the new indices of columns and rows in **T** can be calculated as follows:

$$\mathbf{V}(q) = \min\{\min_{1\leq i\leq(q-1)}\{\mathbf{T}(i,q)-\mathbf{U}(i)\}, \mathbf{T}(q,q)\} \tag{5.4}$$

$$\mathbf{U}(q) = \min_{1\leq i\leq q}\{\mathbf{T}(q,i)-\mathbf{V}(i)\} \tag{5.5}$$

where $q = r+1, r+2, \cdots, d$ is the number of columns in the matrix **T**. After calculating and updating all the dual variables (**U**,**V**) and **T**, I perform t (see line 58) iterations of a single stage of the basic Hungarian to obtain the optimal matching $\mathbf{X}^*_{n,k}$ [147,148,150,152]. The complexity of these iterations is therefore $\mathcal{O}(t\mathcal{K}^2)$, where t is the maximum number of changes as depicted in line 57 in the proposed subchannel assignment algorithm (i.e., **Algorithm** 4). The proof of optimality and the analysis of complexity of **Algorithm** (i.e. $\mathcal{O}(t\mathcal{K}^2)$) 4 for a given number of subchannel requirement are provided in **Appendix A** and **Appendix B**, respectively.

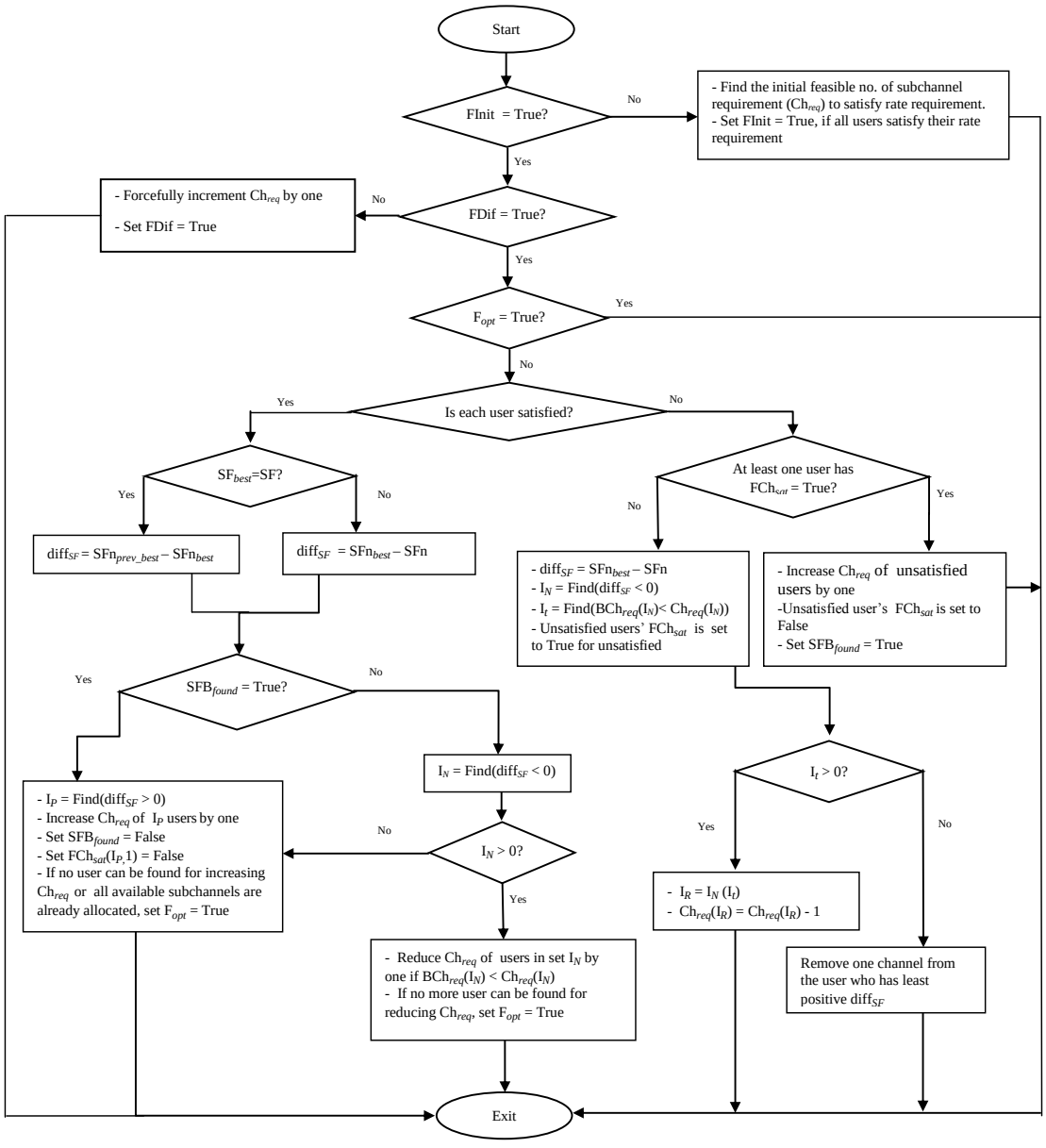

Figure 5.3: Algorithm steps to update the number of subchannels.

Table 5.2: Notations used in the flow chart in Fig. 5.3

Notation	**Definition**
$FInit$	Availability of initial feasible upper bound
$FDif$	Start of the SF difference based update
F_{opt}	Availability of optimal solution
SFB_{found}	Availability of new bound due to the increment of unsatisfied users' subchannel requirements
FCh_{sat}	Each user is satisfied with its required rate or not
BCh_{req}	Current best number of subchannel requirement of users
Ch_{req}	Number of subchannels allocated to each user
SF_{best}	Current best spectral footprint
SF	Current value of spectral footprint
SFn	Collection of SFs of individual users
SFn_{best}	Collection of the current best SFs of individual users
SFn_{prev_best}	Collection of the best SFs before finding current SFn_{best}

Fig. 5.3 shows the flowchart to update the number of subchannels required by each user based on the difference in spectral footprint of each user in consecutive iterations. To maintain the readability, all the notations used in the flowchart are shown in Table 5.2. The difference in spectral footprint of each user is calculated by deducting the previous iteration's spectral footprint from the spectral footprint in the present iteration unless mentioned otherwise (see the true case for $(SF_{best} = SF)$ in Fig. 5.3). A negative value of the SF difference indicates that the increment of subchannel of a particular user increases the spectral footprint whereas a positive value of the difference in spectral footprint indicates that there is a possibility to further reduce the spectral footprint by allocating more subchannels to that user. In this algorithm, the initial feasible subchannel requirement is obtained by increasing the subchannel requirement of unsatisfied users (Ch_{req}) one by one until all users are satisfied with their rate requirements. Obviously, this is the upper bound of the solution for the SF minimization problem. With this initial solution I cannot predict possible channel increment of users to reduce the total spectral footprint. Letting the initial solution as the present best available solution, the channel requirement of each user

(Ch_{req}) is increased by one to calculate the difference in SF for the new subchannel assignment and power allocation. After this forceful increment of number of subchannels the flag $FDif$ is set to $True$ since the process of updating the number of subchannel is based on the difference in SF starts.

Note that every iteration for channel update is followed by a rate satisfaction check. Hence, based on the rate satisfaction of users and the SF difference, I seek to obtain a better bound until there is no change in the bound as shown in Fig. 5.3.

5.3.2 Power Allocation

After obtaining the optimal subchannel assignment, $\mathbf{X}^*_{n,k}$, by solving the master problem in Section 5.3.1, I find $P_{n,k}$ that minimizes the spectral footprint as follows:

$$
\begin{aligned}
\min \ & \Big[F_B^*\Big]^{\alpha}\Big[\sum_{n=1}^{N}\sum_{k=1}^{\mathcal{K}} P_{n,k}\Big]^{\beta} \\
\text{s.t.} \ & \sum_{k=1}^{\mathcal{K}} X^*_{n,k} B\log\left(1+\frac{P_{n,k}h_{n,k}}{\eta+\sum_{p\in\mathcal{P}} I_{p,n,k}}\right) \geq \phi_n, \forall n \\
& g_{p,k}P_{n,k} \leq I^p_{th,k}, \ \ \forall\, \omega_k \leq \omega_{th}, p \in \mathcal{P}, \forall k \\
& \sum_{n=1}^{N}\sum_{k=1}^{\mathcal{K}} P_{n,k} \leq P^{max} \\
& P_{n,k}h_{n,k} \geq \Gamma_n, \forall n, \forall k \\
& P_{n,k} \geq 0, \forall n, k.
\end{aligned}
\tag{5.6}
$$

This power allocation subproblem can be solved by formulating the Lagrangian as follows:

$$\mathcal{L}(\mathbf{P},\lambda,\mu,\gamma,\nu)=\Big[F_B^*\Big]^{\alpha}\Big[\sum_{n=1}^{N}\sum_{k=1}^{\mathcal{K}}P_{n,k}\Big]^{\beta}+\sum_{p\in\mathcal{P}}\sum_{k=1}^{\mathcal{K}}\mu_{p,k}\Big(g_{p,k}P_{n,k}-I_{th,k}^{p}\Big)$$
$$+\sum_{n=1}^{N}\lambda_n\Big(\phi_n-\sum_{k=1}^{\mathcal{K}}X_{n,k}^{*}B\log\Big(1+\frac{P_{n,k}h_{n,k}}{\eta+\sum_{p\in\mathcal{P}}I_{p,n,k}}\Big)\Big)$$
$$+\gamma\Big(\sum_{n=1}^{N}\sum_{k=1}^{\mathcal{K}}P_{n,k}-P^{max}\Big)+\sum_{n=1}^{N}\sum_{k=1}^{\mathcal{K}}\nu_{n,k}\Big(\Gamma_n-P_{n,k}h_{n,k}\Big) \tag{5.7}$$

where $\lambda_n, \mu_{p,k}, \gamma$, and $\nu_{n,k}$ are Lagrangian multipliers [146]. Hence, the optimal power allocation at $(t+1)$-th iteration ($P_{n,k}(t+1)$) for a given subchannel assignment can be obtained by yielding $\dfrac{\partial\mathcal{L}(\mathbf{P},\lambda,\mu,\gamma,\nu)}{\partial P_{n,k}}=0$ as in (5.8) [146].

$$P_{n,k}(t+1)=\left[\frac{B\lambda_n X_{n,k}^{*}}{\beta[F_B^*]^{\alpha}\Big[\sum_{n=1}^{N}\sum_{k=1}^{\mathcal{K}}P_{n,k}(t)\Big]^{\beta-1}+\sum_{p\in\mathcal{P}}\mu_{p,k}g_{p,k}+\gamma-\nu_{n,k}h_{n,k}}-\frac{\eta+\sum_{p\in\mathcal{P}}I_{p,n,k}}{h_{n,k}}\right]^{+} \tag{5.8}$$

The Lagrangian multipliers can be updated in each iteration as follows [146]:

$$\lambda_n(t+1)=\Big[\lambda_n(t)+\delta(t)\Big(\phi_n-\sum_{k=1}^{\mathcal{K}}X_{n,k}^{*}B\log\Big(1+\frac{P_{n,k}(t)h_{n,k}}{\eta+\sum_{p\in\mathcal{P}}I_{p,n,k}}\Big)\Big)\Big]^{+} \tag{5.9}$$

$$\mu_{p,k}(t+1)=\Big[\mu_{p,k}(t)+\delta(t)\Big(g_{p,k}P_{n,k}-I_{th,k}^{p}\Big)\Big]^{+} \tag{5.10}$$

$$\nu_{n,k}(t+1)=\Big[\nu_{n,k}(t)+\delta(t)\Big(\Gamma_n-P_{n,k}h_{n,k}\Big)\Big]^{+} \tag{5.11}$$

$$\gamma(t+1)=\Big[\gamma(t)+\delta(t)\Big(\sum_{n=1}^{N}\sum_{k=1}^{\mathcal{K}}P_{n,k}-P^{max}\Big)\Big]^{+} \tag{5.12}$$

where $\delta(t)$ is the step size in the t-th iteration and can be updated as described in [146]. Hence, the power allocation algorithm can be presented as in **Algorithm** 6.

Remark: Obtaining good initial feasible transmit power is important since I adopt Lagrangian technique to allocate transmit power and it affects to the convergence of the algorithm. Note that at first we do not know the exact number of subchannels required to achieve the given rate requirement of users. Hence, I calculate the minimum transmit power required to decode a signal on each subchanel for a given user by considering the equality

Algorithm 6 Power Allocation Algorithm

Input: $\{\mathcal{K}_n\}, \{h_{n,k}\}, \{I_{p,n,k}\}, \{\omega_k\}, \{I^p_{th,k}\}, , \{\Gamma_n\}, \eta, \mathcal{K}, N, \Delta_{th}, P^{max}$
Initialization: $t \leftarrow 0, \lambda_n(0) \leftarrow \phi_n, \mu_{p,k}(0) \leftarrow 10^6, \gamma(0) \leftarrow 10^6, \nu_{n,k}(0) \leftarrow 0$
while $\Delta \geq \Delta_{th}$ **do**
  for $\forall n \in N$ **do**
    for $k = 1$ **to** $\mathcal{K}_n$ **do**
      $P_{n,k\_old} \leftarrow P_{n,k}$
      Calculate $P_{n,k}$ by using equation (5.8)
      $\Delta_{n,k} = P_{n,k\_old} - P_{n,k}$
      Update $\mu_{p,k}$ as in (5.10)
      Update $\nu_{n,k}$ as in (5.11)
    end for
    Update λ_n as in (5.9)
  end for
  Update γ as in (5.12)
  Update $\Delta = |\sum_{n=1}^{N} \sum_{k=1}^{\mathcal{K}} \Delta_{n,k}|$
  $t \leftarrow (t+1)$
  $\delta(t+1) \leftarrow \delta(t)/t^2$
end while
Output: $\{P_{n,k}\}$

of the sensitivity constraint in (1.5). Then, I check the violation of interference constraint in (1.3) for the calculated power. If the interference is not violated for a particular power I assume that power as a feasible power though I do not consider the rate constraint. This is acceptable and a good starting point since I do not know the exact number of subchannels that should be allocated to achieve a given rate requirement of users. Further, if the minimum transmit power, that I obtained by equating the sensitivity constraint in (1.5), violates interference constraint in (1.3) then I do not allocate power on that subchannel.

5.3.3 Complete Resource Allocation Algorithm

So far I have separately developed the algorithms for subchannels assignment, updating the number of subchannels required for each user, and power allocation. One iteration of the resource allocation algorithm is completed after executing the power allocation algorithm followed by the subchannel assignment algorithm. Then, new spectral footprint (i.e.,

$F_B^{\alpha} F_P^{\beta}$) for the corresponding subchannel assignment and power allocation is calculated. The new subchannel requirement of each user ($\mathcal{K}_n$) for the next iteration is calculated by using the algorithm for updating the number of subchannels which is presented in Fig. 5.3. This iterative allocation continues until the difference in spectral footprint (Δ_{SF}) drops below a given threshold. The complete resource allocation algorithm for minimizing SF is presented in **Algorithm** 7.

Note that **Algorithm** 1 is optimal for a given number of subchannel requirement. However, since I use the Lagrangian formulation, the power allocation algorithm converges to a local optima. Further, the algorithm to update the number of subchannels required by each user (in Fig. 3) is optimal if and only if the maximum increment of channel requirement for a user in a particular iteration is one. Otherwise, the subchannel update algorithm is not optimal. Therefore, the overall algorithm converges to a local optima although the maximum increment of subchannel requirement for a user in a particular iteration is one.

5.4 Spectral Footprint Analysis for a Single User Scenario

In this section, I obtain a closed-form expression for the optimal number of subchannels to minimize the spectral footprint under certain assumptions. Specially, I assume that there exists a single user in CRN and the subchannel gains between the user and the CR-BS are sufficiently good. The activities of PUs over the subchannels are assumed to be similar. Under these conditions the subchannels can be allocated to the user in a greedy manner. First, the cost for assigning the k-th subchannel to the user is calculated as: $c_k = \frac{\eta + \sum_{p \in \mathcal{P}} I_{p,k}}{(1-\omega_k) B h_k}$. The calculated cost values are sorted in an ascending order and the first κ, $\kappa \leq \mathcal{K}$, subchannels are assigned to the user. Hence, the power minimization problem for the given κ can be

Algorithm 7 Complete Algorithm for SF Minimization

Input: $\psi = \Big\{\{\mathcal{K}_n\}, \{h_{n,k}\}, \{I_{p,n,k}\}, \{\omega_k\}, \eta, \mathcal{K}, N\Big\}$, $\xi = \Big\{\{\phi_n\}, \{I^p_{th,k}\}, \{\Gamma_n\}, P^{max}\Big\}$, Δ_{th}, Δ_{SF}, $\Delta_{SF_{th}}$
$\Lambda = \Big\{\{SFn\}, \{SFn_{best}\}, \{SFn_{prev\_best}\}, SF, SF_{best}, \ SFB_{found}, BCh_{req}, FInit, FDif, F_{opt}\Big\}$, F_0, α, β
Initialization: $\{P_{n,k\_old}\} \leftarrow \{0\}$, $\{SFn_{best}\} \leftarrow \{0\}$, $\{SFn_{prev\_best}\} \leftarrow \{0\}$, $\{SF_{best}\} \leftarrow \{10^{10}\}$, $SF_{prev} \leftarrow 0$, $\{\mathcal{K}_n\} \leftarrow 1$ and $\{P_{n,k}\} \leftarrow 1$
while $\Delta_{SF} \geq \Delta_{SF_{th}}$ **do**
  $\{X^*_{n,k}\} \leftarrow Subchannel\_Assignment(\psi, F_0)$
  \\Using **Algorithm 4**
  $\{P^*_{n,k}\} \leftarrow Power\_Allocation(\psi, \xi, \alpha, \beta, \Delta_{th})$
  \\Using **Algorithm 6**
  $SF = \Big[\sum_{n=1}^{N}\sum_{k=1}^{\mathcal{K}} \frac{BX^*_{n,k}}{(1-\omega_k)}\Big]^{\alpha}\Big[\sum_{n=1}^{N}\sum_{k=1}^{\mathcal{K}} P^*_{n,k}\Big]^{\beta}$
  $\{SFn\} = \Big[\sum_{k=1}^{\mathcal{K}} \frac{BX^*_{n,k}}{(1-\omega_k)}\Big]^{\alpha}\Big[\sum_{k=1}^{\mathcal{K}} P^*_{n,k}\Big]^{\beta}, \quad \forall n$
  $\{rate_n\} = \sum_{k=1}^{\mathcal{K}} X^*_{n,k} B\log\left(1+\frac{P^*_{n,k}h_{n,k}}{\eta+\sum_{p\in\mathcal{P}} I_{p,n,k}}\right), \quad \forall n$
  if $\{rate_n\} > \{\phi_n\}$ **then**
    if $SF_{best} > SF$ **then**
      $\{SFn_{prev\_best}\} \leftarrow \{SFn_{best}\}$
      $\{SFn_{best}\} \leftarrow \{SFn\}$
      $SF_{best} \leftarrow SF$
      $BCh_{req}(n) \leftarrow \{\mathcal{K}_n\}$
    end if
  end if
  $\{\mathcal{K}_n\} \leftarrow Update\_NumberOfSubchannels(\Lambda)$ \\Using **flowchart** in Fig. 5.3
  $\Delta_{SF} \leftarrow |SF - SF_{prev}|$
  $SF_{prev} \leftarrow SF$
end while
Output: $X^*_{n,k}, \{P^*_{n,k}\}$

written as follows:

$$\begin{aligned} &\min \Big[\sum_{k=1}^{\kappa} \frac{B}{(1-\omega_k)}\Big]^{\alpha}\Big[\sum_{k=1}^{\kappa} P_k\Big]^{\beta} \\ &\text{s.t.} \sum_{k=1}^{\kappa} B\log\left(1+\frac{P_k h_k}{\eta+\sum_{p\in\mathcal{P}} I_{p,k}}\right) \geq \phi \\ &\quad g_{p,k}P_k \leq I^p_{th,k},\ \ \forall\, \omega_k \leq \omega_{th}, p \in \mathcal{P}, \forall k \\ &\quad P_{n,k} \geq 0, \forall n, k. \end{aligned} \tag{5.13}$$

The optimal power for the problem in (5.13) can be obtained by formulating the Lagrangian and solving its dual problem. Hence, the optimal power on the k-th subchannel can be expressed as

$$P_k = \begin{cases} \Big[\frac{2^{\frac{\phi}{\kappa B}}}{\prod_{k=1}^{\kappa}(H_k)^{\frac{1}{\kappa}}} - \frac{1}{H_k}\Big]^{+}, & P_k \leq \min_{p\in\mathcal{P}}\Big(\frac{I^p_{th,k}}{g_{p,k}}\Big) \\ \min_{p\in\mathcal{P}}\Big(\frac{I^p_{th,k}}{g_{p,k}}\Big), & \text{otherwise} \end{cases} \tag{5.14}$$

(5.15)

where H_k is the CINR and can be expressed as: $H_k = \dfrac{h_k}{\eta+\sum_{p\in\mathcal{P}} I_{p,k}}$. Hence, for the special case of $P_k \leq \min_{p\in\mathcal{P}}\Big(\frac{I^p_{th,k}}{g_{p,k}}\Big)$, the problem of finding κ that minimizes the spectral footprint can be written as follows:

$$\min_{\kappa}\Big\{\Big[\sum_{k=1}^{\kappa} \frac{B}{(1-\omega_k)}\Big]^{\alpha}\Big[\sum_{k=1}^{\kappa}\Big(\frac{2^{\frac{\phi}{\kappa B}}}{\prod_{k=1}^{\kappa}(H_k)^{\frac{1}{\kappa}}} - \frac{1}{H_k}\Big)\Big]^{\beta}\Big\}. \tag{5.16}$$

Assuming perfect channel state information at the user, the CINR on the k-th subchannel can be written with the help of average CINR $\bar{H}$ as: $H_k = \bar{H} + \Delta H_k$. Hence, the expression in (5.16) can be modified as follows:

$$\min_{\kappa}\Big\{\frac{B^{\alpha}}{\bar{H}^{\beta}}\Big[\sum_{k=1}^{\kappa} \frac{1}{(1-\omega_k)}\Big]^{\alpha}\Big[\sum_{k=1}^{\kappa}\Big(\frac{2^{\frac{\phi}{\kappa B}}}{\prod_{k=1}^{\kappa}(1+\frac{\Delta H_k}{\bar{H}})^{\frac{1}{\kappa}}} - \frac{1}{(1+\frac{\Delta H_k}{\bar{H}})}\Big)\Big]^{\beta}\Big\}. \tag{5.17}$$

Assuming that the variation of CINR over all subchannels is small (i.e., $\frac{\Delta H_k}{\bar{H}} \approx 0$) and

the PU activity factor is approximately same (i.e., $\omega_k \approx \omega$), the above expression can be written as

$$\min_{\kappa}\Big\{\frac{B^{\alpha}\,\Omega}{\bar{H}^{\beta}(1-\omega)^{\alpha}}\Big\} \tag{5.18}$$

where $\Omega = \kappa^{(\alpha+\beta)}(2^{\frac{\phi}{\kappa B}}-1)^{\beta}$. Since Ω in equation (5.18) depends on the optimal number of subchannels (κ), the expression in (5.18) implies minimization over κ. Hence, I can interpret Ω as the optimization metric which minimizes the spectral footprint in an asymptotic scenario. The value of κ that minimizes the spectral footprint in (5.18) can be obtained by yielding the derivative with respect to κ and finding its roots by equating it to zero. Hence, the roots can be obtained from

$$\kappa^{(\alpha+\beta-1)}(2^{\frac{\phi}{\kappa B}}-1)^{\beta-1}\big[(\alpha+\beta)(2^{\frac{\phi}{\kappa B}}-1)-\beta 2^{\frac{\phi}{\kappa B}}\log(2^{\frac{\phi}{\kappa B}})\big]=0.$$

It is required to allocate at least one subchannel to the user for satisfying its rate requirement. Hence, the number of subchannels (κ) obtained by yielding $\kappa^{(\alpha+\beta-1)} = 0$ and $(2^{\frac{\phi}{\kappa B}}-1) = 0$ are no longer a feasible solution for (5.18). However, the $[(\alpha+\beta)-\beta(2^{\frac{\phi}{\kappa B}}-1)^{\beta-2}2^{\frac{\phi}{\kappa B}}\log(2^{\frac{\phi}{\kappa B}})] = 0$ yields a closed-form solution for κ. Hence, the κ that minimizes SF can be derived in closed-form as in (5.19), where $\mathrm{Lambertw}(.)$ is the Lambert W function defined in [153].

$$\kappa = \frac{\phi}{B\Big(\log_2\Big[-\frac{(\alpha+\beta)}{\beta}\Big]-\log_2\Big[\mathrm{Lambertw}\Big(-\frac{(\alpha+\beta)}{\beta}\exp\big(-\frac{(\alpha+\beta)}{\beta}\big)\Big)\Big]\Big)},\ \beta>0. \tag{5.19}$$

The minimum SF for the asymptotic analysis in the single user case can thus be obtained by substituting the value of κ in (5.18). For this special case, the optimal number of subchannels required to satisfy the user's demand does not directly depend on the CINR and this effect can be clearly observed in (5.19). In general, the optimal number of sub-

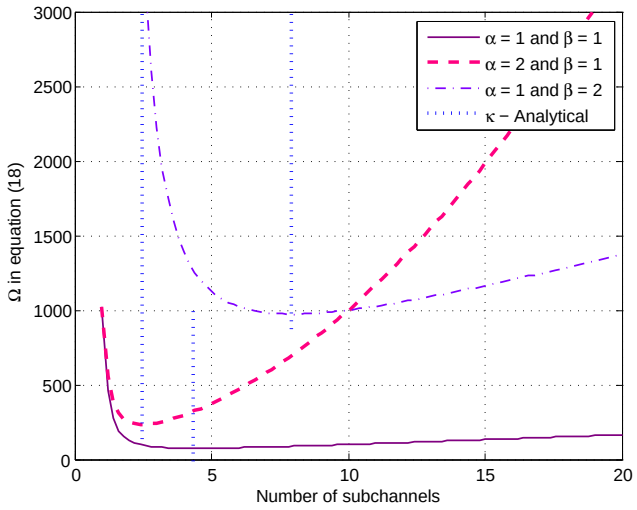

Figure 5.4: Behaviour of Ω (see (5.18)) when there is a single user in the network.

channels required to satisfy users' demands indirectly depends on the collective view of CINR in terms of the summation and the product as shown in (5.17). Interestingly, there is no difference in κ when the footprint weighting parameters are equal, i.e., $\alpha = \beta$.

5.5 Simulation Results and Discussions

5.5.1 Simulation Parameters

I present simulation results and compare the performance of our proposed resource allocation algorithm with the traditional power minimization (waterfilling) algorithm. The important simulation parameters are as follows: total number of subchannels is $\mathcal{K} = 30$, bandwidth of each subchannel (B) is 10 kHz, spectral density of noise N_0 is -174 dBm/Hz, the path-loss exponent is 3, and the standard deviation of shadowing is 8 dB. The minimum required received power at the SU receivers is -100 dBm and the maximum allowable interference at the PUs is calculated such that they can maintain a minimum SINR of 15dB. The cognitive users are placed randomly in a 500 m $\times$ 500 m grid.

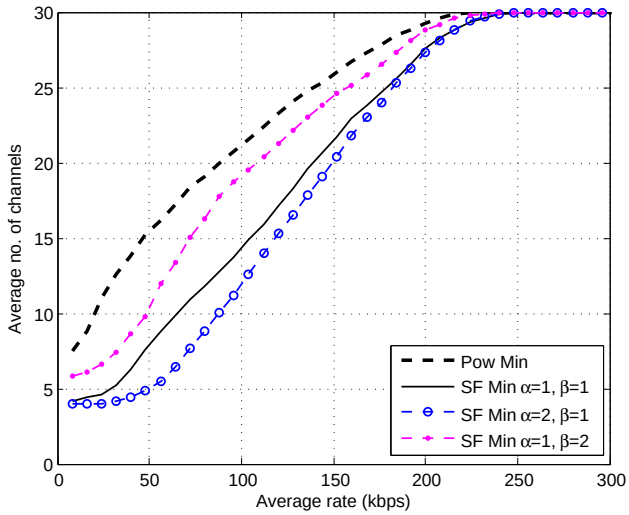

Figure 5.5: Average number of subchannel requirement when there are 4 SUs in the network.

5.5.2 Results

Fig. 5.4 shows the behaviour of the Ω (see (5.18)) for the single SU case. The Ω value is plotted for several combination of bandwidth and power weighting parameters (α and β, respectively) when the minimum rate requirement of the SU (ϕ_n) is 100kbps. Further, the optimal number of subchannel requirement (κ), which is obtained through the asymptotic analysis is also plotted by vertical dash lines to compare our asymptotic results. Fig. 5.4 clearly reveals that the dash lines match exactly with the minimum of Ω curves validating our analysis.

Fig. 5.5 shows the average number of subchannels required per user to satisfy its rate requirement when there are 4 SUs in the network. The channel requirement is plotted for several weighting values of α and β. This figure reveals that the number of subchannel requirement varies with the weighting factors. Further, the case with $\alpha = 0$ and $\beta = 1$ presents the power minimization scenario which is plotted by using the power minimization. As expected, the power minimization consumes as many subchannels as possible

to reduce the power utilization. I can clearly observe that the increase of the bandwidth weighting factor (α) reduces the number of subchannels utilized to satisfy users' rate requirements. This fact is revealed by the curves corresponding to ($\alpha = 1$ and $\beta = 1$) and ($\alpha = 2$ and $\beta = 1$). Further, I can clearly see that the spectral footprint minimization technique uses a fewer number of subchannels at the expense of a slight increase in transmit power (as shown in Fig. 5.6).

Fig. 5.6 depicts the effect of weighting factor in the power allocation. The $\alpha = 0$ and $\beta = 1$ case (power minimization) is plotted as the benchmark to compare the performance of the generalized spectral footprint minimization approach. I observe that the increase of the bandwidth weighting factor (α) slightly increases the transmit power of SUs while reducing the number of subchannels utilized to satisfy users' rate requirements (compare Fig. 5.5 and 5.6). This fact is revealed by the curves corresponding to ($\alpha = 1$ and $\beta = 1$) and ($\alpha = 2$ and $\beta = 1$).

In Fig. 5.7, the spectral footprint is plotted for several combinations of the weighting factors. With the power minimization, the spectral footprint is always higher in low rate requirement region when compared to that with the spectral footprint minimization approach. This is due to the fact that the power minimization algorithm uses as many subchannels as possible to reduce the transmit power. Further, these curves reveal that the generalized SF minimization approach has more flexibility to adapt to the environment when the rate requirement of SUs lies in the low to medium region. This is possible since the SUs do not reach the maximum allowable interference threshold in most of the times. Therefore, the SUs have the opportunity to increase their transmit powers until the interference threshold is reached. Moreover, it is important to notice that, at the high rate requirement scenarios, since all the available subchannels are utilized, the performance metrics of both power minimization and spectral footprint minimization algorithms converge to the same value.

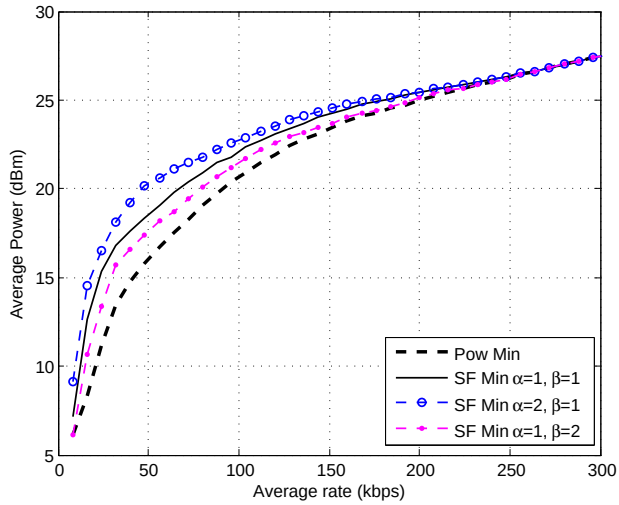

Figure 5.6: Average transmit power of users when there are 4 SUs in the network.

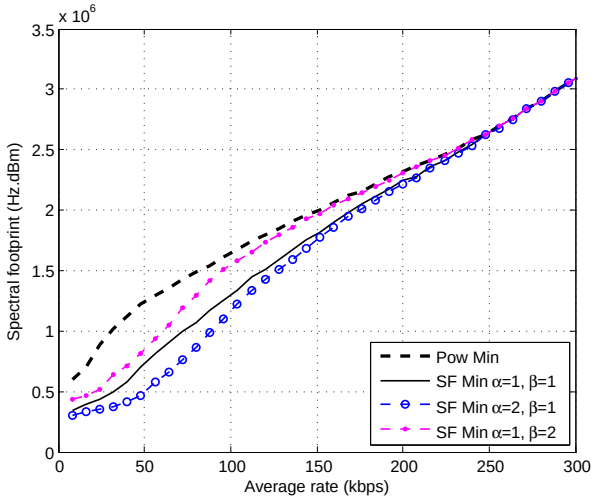

Figure 5.7: Spectral footprint when there are 4 SUs in the network.

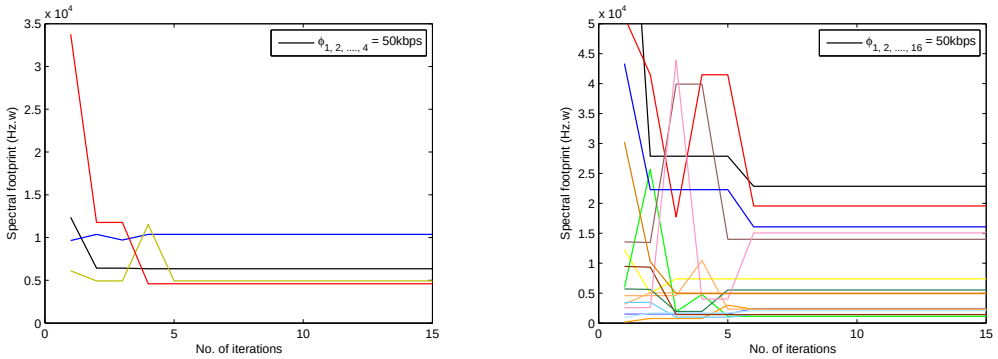

(a) Convergence of the proposed resource allocation algorithm when $N = 4$ and $\phi_n = 50$ kbps.

(b) Convergence of the proposed resource allocation algorithm when $N = 16$ and $\phi_n = 50$ kbps.

Figure 5.8: Convergence of the proposed resource allocation algorithm.

The convergence behavior of the proposed resource allocation algorithm is shown in Fig. 5.8(a) and Fig. 5.8(b) for different combinations of users with equal minimum rate requirements. I can clearly observe that the proposed algorithm converges within 10 iterations when there are 16 users. By comparing Fig. 5.8(a) and Fig. 5.8(b) I observe that the percentage increase of iteration per user is $\approx \frac{6-5}{16-4} = 8.33\%$. That is, the number of users does not impact for the convergence of resource allocation algorithm significantly.

Fig. 5.9 shows the performance of the proposed resource allocation algorithm with respect to the optimal resource allocation algorithm when there is two users ($N = 2$) and five subchannels ($\mathcal{K} = 5$). The optimal curves are plotted by using a brute-force search. Specially, Fig. 5.9(a), Fig. 5.9(b), and Fig. 5.9(c) clearly reveal that the performance gap between the optimal and proposed approach is not significant.

5.6 Conclusion

In this chapter, I have proposed a downlink resource allocation algorithm for cognitive radio networks based on the generalized spectral footprint minimization. Specifically, I have minimized the spectral footprint in terms of weighted bandwidth and power product

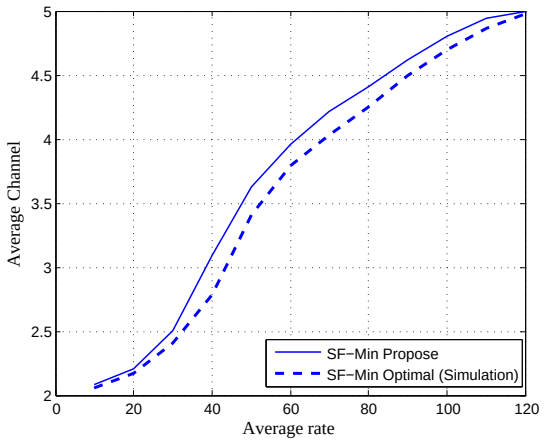

(a) Average number of subchannels

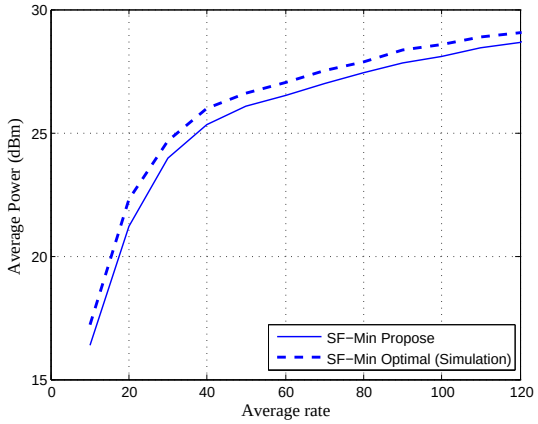

(b) Average Power

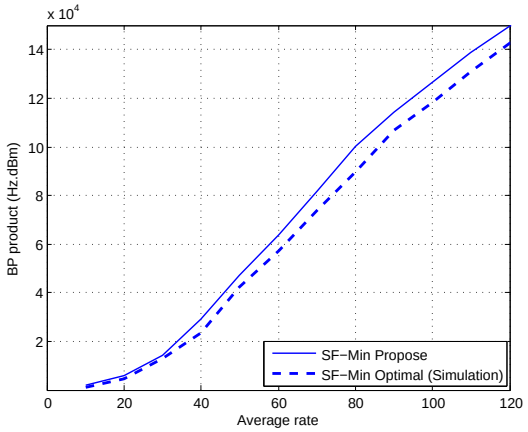

(c) Average spectral footprint

Figure 5.9: Comparison of the proposed resource allocation algorithm with the optimal resource allocation algorithm based on simulations when $N = 2$, $\mathcal{K} = 5$, $\omega_k = [0.2,\ 0.3,\ 0.4,\ 0.5,\ 0.6]$, $\alpha = 1$ and $\beta = 1$. 140

which allows me to improve the spectrum utilization by optimally selecting the weighting factors. I have compared the performance of our spectral footprint minimization approach with the power minimization and an approach based on brute-force search. The simulation results have shown that, when compared to the traditional power minimization approach, the spectral footprint minimization technique uses a fewer number of subchannels to satisfy a given rate requirement at the expense of a slight increase in the transmit power. Specially, a low-complexity subchannel assignment algorithm based on the modified Hungarian algorithm has been proposed. When the total number of available subchannels is $\mathcal{K}$, the computational complexity of the proposed subchannel assignment algorithm is $\mathcal{O}(t\mathcal{K}^2)$ for t number of new subchannel assignments. I have obtained a closed-form expression for the optimal number of subchannels when there is a single user in the network. Specially, I have shown that the optimal number of subchannels required by users does not depend on the value of weighting factors (α and β) when $\alpha = \beta$.

Chapter 6

Conclusion and Future Directions

6.1 Conclusion

In this dissertation, I have studied three different aspects of centralized cognitive radio networks, namely, learning-based cooperative spectrum sensing, generalized spectral footprint-based resource allocation, and dynamic common control-based medium access control protocol.

In Chapter 3, I have designed cooperative spectrum sensing (CSS) mechanisms for centralized cognitive radio networks (CRNs) based on unsupervised and supervised learning techniques. I have proposed to use unsupervised classifiers such as K-means clustering and Gaussian mixture model (GMM) for CSS, whereas the support vector machine (SVM) and weighted K-nearest-neighbor classifiers have been proposed for CSS under supervised learning. The proposed SVM classifier achieves the highest detection performance compared to the other CSS algorithms by mapping the feature space into the higher dimensional space with the help of kernel functions, namely, linear kernel and polynomial kernel functions. The unsupervised K-means clustering scheme which achieves the performance very close to the supervised SVM-Linear classifier is a promising candidate for CSS in CRNs due to its flexibility in practical implementation (i.e. due to the unsupervised learning), and lower training and classification delay. Further, the testing energy vectors which are used

for CSS in K-mean clustering can be used as a training energy vector in K-mean clustering. Therefore, K-mean clustering based CSS is highly adaptive to the dynamically changing environment and provide a cost effective solution to the CSS in CRNs. In particular, the weighted KNN cognitive classifier requires very small amount of time for training the classifier. Hence, the weighted KNN classifier is well suited for CSS which requires updating training energy vectors on-the-fly.

More importantly, the unsupervised K-means clustering and the supervised SVM with the linear kernel are promising approaches for CSS in CRNs. In practical implementation, it is important to obtain accurate training energy vectors since inaccurate training of the classifier results in inaccurate decision. The proposed CSS approaches can be further improved to gradually train the classifiers by using the energy vectors obtained one-by-one on the fly. This facilitates the classifiers to adapt to the varying environment without training all over again.

In chapter 4, I have proposed a solution to a long standing problem in designing cognitive medium access control (MAC) protocols. Specially, all the previous studies in the literature assumed that there exists a dedicated common control channel (CCC) owned by the cognitive operators. This assumption itself challenges the definition of the cognitive radios. Hence, in this chapter, I have proposed a novel dynamic CCC-MAC (DCCC-MAC) protocol for CRNs by replacing the assumption of having a dedicated CCC for cognitive MAC protocols. In particular, the proposed DCCC-MAC protocol is capable to withstand against control channel jamming problem in wireless networks due to the dynamic nature of the CCC. In the this protocol, the CCC for a given frame is selected using a support vector machine-based approach and the set of primary users idle channels for the given frame duration in the network is given as a by-product of CCC selection process. Hence this improves the detection probability while mitigating the hidden terminal problem in CRNs.

Moreover, this protocol mitigates not only the hidden terminal problem in CRNs but also it mitigates the multichannel hidden terminal problem in the existing multichannel MAC protocols by prioritizing the channel access of scheduled secondary users. Specially, the system throughput has been analyzed in closed-form and simulation results have validated the correctness of our analysis.

In Chapter 5, I have proposed a novel downlink resource allocation scheme for OFDMA-based cognitive radio networks based on the generalized spectral footprint minimization. Since the generalized spectral footprint is defined as the product of weighted bandwidth and power, it allows us to improve the spectrum utilization by optimally selecting the weighting factors. In particular, the simulation results have shown that, when compared to the traditional power minimization approach, the spectral footprint minimization technique uses fewer number of subchannels to satisfy a given rate requirement at the expense of a slight increase in the transmit power. Moreover, for CRNs, a generalized spectral footprint based allocation paves the way to utilize the available radio resources (spectrum and power) optimally and opportunistically due to the flexibility in weighting bandwidth and power footprint depending on the network operators objectives.

The modified Hungarian based low complex subchannel allocation algorithm can be applied not only for the OFDMA based subchannel allocation but also for any iterative assignment problem. When the total number of available subchannels is $\mathcal{K}$, the computational complexity of the proposed subchannel assignment algorithm is $\mathcal{O}(t\mathcal{K}^2)$ for t number of new subchannel assignments. To observe the insight of the system performance, I have obtained a closed-form expression for the optimal number of subchannels requirement to satisfy a given rate requirement when there is a single user in the network. Specially, I have shown that the optimal number of subchannels required by users does not depend on the value of weighting factors (α and β) when $\alpha = \beta$.

6.2 Future Directions

As future work, some interesting ideas can be explored as discussed below.

6.2.1 Improved Cooperative Spectrum Sensing

The cognitive radios sense and opportunistically access the spectrum when the primary users are not utilizing the spectrum. This cognitive transmission may leads to collision with primary transmission since CRs do not have any idea about the PUs' behaviour in the network. However, the effect of this collision due to harmful interference can be mitigated if CRs can identify the MAC protocols (i.e. TDMA, CSMA/CA, pure ALOHA, Slotted ALOHA and etc.) which are utilized by the PUs. To identify the primary MAC protocols, the CRs can exploit the techniques used in the learning based cooperative spectrum sensing. However, identifying suitable feature space which can be used to clearly differentiate these protocols is a daunting task. Specially, the average received power, variation of received power, channel busy duration and channel idle duration will be good candidates to treat as features in the process of identifying primary MAC protocol by using proposed techniques. As an example, if a TDMA-based MAC protocol is used in primary network, then the PUs transmit packets in the scheduled time slots. Therefore, we cannot expect collision between primary transmission, and therefore, the received power at a CR is expected to be low. However, if primary network uses ALOHA based approach, then collision occurs while generating comparatively high energy level (received power) at CRs. Specially, the receiving energy variation is also significant in these two protocols. Hence, we can use received energy and its variation for identifying TDMA and ALOHA-based protocols used in the primary network. On the otherhand, busy time duration also can be utilized to differentiate TDMA and pure ALOHA protocols. The channel busy duration in TDMA-based approach is integer multiple of time slot duration whereas the channel busy duration is not

necessarily an integer multiple of time slot duration since PUs transmission duration can be overlapped causing collisions.

In the proposed cooperative spectrum sensing schemes and dynamic common control channel-based MAC protocol, the PUs' idle channels and control channel are selected only considering the sensing information. Since we only consider the sensing information in the idle channel selection process, there is no guarantee for the CRs that the detected channel is idle for the whole duration of cognitive transmission. Therefore, it is important to jointly consider the PUs' activity and cooperative spectrum sensing decision in the process of PU idle channel selection and allocation. Specially, I have completely ignored the availability of radio environmental maps in cooperative spectrum sensing. However, the accuracy of the proposed cooperative spectrum sensing schemes can be further improved if we can exploit the REMs contents.

The wireless channel is time-varying. Therefore, the received energy at the CRs from the PUs varies with time. Hence, the initial training sets fed to the classifiers may not give accurate sensing decision at a different time. Also, it is reasonable to assume that the primary networks broadcast some information time-to-time which helps the CRNs to update the training set. Another limitation of the proposed CSS schemes is: if the training set is updated by a single sample, we have to train the classifiers from the very beginning. This is time consuming and the CRs have to hold their transmission within the training duration, which causes underutilization of the radio spectrum. This drawback can be eliminated by introducing incremental learning techniques to the proposed cooperative spectrum sensing scheme.

6.2.2 Extension of the Generalized Spectral Footprint Minimization Model

The proposed generalized spectral footprint based resource allocation technique can be extended to multicell scenario where each cognitive cell consists of a single CR-BS and

several SUs. However, the concept of activity factor needs to be modified to capture inter-cell interference. One way is to define a generalized activity factor to capture the effect of aggregate interference on each subcarrier from both the primary network and the neighboring CBSs. An alternative approach is to determine separate activity factors for interfering secondary cells as well as an activity factor related to the primary network. In this way, the proposed spectral footprint minimization approach for resource allocation can be applied to a new cognitive system model with the modified activity factors and additional cochannel interference constraint.

In an OFDMA-based cellular network in which user equipments (UEs) are allowed to use D2D (also called direct mode) of communication, the D2D links may reuse some of the resource blocks. Generally, the mode of communication is determined through a mode selection algorithm (cellular mode or D2D mode). Assuming that the D2D mode with resource reuse is selected for communication between users, performing the interference-aware resource allocation with QoS constraints can be addressed using our proposed scheme. To this end, we can consider the D2D network as a CRN, while the cellular network acts as the primary network. The resource allocation (i.e., power and spectrum) for D2D should be done by the base station. Intuitively, there exists a relationship between the activity factor defined for a subcarrier and the mode of communication selected for the D2D communication. Actually, D2D communication-enabled networks should have a different notion of definition for the activity factor since PUs activity in different channel is available for both cellular and D2D users.

Let us assume a relay-based network and there are multiple relays to assist its communications. Each relay station (RS) and its corresponding users form a cluster. In this scenario, transmission occurs in two consecutive time slots. In first time slot, the base station transmits it message to the relay stations. Then, in the second time slot, the relay

stations transmit the received messages to the corresponding users. Resource allocation during the second phase of transmission is a special case that can be captured by the proposed scheme. Since all the subchannels are available to all the clusters, the problem of inter-cluster interference will arise and can be readily addressed by modifying the activity factor term in bandwidth footprint in such a way that captures the inter-cluster interference. In this context, relay-based wireless networks can utilize the generalized spectral footprint minimization-based approach for efficient resource allocation. Specially, this scheme facilitates relays to save subchannels from low demand clusters while allowing to exploit them in high demand clusters.

6.2.3 Extension of the DCCC-MAC Protocol

In the proposed DCCC-MAC protocol, the common control channel and the PUs' idle channels are selected by only considering the sensing information. The channel which has the highest possibility to be idle within the considered time slot is selected as the CCC for the current time frame. However, there is no guarantee for the CRs that the available channels are idle for the whole duration of cognitive transmission. Therefore, it is important to jointly consider the PUs' activity and cooperative spectrum sensing decision in the process of selection of CCC and allocation of PU idle channels. The integration of PUs' activity is important since this gives a long-term picture about the appearance of PUs on the considered channel. Further, implementing a mechanism to exploit both the REMs and sensing information while dynamically selecting a control channel is of significant important since this improves the cognitive network performance while avoiding harmful interference at the PUs.

The proposed DCCC MAC protocol has been developed for centralized CRNs. This cannot be applied in a distributed network. Developing a dynamic common control-based distributed MAC protocol would be an interesting and challenging problem.

6.2.4 Full-Duplex Cognitive Radio Networks

Until recently, the concept of simultaneous transmission and reception (i.e., full-duplexing [FD]) in the same time and frequency bands did not seem to be promising due to the overwhelming nature of the so called self-interference generated by a transmitter to its collocated receiver. Fortunately, with the recent advancement in antenna and digital baseband technologies and RF interference cancellation techniques, the self-interference can be reduced close to the level of noise floor in low-power networks [154, 155]. Interestingly, the theoretical gain of FD transmission is equal to twice the spectral efficiency of half-duplex transmission assuming perfect self interference cancellation. Due to this attractive feature, there has been significant interest in FD-enabled wireless applications, especially, the ones with low transmission power and distance requirements such as short-range cognitive radios and device-to-device communications.

All the concepts and algorithms which have been developed in this dissertation assume half-duplex communication scenarios. However, in practical situations, the PU behaviour is random and the PUs may become active on a channel which is currently being used by a CR. This change in PU activity cannot be immediately detected by the CRs due to the inherent limitation of half-duplex communication. This may cause unexpected interference and delay to PU communications. This unexpected interference and delay caused to the PUs by cognitive transmissions can be eliminated by simultaneous transmission-and-sensing on the same channel. At the same time, the CRs can implement simultaneous transmission-and-reception that improves the spectral efficiency. However, the simultaneous transmission-and-sensing and transmission-and-reception-based cognitive communication offers a trade-off between the spectrum awareness and spectrum efficiency. Hence, the FD-enabled CRNs should optimize their performance by adaptively switching between these two operational modes. In the context of FD-enabled CRNs, implementing dynamic

common control channel-based MAC protocol, which adaptively switches between two different operational modes, is challenging. Further, the generalized spectral foortprint minimization-based resource allocation becomes a daunting task since the resource allocation algorithm has to consider both the uplink and downlink channel jointly. Further, if the cognitive base station also uses full-duplex communication with two different users (i.e., start receiving from one CR while transmitting to other CR) then this generalized spectrum allocation problem becomes much more challenging.

Bibliography

[1] I. Akyildiz, W.-Y. Lee, M. C. Vuran, and S. Mohanty, "A survey on spectrum management in cognitive radio networks," *Communications Magazine, IEEE*, vol. 46, no. 4, pp. 40–48, April 2008.

[2] L. B. Le and E. Hossain, "Resource allocation for spectrum underlay in cognitive radio networks," *Wireless Communications, IEEE Transactions on*, vol. 7, no. 12, pp. 5306–5315, December 2008.

[3] P. Hu and M. Ibnkahla, "Cm-mac: A cognitive mac protocol with mobility support in cognitive radio ad hoc networks," in *Communications (ICC), 2012 IEEE International Conference on*, June 2012, pp. 430–434.

[4] m. naeem, A. Anpalagan, M. Jaseemuddin, and D. Lee, "Resource allocation techniques in cooperative cognitive radio networks," *Communications Surveys Tutorials, IEEE*, vol. 16, no. 2, pp. 729–744, Second 2014.

[5] M. Timmers, S. Pollin, A. Dejonghe, L. Van der Perre, and F. Catthoor, "A distributed multichannel mac protocol for multihop cognitive radio networks," *Vehicular Technology, IEEE Transactions on*, vol. 59, no. 1, pp. 446–459, Jan 2010.

[6] G. Bianchi, "Performance analysis of the ieee 802.11 distributed coordination function," *Selected Areas in Communications, IEEE Journal on*, vol. 18, no. 3, pp. 535–547, March 2000.

[7] FCC:, "Et docket no 02-135 spectrum policy task force report," Federal Communications Comission (FCC), Tech. Rep.

[8] ——, "Et docket no 02-155 spectrum policy task force report," Federal Communications Comission (FCC), Tech. Rep.

[9] ——, "Et docket no 03-222 notice of proposed rule making and order," Federal Communications Comission (FCC), Tech. Rep., December 2003.

[10] J. Mitola, "Cognitve radio: An integrated agent architecture for software define radio," Ph.D. dissertation, KTH, 2000.

[11] E. Hossain and V. K. Bhargava, *Cognitive Wireless Communication Networks*. Springer, 2007.

[12] Haykin, "Cognitive radio: brain-empowered wireless communications," *IEEE Journal on Selected Areas in Communications*, vol. 23, pp. 201–220, February 2005.

[13] P. Kolotzy, "Next generation communications: Kickoff meeting," in Proc. DARAPA, Tech. Rep.

[14] A. Fragkiadakis, E. Tragos, and I. Askoxylakis, "A survey on security threats and detection techniques in cognitive radio networks," *Communications Surveys Tutorials, IEEE*, vol. 15, no. 1, pp. 428–445, First 2013.

[15] A. Attar, H. Tang, A. Vasilakos, F. Yu, and V. Leung, "A survey of security challenges in cognitive radio networks: Solutions and future research directions," *Proceedings of the IEEE*, vol. 100, no. 12, pp. 3172–3186, Dec 2012.

[16] S. V. Fragkiadakis A and P. N., "Anomaly-based intrusion detection algorithms for wireless networks," *The 8th WWIC 2010*, June 2010.

[17] T. T. A. Fragkiadakis, E. Tragos and I. Askoxylakis, "Design and performance evaluation of a lightweight wireless early warning intrusion detection prototype," *EURASIP Journal on Wireless Communications and Networking*, no. 12, pp. 1–18, 2012.

[18] A. Houjeij, W. Saad, and T. Basar, "Evading eavesdroppers in adversarial cognitive radio networks," in *Global Communications Conference (GLOBECOM), 2013 IEEE*, Dec 2013, pp. 611–616.

[19] J. H. M. Raya and I. Aad, "Domino: A system to detect greedy behavior in ieee 802.11 hotspots," 2010, pp. 1–8.

[20] Z. Jin, S. Anand, and K. Subbalakshmi, "Detecting primary user emulation attacks in dynamic spectrum access networks," in *Communications, 2009. ICC '09. IEEE International Conference on*, June 2009, pp. 1–5.

[21] Y. Liu, P. Ning, and H. Dai, "Authenticating primary users' signals in cognitive radio networks via integrated cryptographic and wireless link signatures," in *Security and Privacy (SP), 2010 IEEE Symposium on*, May 2010, pp. 286–301.

[22] A. Alahmadi, M. Abdelhakim, J. Ren, and T. Li, "Defense against primary user emulation attacks in cognitive radio networks using advanced encryption standard," *Information Forensics and Security, IEEE Transactions on*, vol. 9, no. 5, pp. 772–781, May 2014.

[23] F. Yu, H. Tang, M. Huang, Z. Li, and P. Mason, "Defense against spectrum sensing data falsification attacks in mobile ad hoc networks with cognitive radios," in *Military Communications Conference, 2009. MILCOM 2009. IEEE*, Oct 2009, pp. 1–7.

[24] A. Min, K. Shin, and X. Hu, "Attack-tolerant distributed sensing for dynamic spectrum access networks," in *Network Protocols, 2009. ICNP 2009. 17th IEEE International Conference on*, Oct 2009, pp. 294–303.

[25] Y. E. Sagduyu, "Securing cognitive radio networks with dynamic trust against spectrum sensing data falsification," in *Military Communications Conference (MILCOM), 2014 IEEE*, Oct 2014, pp. 235–241.

[26] C. Cordeiro, K. Challapali, D. Birru, and N. Sai Shankar, "Ieee 802.22: the first worldwide wireless standard based on cognitive radios," in *New Frontiers in Dynamic Spectrum Access Networks, 2005. DySPAN 2005. 2005 First IEEE International Symposium on*, Nov 2005, pp. 328–337.

[27] C. Stevenson, G. Chouinard, Z. Lei, W. Hu, S. Shellhammer, and W. Caldwell, "Ieee 802.22: The first cognitive radio wireless regional area network standard," *Communications Magazine, IEEE*, vol. 47, no. 1, pp. 130–138, January 2009.

[28] O. Leon, J. Hernandez-Serrano, and M. Soriano, "A new cross-layer attack to tcp in cognitive radio networks," in *Cross Layer Design, 2009. IWCLD '09. Second International Workshop on*, June 2009, pp. 1–5.

[29] W. Wang, Y. Sun, H. Li, and Z. Han, "Cross-layer attack and defense in cognitive radio networks," in *Global Telecommunications Conference (GLOBECOM 2010), 2010 IEEE*, Dec 2010, pp. 1–6.

[30] O. L. J. Hernandez-Serrano and M. Soriano, "Modeling the lion attack in cognitive radio networks," *EURASIP Journal on Wireless Communications and Networking*, 2011.

[31] D. N. E. Hossain and Z. Han, *Dynamic Spectrum Access and Management in Cognitive Communication Networks*. Cambridge University Press, 2009.

[32] S. Dudley, W. Headley, M. Lichtman, E. Imana, X. Ma, M. Abdelbar, A. Padaki, A. Ullah, M. Sohul, T. Yang, and J. Reed, "Practical issues for spectrum management with cognitive radios," *Proceedings of the IEEE*, vol. 102, no. 3, pp. 242–264, March 2014.

[33] I. S. for Information technology Local and metropolitan area networks Specific requirements, "Part 22: Cognitive wireless ran medium access control (mac) and physical layer (phy) specifications: Policies and procedures for operation in the tv bands," *IEEE Std 802.22-2011*, pp. 1–680, July 2011.

[34] J. Wang, M. S. Song, S. Santhiveeran, K. Lim, G. Ko, K. Kim, S. H. Hwang, M. Ghosh, V. Gaddam, and K. Challapali, "First cognitive radio networking standard for personal/portable devices in tv white spaces," in *New Frontiers in Dynamic Spectrum, 2010 IEEE Symposium on*, April 2010, pp. 1–12.

[35] K. Shin, H. Kim, A. Min, and A. Kumar, "Cognitive radios for dynamic spectrum access: from concept to reality," *Wireless Communications, IEEE*, vol. 17, no. 6, pp. 64–74, December 2010.

[36] D. Wang, D. Evans, and R. Krasinski, "Ieee 802.15.4j: extend ieee 802.15.4 radio into the mban spectrum [industry perspectives]," *Wireless Communications, IEEE*, vol. 19, no. 5, pp. 4–5, Oct 2012.

[37] I. S. for Local and metropolitan area networks.

[38] T. Doumi, "Spectrum considerations for public safety in the united states," *Communications Magazine, IEEE*, vol. 44, no. 1, pp. 30–37, Jan 2006.

[39] N. Jesuale and B. Eydt, "A policy proposal to enable cognitive radio for public safety and industry in the land mobile radio bands," in *New Frontiers in Dynamic Spectrum Access Networks, 2007. DySPAN 2007. 2nd IEEE International Symposium on*, April 2007, pp. 66–77.

[40] U. D. of Energy, "Communications requirements of smart grid technologies," Tech. Rep., October 2010.

[41] I. . working group, "Official ieee 802.11 working group project timelines," Retrieved 26.11.2014, Tech. Rep., November 2014. [Online]. Available: http://grouper.ieee.org/groups/802/11/Reports/802.11_Timelines.htm

[42] B. Wang and K. Liu, "Advances in cognitive radio networks: A survey," *Selected Topics in Signal Processing, IEEE Journal of*, vol. 5, no. 1, pp. 5–23, Feb 2011.

[43] Tech. Rep.

[44] B. Lo, "A survey of common control channel design in cognitive radio networks," *Physical Communication*, vol. 4, no. 1, pp. 26–39, March 2011.

[45] S. Srinivasa and S. Jafar, "The throughput potential of cognitive radio: A theoretical perspective," in *Signals, Systems and Computers, 2006. ACSSC '06. Fortieth Asilomar Conference on*, Oct 2006, pp. 221–225.

[46] J. M. Peha and S. Panichpapiboon, "Real-time secondary market for spectrum," Telecommunication Policy, Tech. Rep., 2004.

[47] G. Li, S. Srikanteswara, and C. Maciocco, "Interference mitigation for wlan devices using spectrum sensing," in *Consumer Communications and Networking Conference, 2008. CCNC 2008. 5th IEEE*, Jan 2008, pp. 958–962.

[48] L. Gavrilovska, D. Denkovski, V. Rakovic, and M. Angjelichinoski, "Medium access control protocols in cognitive radio networks: Overview and general classification," *Communications Surveys Tutorials, IEEE*, vol. 16, no. 4, pp. 2092–2124, Fourthquarter 2014.

[49] K. C. C. Cordeiro and M. Ghosh, "Cognitive phy and mac layers for dynamic spectrum access and sharing of tv bands," in *1st Int. Workshop TAPAS, Boston, MA, USA*, August 2006, pp. 1–10.

[50] H. Kim and K. G. Shin, "In-band spectrum sensing in cognitive radio networks: Energy detection or feature detection?" in *Proceedings of the 14th ACM International Conference on Mobile Computing and Networking*, ser. MobiCom '08, 2008, pp. 14–25.

[51] M. Oner and F. Jondral, "On the extraction of the channel allocation information in spectrum pooling systems," *Selected Areas in Communications, IEEE Journal on*, vol. 25, no. 3, pp. 558–565, April 2007.

[52] W. Han, J. Li, Z. Li, J. Si, and Y. Zhang, "Efficient soft decision fusion rule in cooperative spectrum sensing," *Signal Processing, IEEE Transactions on*, vol. 61, no. 8, pp. 1931–1943, April 2013.

[53] J. Ma and Y. Li, "Soft combination and detection for cooperative spectrum sensing in cognitive radio networks," in *Global Telecommunications Conference, 2007. GLOBECOM '07. IEEE*, Nov 2007, pp. 3139–3143.

[54] K. M. Thilina, K. W. Choi, N. Saquib, and E. Hossain, "Machine learning techniques for cooperative spectrum sensing in cognitive radio networks," *Selected Areas in Communications, IEEE Journal on*, vol. 31, no. 11, pp. 2209–2221, November 2013.

[55] W. Gabran, P. Pawelczak, and D. Cabric, "Throughput and collision analysis of multichannel multistage spectrum sensing algorithms," *Vehicular Technology, IEEE Transactions on*, vol. 60, no. 7, pp. 3309–3323, Sept 2011.

[56] Z. Zhang, H. Jiang, P. Tan, and J. Slevinsky, "Channel exploration and exploitation with imperfect spectrum sensing in cognitive radio networks," *Selected Areas in Communications, IEEE Journal on*, vol. 31, no. 3, pp. 429–441, March 2013.

[57] L. Wang, X. Chen, Z. Zhao, and H. Zhang, "Exploration vs exploitation for distributed channel access in cognitive radio networks: A multi-user case study," in *Communications and Information Technologies (ISCIT), 2011 11th International Symposium on*, Oct 2011, pp. 360–365.

[58] M. Bkassiny, S. Jayaweera, Y. Li, and K. Avery, "Optimal and low-complexity algorithms for dynamic spectrum access in centralized cognitive radio networks with fading channels," in *Vehicular Technology Conference (VTC Spring), 2011 IEEE 73rd*, May 2011, pp. 1–5.

[59] Z. Khan, J. Lehtomaki, L. DaSilva, and M. Latva-aho, "Autonomous sensing order selection strategies exploiting channel access information," *Mobile Computing, IEEE Transactions on*, vol. 12, no. 2, pp. 274–288, Feb 2013.

[60] S. Lim and T.-J. Lee, "A self-scheduling multi-channel cognitive radio mac protocol based on cooperative communications," *IEICE Trans. Commun.*, vol. 94-B, no. 6, p. 16571668, June 2011.

[61] D. Hu and S. Mao, "A sensing error aware mac protocol for cognitive radio networks," *Res. Article ICST Trans. Mobile Commun. Appl.*, vol. 12, no. 7-9, pp. 1–22, August 2012.

[62] B. Canberk, I. Akyildiz, and S. Oktug, "Primary user activity modeling using first-difference filter clustering and correlation in cognitive radio networks," *Networking, IEEE/ACM Transactions on*, vol. 19, no. 1, pp. 170–183, Feb 2011.

[63] M. Masonta, M. Mzyece, and N. Ntlatlapa, "Spectrum decision in cognitive radio networks: A survey," *Communications Surveys Tutorials, IEEE*, vol. 15, no. 3, pp. 1088–1107, Third 2013.

[64] M. U. P. Kaur and A. Khosla, "Adaptive bandwidth allocation scheme for cognitive radios," vol. 2, no. 4, p. 3541, June 2010.

[65] Q. Liang, S. Han, F. Yang, G. Sun, and X. Wang, "A distributed-centralized scheme for short- and long-term spectrum sharing with a random leader in cognitive radio networks," *Selected Areas in Communications, IEEE Journal on*, vol. 30, no. 11, pp. 2274–2284, December 2012.

[66] K. Shashika Manosha, N. Rajatheva, and M. Latva-aho, "Overlay/underlay spectrum sharing for multi-operator environment in cognitive radio networks," in *Vehicular Technology Conference (VTC Spring), 2011 IEEE 73rd*, May 2011, pp. 1–5.

[67] Q. Zhao, L. Tong, A. Swami, and Y. Chen, "Decentralized cognitive mac for opportunistic spectrum access in ad hoc networks: A pomdp framework," *Selected Areas in Communications, IEEE Journal on*, vol. 25, no. 3, pp. 589–600, April 2007.

[68] K. M. Thilina, E. Hossain, and D. Kim, "Dccc-mac: A dynamic common control channel-based mac protocol for cellular cognitive radio networks," *Vehicular Technology, IEEE Transactions on*.

[69] H. Bany Salameh, M. Krunz, and O. Younis, "Cooperative adaptive spectrum sharing in cognitive radio networks," *Networking, IEEE/ACM Transactions on*, vol. 18, no. 4, pp. 1181–1194, Aug 2010.

[70] H. Zheng and L. Cao, "Device-centric spectrum management," in *New Frontiers in Dynamic Spectrum Access Networks, 2005. DySPAN 2005. 2005 First IEEE International Symposium on*, Nov 2005, pp. 56–65.

[71] A. Attar, M. Nakhai, and A. Aghvami, "Cognitive radio game for secondary spectrum access problem," *Wireless Communications, IEEE Transactions on*, vol. 8, no. 4, pp. 2121–2131, April 2009.

[72] Z. Khan, S. Glisic, L. DaSilva, and J. Lehtomaki, "Modeling the dynamics of coalition formation games for cooperative spectrum sharing in an interference channel," *Computational Intelligence and AI in Games, IEEE Transactions on*, vol. 3, no. 1, pp. 17–30, March 2011.

[73] I. Christian, S. Moh, I. Chung, and J. Lee, "Spectrum mobility in cognitive radio networks," *Communications Magazine, IEEE*, vol. 50, no. 6, pp. 114–121, June 2012.

[74] T. Yucek and H. Arslan, "A survey of spectrum sensing algorithms for cognitive radio applications," *Communications Surveys Tutorials, IEEE*, vol. 11, no. 1, pp. 116–130, First 2009.

[75] J. Dong, H. Liu, and X. Wu, "Spectrum sensing techniques in practical cognitive radio applications," in *Communication Technology (ICCT), 2010 12th IEEE International Conference on*, Nov 2010, pp. 293–296.

[76] S. Atapattu, C. Tellambura, and H. Jiang, "Energy detection based cooperative spectrum sensing in cognitive radio networks," *Wireless Communications, IEEE Transactions on*, vol. 10, no. 4, pp. 1232–1241, April 2011.

[77] K. M. Thilina, K. W. Choi, N. Saquib, and E. Hossain, "Pattern classification techniques for cooperative spectrum sensing in cognitive radio networks: Svm and w-knn approaches," in *Global Communications Conference (GLOBECOM), 2012 IEEE*, Dec 2012, pp. 1260–1265.

[78] J. Unnikrishnan and V. Veeravalli, "Cooperative sensing for primary detection in cognitive radio," *Selected Topics in Signal Processing, IEEE Journal of*, vol. 2, no. 1, pp. 18–27, Feb 2008.

[79] E. Peh, Y.-C. Liang, Y. L. Guan, and Y. Zeng, "Optimization of cooperative sensing in cognitive radio networks: A sensing-throughput tradeoff view," *Vehicular Technology, IEEE Transactions on*, vol. 58, no. 9, pp. 5294–5299, Nov 2009.

[80] J. Ma, G. Zhao, and Y. Li, "Soft combination and detection for cooperative spectrum sensing in cognitive radio networks," *Wireless Communications, IEEE Transactions on*, vol. 7, no. 11, pp. 4502–4507, November 2008.

[81] M. H. A. Ashraf M. Aziz, Ahmed M. ElBakly and G. A. Hamid, "A new soft-fusion approach for multiple-receiver wireless communication systems," *ETRI Journal*, vol. 33, no. 3, pp. 310–319, June 2011.

[82] K. W. Choi, E. Hossain, and D. I. Kim, "Cooperative spectrum sensing under a random geometric primary user network model," *Wireless Communications, IEEE Transactions on*, vol. 10, no. 6, pp. 1932–1944, June 2011.

[83] C. Cortes and V. Vapnik, "Support-vector networks," *Kluwer Academic Publishers, Boston*, 2095.

[84] P. E. H. O. Richard, Duda and D. G. Stork, *Pattern Classification*. (2nd edition), Wiley, New York, 2001.

[85] Y. Zhao, D. Raymond, C. da Silva, J. Reed, and S. Midkiff, "Performance evaluation of radio environment map-enabled cognitive spectrum-sharing networks," in *Military Communications Conference, 2007. MILCOM 2007. IEEE*, Oct 2007, pp. 1–7.

[86] S. Grimoud, B. Sayrac, S. Ben Jemaa, and E. Moulines, "An algorithm for fast rem construction," in *Cognitive Radio Oriented Wireless Networks and Communications (CROWNCOM), 2011 Sixth International ICST Conference on*, June 2011, pp. 251–255.

[87] F. ICT-248351, Tech. Rep.

[88] P. Li, S. Guo, W. Zhuang, and B. Ye, "On efficient resource allocation for cognitive and cooperative communications," *Selected Areas in Communications, IEEE Journal on*, vol. 32, no. 2, pp. 264–273, February 2014.

[89] K. Thilina, E. Hossain, and M. Moghadari, "Cellular ofdma cognitive radio networks: Generalized spectral footprint minimization," *Vehicular Technology, IEEE Transactions on*, vol. PP, no. 99, pp. 1–1, 2014.

[90] Q. Qi, A. Minturn, and Y. Yang, "An efficient water-filling algorithm for power allocation in ofdm-based cognitive radio systems," in *Systems and Informatics (ICSAI), 2012 International Conference on*, May 2012, pp. 2069–2073.

[91] L. B. Le, P. Mitran, and C. Rosenberg, "Queue-aware subchannel and power allocation for downlink ofdm-based cognitive radio networks," in *Wireless Communications and Networking Conference, 2009. WCNC 2009. IEEE*, April 2009, pp. 1–6.

[92] K. Thilina, M. Moghadari, and E. Hossain, "Generalized spectral footprint minimization for ofdma-based cognitive radio networks," in *2014 IEEE International Conference on Communications (ICC)*, June 2014, pp. 1657–1662.

[93] S. Sadr, A. Anpalagan, and K. Raahemifar, "Radio resource allocation algorithms for the downlink of multiuser ofdm communication systems," *Communications Surveys Tutorials, IEEE*, vol. 11, no. 3, pp. 92–106, rd 2009.

[94] D. Ngo, C. Tellambura, and H. Nguyen, "Resource allocation for ofdma-based cognitive radio multicast networks with primary user activity consideration," *Vehicular Technology, IEEE Transactions on*, vol. 59, no. 4, pp. 1668–1679, May 2010.

[95] L. Zheng and C. W. Tan, "Maximizing sum rates in cognitive radio networks: Convex relaxation and global optimization algorithms," *Selected Areas in Communications, IEEE Journal on*, vol. 32, no. 3, pp. 667–680, March 2014.

[96] F. P. Kelly, "Charging and rate control for elastic traffic," *European Trans. on Telecommun.*, vol. 8, pp. 33–37, 1997.

[97] O. El Ferkouss and W. Ajib, "Game theory based resource allocation for cognitive radio networks," in *Global Communications Conference (GLOBECOM), 2012 IEEE*, Dec 2012, pp. 1174–1179.

[98] Y. W. B. Wang and K. J. R. Liu, "Game theory for cognitive radio networks: an overview," *International J. Comput. Telecommun. Netw.*, vol. 54, no. 14, p. 2537j2574, October 2010.

[99] K. Shashika Manosha and N. Rajatheva, "Joint power and rate control for spectrum underlay in cognitive radio networks with a novel pricing scheme," in *Vehicular Technology Conference Fall (VTC 2010-Fall), 2010 IEEE 72nd*, Sept 2010, pp. 1–5.

[100] K. Akkarajitsakul, E. Hossain, and D. Niyato, "Distributed resource allocation in wireless networks under uncertainty and application of bayesian game," *Communications Magazine, IEEE*, vol. 49, no. 8, pp. 120–127, August 2011.

[101] T. Krishna and A. Das, "A survey on mac protocols in osa networks," *Computer Networks, Elsevier Journal*, vol. 53, no. 9, pp. 214–218, March 2009.

[102] P. Ren, Y. Wang, Q. Du, and J. Xu, "A survey on dynamic spectrum access protocols for distributed cognitive wireless networks." *EURASIP J. Wireless Comm. and Networking*, vol. 2012, p. 60, 2012.

[103] A. De Domenico, E. Strinati, and M. Di Benedetto, "A survey on mac strategies for cognitive radio networks," *Communications Surveys Tutorials, IEEE*, vol. 14, no. 1, pp. 21–44, First 2012.

[104] K. Chowdhury and I. Akyldiz, "Ofdm-based common control channel design for cognitive radio ad hoc networks," *Mobile Computing, IEEE Transactions on*, vol. 10, no. 2, pp. 228–238, Feb 2011.

[105] T. Chen, M. Matinmikko, and H. Zhang, "A novel control channel management in cogmesh networks," in *Vehicular Technology Conference (VTC Fall), 2011 IEEE*, Sept 2011, pp. 1–6.

[106] K. Bian, J.-M. Park, and R. Chen, "Control channel establishment in cognitive radio networks using channel hopping," *Selected Areas in Communications, IEEE Journal on*, vol. 29, no. 4, pp. 689–703, April 2011.

[107] G.-Y. Chang, W.-H. Teng, H.-Y. Chen, and J.-P. Sheu, "Novel channel-hopping schemes for cognitive radio networks," *Mobile Computing, IEEE Transactions on*, vol. 13, no. 2, pp. 407–421, Feb 2014.

[108] N. Theis, R. Thomas, and L. DaSilva, "Rendezvous for cognitive radios," *Mobile Computing, IEEE Transactions on*, vol. 10, no. 2, pp. 216–227, Feb 2011.

[109] C. Li and C. Li, "Opportunistic spectrum access in cognitive radio networks," in *Neural Networks, 2008. IJCNN 2008. (IEEE World Congress on Computational Intelligence). IEEE International Joint Conference on*, June 2008, pp. 3412–3415.

[110] D. Cabric, S. Mishra, and R. Brodersen, "Implementation issues in spectrum sensing for cognitive radios," in *Signals, Systems and Computers, 2004. Conference Record of the Thirty-Eighth Asilomar Conference on*, vol. 1, Nov 2004, pp. 772–776 Vol.1.

[111] S. M. M. A. Sahai, R. Tandra and N. Hoven, "Fundamental design tradeoffs in cognitive radio systems," in *in Proc. of TAPAS06, Boston*, Aug 2006.

[112] A. Ghasemi and E. S. Sousa, "Spectrum sensing in cognitive radio networks: The cooperation-processing tradeoff," *Wireless Commun. and Mobile Comput.*, vol. 7, no. 9, p. 10491060, Nov 2007.

[113] J. Ma and Y. Li, "Soft combination and detection for cooperative spectrum sensing in cognitive radio networks," in *Global Telecommunications Conference, 2007. GLOBECOM '07. IEEE*, Nov 2007, pp. 3139–3143.

[114] G. Ding, Q. Wu, J. Wang, and X. Zhang, "Joint cooperative spectrum sensing and resource scheduling for cognitive radio networks with soft sensing information," in *Information Computing and Telecommunications (YC-ICT), 2010 IEEE Youth Conference on*, Nov 2010, pp. 291–294.

[115] Z. Quan, W.-K. Ma, S. Cui, and A. Sayed, "Optimal linear fusion for distributed detection via semidefinite programming," *Signal Processing, IEEE Transactions on*, vol. 58, no. 4, pp. 2431–2436, April 2010.

[116] W. Zhang and K. Letaief, "Cooperative spectrum sensing with transmit and relay diversity in cognitive radio networks - [transaction letters]," *Wireless Communications, IEEE Transactions on*, vol. 7, no. 12, pp. 4761–4766, December 2008.

[117] A. Agostini and E. Celaya, "Reinforcement learning with a gaussian mixture model," in *in Proc. Int. Joint Conf. on Neural Networks (IJCNN10), Barcelona, Spain*, 2010.

[118] N. L. A. Dempster and D. Rubin, "Maximum likelihood from incomplete data via the em algorithm," *Journal of the Royal Statistical Society. Series B (Methodological)*, vol. 39, no. 1, pp. 1–38, December 1977.

[119] J. S. Taylor and N. Cristianini, *Kernel Methods for Pattern Analysis*. Cambridge University Press, Cambridge, UK, 2004.

[120] H. Huang, Z. Zhang, P. Cheng, and P. Qiu, "Opportunistic spectrum access in cognitive radio system employing cooperative spectrum sensing," in *Vehicular Technology Conference, 2009. VTC Spring 2009. IEEE 69th*, April 2009, pp. 1–5.

[121] C. Li and C. Li, "Opportunistic spectrum access in cognitive radio networks," in *Neural Networks, 2008. IJCNN 2008. (IEEE World Congress on Computational Intelligence). IEEE International Joint Conference on*, June 2008, pp. 3412–3415.

[122] J. Mo, H.-S. So, and J. Walrand, "Comparison of multichannel mac protocols," *Mobile Computing, IEEE Transactions on*, vol. 7, no. 1, pp. 50–65, Jan 2008.

[123] S. Zhuo, Z. Wang, Y.-Q. Song, Z. Wang, and L. Almeida, "iqueue-mac: A traffic adaptive duty-cycled mac protocol with dynamic slot allocation," in *Sensor, Mesh*

and Ad Hoc Communications and Networks (SECON), 2013 10th Annual IEEE Communications Society Conference on, June 2013, pp. 95–103.

[124] H. Wang, H. Qin, and L. Zhu, "A survey on mac protocols for opportunistic spectrum access in cognitive radio networks," in *Computer Science and Software Engineering, 2008 International Conference on*, vol. 1, Dec 2008, pp. 214–218.

[125] M. Zia, F. Qureshi, and S. Shah, "Energy efficient cognitive radio mac protocols for adhoc network: A survey," in *Computer Modelling and Simulation (UKSim), 2013 UKSim 15th International Conference on*, April 2013, pp. 140–143.

[126] L. Ma, X. Han, and C.-C. Shen, "Dynamic open spectrum sharing mac protocol for wireless ad hoc networks," in *New Frontiers in Dynamic Spectrum Access Networks, 2005. DySPAN 2005. 2005 First IEEE International Symposium on*, Nov 2005, pp. 203–213.

[127] J. So and N. Vaidya, "Multi-channel mac for ad hoc networks: Handling multi-channel hidden terminals using a single transceiver," in *in Proc. of ACM MobiHoc*, 2004.

[128] L. Le and E. Hossain, "A mac protocol for opportunistic spectrum access in cognitive radio networks," in *Wireless Communications and Networking Conference, 2008. WCNC 2008. IEEE*, March 2008, pp. 1426–1430.

[129] C. Cordeiro and K. Challapali, "C-mac: A cognitive mac protocol for multi-channel wireless networks," in *New Frontiers in Dynamic Spectrum Access Networks, 2007. DySPAN 2007. 2nd IEEE International Symposium on*, April 2007, pp. 147–157.

[130] S. M. Kamruzzaman, "An energy efficient multichannel mac protocol for cognitive radio ad hoc networks," *Int. J. Commun. Netw. Info. Sec. (IJCNIS)*, vol. 2, no. 2, p. 112119, Aug 2010.

[131] J. Jia, Q. Zhang, and X. Shen, "Hc-mac: A hardware-constrained cognitive mac for efficient spectrum management," *Selected Areas in Communications, IEEE Journal on*, vol. 26, no. 1, pp. 106–117, Jan 2008.

[132] B. Hamdaoui and K. Shin, "Os-mac: An efficient mac protocol for spectrum-agile wireless networks," *Mobile Computing, IEEE Transactions on*, vol. 7, no. 8, pp. 915–930, Aug 2008.

[133] A.-C. Hsu, D. Wei, and C.-C. Kuo, "A cognitive mac protocol using statistical channel allocation for wireless ad-hoc networks," in *Wireless Communications and Networking Conference, 2007.WCNC 2007. IEEE*, March 2007, pp. 105–110.

[134] J. Jang and K. B. Lee, "Transmit power adaptation for multiuser ofdm systems," *Selected Areas in Communications, IEEE Journal on*, vol. 21, no. 2, pp. 171–178, Feb 2003.

[135] R. Wang, V. Lau, and Y. Cui, "Decentralized fair scheduling in two-hop relay-assisted cognitive ofdma systems," *Selected Topics in Signal Processing, IEEE Journal of*, vol. 5, no. 1, pp. 171–181, Feb 2011.

[136] T. Weiss, J. Hillenbrand, A. Krohn, and F. Jondral, "Mutual interference in ofdm-based spectrum pooling systems," in *Vehicular Technology Conference, 2004. VTC 2004-Spring. 2004 IEEE 59th*, vol. 4, May 2004, pp. 1873–1877 Vol.4.

[137] P. Kaligineedi, G. Bansal, and V. Bhargava, "Power loading algorithms for ofdm-based cognitive radio systems with imperfect sensing," *Wireless Communications, IEEE Transactions on*, vol. 11, no. 12, pp. 4225–4230, December 2012.

[138] K. W. Choi, E. Hossain, and D. I. Kim, "Downlink subchannel and power allocation in multi-cell ofdma cognitive radio networks," *Wireless Communications, IEEE Transactions on*, vol. 10, no. 7, pp. 2259–2271, July 2011.

[139] X. Liu and W. Wang, "On the characteristics of spectrum-agile communication networks," in *New Frontiers in Dynamic Spectrum Access Networks, 2005. DySPAN 2005. 2005 First IEEE International Symposium on*, Nov 2005, pp. 214–223.

[140] Y. Hou, Y. Shi, and H. Sherali, "Optimal spectrum sharing for multi-hop software defined radio networks," in *INFOCOM 2007. 26th IEEE International Conference on Computer Communications. IEEE*, May 2007, pp. 1–9.

[141] Y. Tachwali, B. Lo, I. Akyildiz, and R. Agusti, "Multiuser resource allocation optimization using bandwidth-power product in cognitive radio networks," *Selected Areas in Communications, IEEE Journal on*, vol. 31, no. 3, pp. 451–463, March 2013.

[142] Z. Jian and Z. Qi, "A novel adaptive resource allocation algorithm for multiuser ofdm-based cognitive radio systems," in *Network Computing and Information Security (NCIS), 2011 International Conference on*, vol. 2, May 2011, pp. 442–445.

[143] I. Toufik and R. Knopp, "Channel allocation algorithms for multi-carrier systems," in *Vehicular Technology Conference, 2004. VTC2004-Fall. 2004 IEEE 60th*, vol. 2, Sept 2004, pp. 1129–1133 Vol. 2.

[144] Y. Zhao, D. Raymond, C. da Silva, J. Reed, and S. Midkiff, "Performance evaluation of radio environment map-enabled cognitive spectrum-sharing networks," in *Military Communications Conference, 2007. MILCOM 2007. IEEE*, Oct 2007, pp. 1–7.

[145] Y. Zhao, L. Morales, J. Gaeddert, K. Bae, J.-S. Um, and J. Reed, "Applying radio environment maps to cognitive wireless regional area networks," in *New Frontiers in Dynamic Spectrum Access Networks, 2007. DySPAN 2007. 2nd IEEE International Symposium on*, April 2007, pp. 115–118.

[146] S. Boyd, *Convex Optimization*. Cambridge University Press, 7th ed., 2009.

[147] Z. Han, Z. Ji, and K. Liu, "Fair multiuser channel allocation for ofdma networks using nash bargaining solutions and coalitions," *Communications, IEEE Transactions on*, vol. 53, no. 8, pp. 1366–1376, Aug 2005.

[148] H. W. Kuhn, "The hungarian method for the assignment problem," *Naval Research Logistics Quarterly 2*, vol. 2, pp. 83–97, 1955.

[149] C. H. Papadimitrious and K. Steiglitz, *Combinatorial Optimization: Algorithms and Complexity*. Dover Publications, 1998.

[150] G. Sirinivas, "Assignment problem - hungarian algorithm," Department of Management Studies, IIT Madras, Tech. Rep. [Online]. Available: https://www.youtube.com/watch?v=BUGIhEecipE

[151] J. Munkres, "Algorithms for the assignment and transportation problems," *Journal of the Society for Industrial and Applied Mathematics 5*, March 1957.

[152] I. H. Toroslu and G. Ucoluk, "Incremental assignment problem," *Information Sciences*, 2007.

[153] D. E. G. H. D. J. J. R. M. Corless, G. H. Gonnet and D. E. Knuth, "On the lambert w function," *Advances in Computational Mathematics*, 1996.

[154] G. P. A. Sahai and A. Sabharwal, "Pushing the limits of full duplex: Design and real-time implementation," in Rice University Technical Report TREE1104, Tech. Rep., 2011.

[155] K. M. Thilina, H. Tabassum, E. Hossain, and D. Kim, "Medium access control design for full duplex wireless systems: challenges and approaches," *Communications Magazine, IEEE*, vol. 53, no. 5, pp. 112–120, May 2015.

[156] J. A. Bondy and U. S. R. Murty, *Graph Theory with Applications*. North Holland, Amsterdam, 1976.

Appendix A

A.1 Proof of Optimality of Algorithm 4 for a given number of subchannel requirement

In **Algorithm** 4, I apply Hungarian algorithm in the first iteration to obtain the best subchannel assignment for users. Hence, the subchannel assignment in the first iteration as given by the Hungarian algorithm is optimal [148, 151]. From the second iteration onward, I exploit localized information (the dual variables corresponding to the rows and the columns of **T**) in the previous iteration to obtain new subchannel assignment. To prove the optimality of the new subchannel assignment for the given number of subchannel requirement of users, I have to prove that the calculated dual variables corresponding to the updated rows and columns in **T** lead to an optimal assignment. Hence, I have to prove the optimality for the following cases:

- *Case I*: If the number of subchannel requirement of a particular user in the current iteration is less than the previous iteration, we should remove excess number of subchannes from that user by replacing Big-M values in the excess row entries.

- *Case II*: If the number of subchannel requirement of a particular user in the current iteration is greater than the previous iteration, I should include additional rows equal to the increased number of subchannels for that particular user at the dummy row locations if there are dummy rows in the assignment matrix T.

- *Case III*: If new candidate subchannels which were not previously indexed appear in the index matrix **D** for the current iteration, I should include new cost entries to assignment-cost-table **T**.

Lets denote the index of rows and columns in the assignment-cost-table **T** by two disjoint sets of **X** and **Y**, respectively. In **Algorithm** 4, I always balance the number of rows and columns in **T** by adding dummy rows if it is unbalanced before starting the subchannel assignment process. Hence, I can construct an equal size bipartite graph ($\mathcal{G}$) [148, 149, 151] using set **X** and **Y**, and the elements of assignment-cost-table **T** are the corresponding costs of edges. The element of i-th row and j-th column or the cost of edge between i-th vertex in set **X** and j-th vertex in set **Y** is denoted by $t_{i,j}$. Accordingly, the set of dual variables corresponding to the sets **X** and **Y** are **U** and **V**, respectively. The condition for satisfying the feasibility of the dual variable can be written as follows [148, 149, 151]:

$$\mathbf{U}(i) + \mathbf{V}(j) \leq t_{ij}. \tag{A.1}$$

If the equality of the constraint in (A.1) is fulfilled, then it is a potential matching for the whole subchannel assignment problem. Generally, if the j-th subchannel is assigned to the i-th user then no more assignment is possible for that subchannel. Thus, i-th user is matched to j-th subchannel.

A.1.1 Proof for Case I:

Suppose a particular user's number of subchannel requirement is reduced by one compared to the previous iteration. Then, the corresponding matching or assignment in the previous iteration should be removed from that user and let the vertices that (to be removed) edge is incident are x and y, where $x \in \mathbf{X}$ and $y \in \mathbf{Y}$. Hence, the x-th row in **T** is no longer assigned for that particular user and the x-th row entries are replaced by a Big-M value. As a result, the existing dual variable corresponding to x-th row no longer satisfies the

feasibility condition in (A.1). However, no cost change for the vertices corresponding to each subchannel and all the dual variables in set **V** still satisfy the feasibility constraint. Although I have removed the x-th row by replacing a Big-M value I need to find updated dual variable for this new row entries to maintain the consistency of the algorithm. Hence, the new dual variable for the x-th row (**U**(x)) can be calculated as

$$\mathbf{U}(x) = \min_j\{\mathbf{T}(x,j) - \mathbf{V}(j)\}. \tag{A.2}$$

Since I adjust **U**(x) to the minimum value that satisfies the equality constraint of (A.1), it guarantees at least one matching for the x-th row [150]. Note that, if $\mathbf{U}(x) + \mathbf{V}(y) = \mathbf{T}(x,y)$, then the best matching for the new row is $\mathbf{X}^*_{n,k}(x,y) = 1$. Otherwise, the vertices corresponding to **U**(x) and **V**(y) are the only unmatched vertices in the equality subgraph[1]. Since this unmatched vertex pair is in two separate vertex sets, it is possible to find an augmenting path[2] if there is one. Let us assume that there exists an augmenting path which starts from the vertex x $\in$ **X** and ends at vertex y $\in$ **Y**. Then, I can obtain a perfect matching for the bipartite graph $\mathcal{G}$ by interchanging unmatching and matching edges in the augmenting path [148–151]. Further, it is shown that the subgraph with perfect matching is the minimum weighted matching of any bipartite graph [156]. Hence, the perfect matching that we obtain by interchanging unmatching and matching in the augmenting path is the optimal solution for the bipartite graph $\mathcal{G}$.

Lets assume that I am unable to find an augmenting path which starts from x and ends at y in $\mathcal{G}$. To obtain an augmenting path using the present matching and unmatched vertex pair x and y, first we grow a Hungarian tree[3] rooted at the unmatched vertex x [148–151].

[1]The edges whose cost are equal to the sum of the dual variables of their end vertices and their incident vertices form the equality subgraph [148, 149, 151].

[2]A path which starts and ends with unmatched edges and alternates with matched and unmatched edges is known as an augmenting path [148–151].

[3]All the alternating paths originated from the given unmatched vertex form a Hungarian tree [148–151]. An alternating path is a path that starts from an unmatched edge and alternates between unmatching and matching edges along the path but ends with a matched edge [148–151]. A Hungarian tree can be obtained

In the process of growing the Hungarain tree, all the vertices encountered corresponding to the set **X** and **Y** are included in set **S** and **W**, respectively. Hence, the smallest possible change in a dual variable can be expressed as [150]

$$l = \min_{i \in \mathbf{S}, j \in \{\mathbf{Y}-\mathbf{W}\}} \{\mathbf{U}(i) + \mathbf{V}(j) - t_{i,j}\}. \tag{A.3}$$

Therefore, the modified dual variable for the encountered vertex ν can be written as follows:

$$\mathbf{U}(\nu) = \begin{cases} \mathbf{U}(\nu) + l, & \text{if } \nu \in \mathbf{S} \\ \mathbf{U}(\nu), & \text{otherwise.} \end{cases} \tag{A.4}$$

$$\mathbf{V}(\nu) = \begin{cases} \mathbf{V}(\nu) - l, & \text{if } \nu \in \mathbf{W} \\ \mathbf{V}(\nu), & \text{otherwise.} \end{cases} \tag{A.5}$$

Due to the modification of the dual variables, the alternating paths of the Hungarian tree is extended at least by one edge [150, 156]. Accordingly, I can find a path which starts from the unmatched vertex $x \in \mathbf{X}$ and ends with the unmatched vertex $y \in \mathbf{Y}$. Obviously, this path is an augmenting path. Hence, I can obtain a perfect matching for the bipartite graph $\mathcal{G}$ by interchanging unmatching and matching edges in the augmenting path and this perfect matching is the optimal minimum solution for the bipartite graph $\mathcal{G}$. Thus, by completing one iteration of the above described steps I can obtain the optimal solution for the subchannel assignment problem if a particular user's number of subchannel requirement is reduced by one compared to that in the previous iteration.

A.1.2 Proof for Case II:

The rows of the costs corresponding to the users whose required number of subchannels is increased in the present iteration are replaced at the location of dummy rows in the cost-

easily by following the ticking approach in [150].

assignment-table **T**. This scenario is exactly same as *Case I* except for the values in the newly replaced rows. Hence, the proof for *Case I* applies to *Case II* as well.

A.1.3 Proof for Case III:

Let us assume that one additional subchannel appears in the index matrix **D** compared to the previous iteration. Therefore, I add a new row (x$\in$ **X**) and a column (y$\in$ **Y**) corresponding to the new candidate user and subchannel at the end of **T**, respectively. The dual variables for the new candidate vertices in the extended bipartite graph are calculated with the help of existing dual variables of the perfect matching in the previous iteration. Hence, the feasible dual variable for the new candidate vertices can be calculated as

$$\mathbf{V}(q) = \min\{\min_{1\leq i\leq (q-1)}\{\mathbf{T}(i,q) - \mathbf{U}(i)\}, \mathbf{T}(q,q)\} \tag{A.6}$$

$$\mathbf{U}(q) = \min_{1\leq j\leq q}\{\mathbf{T}(q,j) - \mathbf{V}(j)\} \tag{A.7}$$

where q is the length of the first row/column of **T**. Note that, as we explained in *Case I*, with this dual calculation there is no change for the existing dual variables. If $\mathbf{U}(q) + \mathbf{V}(q) = \mathbf{T}(q,q)$, then the best matching for the new candidates is the edge between the vertices of the dual variable **U**(q) and **V**(q). Hence, I set $\mathbf{X}^*_{n,k}(q,q) = 1$. Otherwise, the vertices corresponding to the dual variable **U**(q) and **V**(q) are the only unmatched vertices in the equality subgraph. The best matching for the unmatched pair can be obtained by following the procedure described under *Case I* and the solution obtained by following the steps in *Case I* is the optimal subchannel assignment.

A.2 Complexity of Algorithm 4 for a given number of subchannel requirement

As I have described in Appendix A.1, one change in the bipartite graph results in at most one change in the corresponding dual variable. If there are t changes in the assignment-cost-table, I can find at most t unmatched pairs. To obtain perfect matching for one unmatched pair I have to perform at most one stage of the Hungarian as described in A.1. To obtain the best matching for the t unmatched pairs I should run at most t stages of the Hungarian. Since the complexity of one stage of the Hungarian algorithm is $\mathcal{O}(\mathcal{K}^2)$, the complexity of the subchannel assignment problem from the second iteration onward is $\mathcal{O}(t\mathcal{K}^2)$. It is important to note that t is always less than or equal to the number of users in the network since the number of subchannels requirement of a user is increased or decreased by one. The equality to the number of users holds if and only if all the users' channel requirements are increased by one. Further, the algorithm becomes a one-shot subchannel assignment problem when the number of users is equal to, or greater than the available number of subchannels and no iteration is required.